Journal of Geodynamics 52 (2011) 344–378

Contents lists available at ScienceDirect

Journal of Geodynamics

journal homepage: http://www.elsevier.com/locate/jog

Review

Future directions in subduction modeling

Taras Gerya

Geophysical Fluid Dynamics Group, Institute of Geophysics, Department of Earth Sciences, Swiss Federal Institute of Technology (ETH-Zurich), Sonneggstrasse, 5, 8092 Zurich, Switzerland

ARTICLE INFO

Article history:
Received 30 September 2010
Received in revised form 17 June 2011
Accepted 19 June 2011
Available online 24 June 2011

Keywords:
Numerical modeling
Plate tectonics
Subduction zones
Slab dynamics
Mantle convection
Magmatic arcs
Subduction initiation and termination

ABSTRACT

During the last four decades, subduction remained one of the most challenging and captivating geodynamic processes investigated with numerical techniques. While significant progress has been made toward deciphering the diverse array of subduction zone observations within the context of modeled physical processes, numerous questions remain regarding multiple aspects of subduction zone dynamics. A review of recent numerical studies highlights a number of open topics that subduction modeling can provide significant insight into in the future:

1. Resolving the controversy of subduction initiation.
2. Constraining robust high-resolution models of terrestrial plate tectonics.
3. Understanding deep slab processes in the mantle.
4. Constraining crustal growth and differentiation in magmatic arcs.
5. Modeling of fluid and melt transport in subduction zones.
6. Deciphering evolution of high- and ultrahigh-pressure rock complexes.
7. Developing geochemical-thermo-mechanical models of subduction.
8. Coupling of subduction models with volcanic and seismic risk assessment.
9. Understanding the onset of plate tectonics on Earth.

Progress in subduction modeling will require strong input from other disciplines (rheology, phase petrology, seismic tomography, geochemistry, numerical analysis, etc.). Indeed, due to the intrinsic complexity of terrestrial subduction processes, the role of geodynamic modeling will inevitably grow and provide an integrative basis for conducting quantitative cross-disciplinary subduction studies combining natural observations, laboratory experiments and modeling.

© 2011 Elsevier Ltd. All rights reserved.

Contents

E-mail address: taras.gerya@erdw.ethz.ch

0264-3707/$ – see front matter © 2011 Elsevier Ltd. All rights reserved.
doi:10.1016/j.jog.2011.06.005

1. Introduction

During the last four decades, since the first 2D numerical geodynamic modeling paper was published by Minear and Toksöz (1970), subduction has remained as one of the most captivating geodynamic processes investigated with analytical and numerical modeling. What is so special about subduction, and why, after 40 years of numerical research and many hundreds of papers published on subduction modeling, does this source of scientific inspiration still remain unsatisfied? First of all, subduction is the core process of terrestrial plate tectonics that provides the primary forces for plate movement and thus the evolution of Earth's surface and interior through geological time. Secondly, subduction zones are a major source of strong seismicity and volcanic activity that greatly affect human life. Thirdly, many first order physical and geological aspects of subduction remain enigmatic and elude full understanding due mainly to limited observations in both time and depth. The limited range of subduction observations necessitates the use additional physical constraints (such as numerical modeling) in most comprehensive studies of subduction processes. Consequently, this approach of combining observational analysis and numerical modeling has become widespread in subduction studies and geodynamics in general.

Realistic modeling of subduction processes is technically challenging and requires advanced 2D and 3D numerical techniques which account for strongly localized deformation at plate interfaces (e.g., van Keken et al., 2008), large viscosity contrasts (e.g., OzBench et al., 2008), a free surface boundary condition (e.g., Schmeling et al., 2008), complex pressure–temperature–stress-dependent visco-elasto-plastic rheologies of rocks (e.g., Hall et al., 2003; Morra et al., 2006; Capitanio et al., 2007; Gerya et al., 2008a; Gerya, 2010), metamorphic phase transformations (e.g., Rüpke et al., 2004; Gerya et al., 2006; Hebert et al., 2009) and water transport in the mantle wedge (Davies and Stevenson, 1992; Iwamori, 1998; Gerya et al., 2002; Arcay et al., 2005; Cagnioncle et al., 2007). Recently, three geodynamic community benchmarks (OzBench et al., 2008; Schmeling et al., 2008; van Keken et al., 2008) tested existing numerical codes ability to satisfy some of these crucial subduction modeling requirements.

Two tendencies currently exist in subduction model design (Fig. 1): simple models and complex models. The first type of models (Fig. 1a) attempt to isolate the influence of one or a small number of physical parameters on subduction process based on notably simplified numerical setups, such as kinematically prescribed models with uniformly dipping slabs in a thermal steady state, constant subduction velocity, free slip upper surface and simple mantle properties (no phase transitions, no compositional buoyancy, simple viscous rheology, constant thermal conductivity, etc.). These models have a relatively limited parameter space and are therefore easier to investigate in a systematic manner. The obvious danger of using such models is that results may not be necessarily applicable to nature since some essential subduction physics may be "thrown away" by over-simplifications. The second type of models (Fig. 1b) tend to investigate subduction in a more realistic manner by taking into account the broadest possible range of complexities relevant to nature: spontaneous rather than kinematically prescribed subduction rates, free erosion/sedimentation surfaces of plates, complex visco-(elasto)-plastic rheologies based on experimentally measured flow laws, phase transformations, fluid/melt transport, etc. These models often produce seemingly realistic subduction scenarios; however, the parameter space for such models is enormous and it is often difficult to isolate influences of individual parameters. Intermediate varieties between these two end-members also exist and attempt to create "minimal complexity" subduction models that are both sufficiently realistic to be applicable to nature and simple enough to be explored in a systematic manner. At present, the details and preferences of subduction model design are yet rather subjective and tend to reflect the technical, educational and aesthetical experience of individual modelers.

In this review I aim to outline the recent tendencies and future directions in numerical subduction modeling, with a particular emphasis of the following points:

- Subduction initiation.
- Fluid and melt transport in subduction zones.
- Subduction channel processes and histories of high-pressure rocks during subduction.
- Small-scale convection and thermal–chemical plumes in the mantle wedge.
- Crustal growth and magmatic arc development.
- Overriding plate dynamics.
- Deep subduction and slab bending processes.
- Termination of subduction and slab break-off.
- Subduction in the early Earth.
- Lateral variability of subduction processes in 3D.

Due to the broad subject variability and extensive subduction modeling literature (e.g., several hundred of papers can be found on ISI), this review is inevitably incomplete, but will hopefully provide a representative "cross-section" of the state of the art in subduction modeling.

2. Subduction initiation

The process of subduction initiation remains enigmatic and controversial, although it is widely accepted that the gravitational instability of old oceanic plates provides the primary driving force for subduction (Vlaar and Wortel, 1976; Davies, 1999). This gravitational instability develops as the density of oceanic lithosphere progressively increases due to surface cooling as the lithosphere moves away from a spreading ridge (Oxburg and Parmentier, 1977). In contrast to the gravitational instabilities that likely drive the subduction initiation process, the bending and shear resistance of the lithosphere acts againts subduction initiation and in some cases may impede it altogether (McKenzie, 1977). Despite this resistance, certain scenarios must lead to subduction initiation and a recent review by Stern (2004 and references therein) proposes two such scenarios ("induced" and "spontaneous") based on both theoretical considerations and natural data. Induced subduction nucleation may follow continued plate convergence after the jamming of a previously active subduction zone (e.g., due to the arrival of a buoyant crust to the trench). This produces regional compression, uplift and underthrusting that may yield a new subduction zone in a new location. Two subtypes of induced initiation, transference and polarity reversal, are distinguished (Stern, 2004 and references therein). Transference initiation moves the new subduction zone outboard of the failed one. Polarity reversal initiation also follows collision, but continued convergence in this case results in a new subduction zone forming behind the magmatic arc. Spontaneous nucleation results from the inherent gravitational instability of a sufficiently old oceanic lithosphere compared to the underlying mantle. It is widely accepted (e.g., Stern, 2004 and references therein) that subduction can initiate spontaneously either at a transform/fracture zone or at a passive continental/arc margin, in a fashion similar to lithospheric delamination.

Numerous hypotheses have been proposed to explain the physical mechanisms of induced and spontaneous subduction initiation, which largely depend on the tectonic setting:

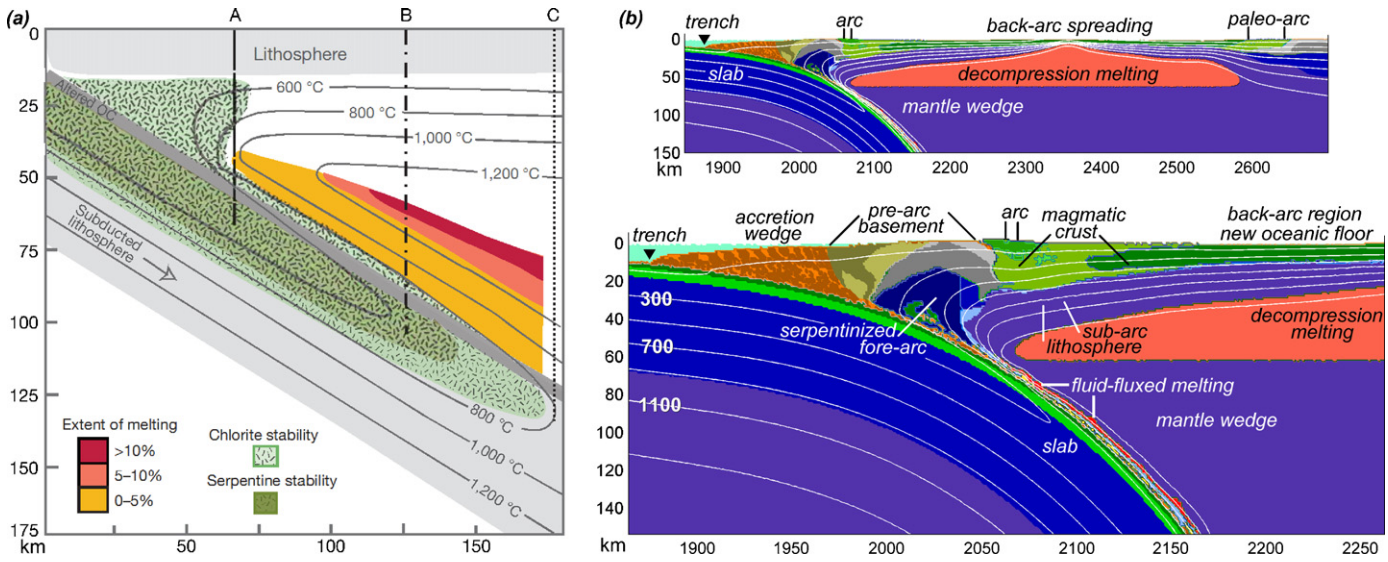

Fig. 1. Examples of (a) simple and (b) complex numerical models of subduction. (a) Finite element model with kinematically prescribed slab, prescribed constant subduction rate, free slip condition on the top, temperature-dependent viscosity and steady temperature field (Grove et al., 2009). (b) Finite difference model with spontaneously bending slab, free erosion/sedimentation upper surface, variable non-prescribed subduction rate, visco-plastic pressure–temperature–stress–dependent rheology, non-steady temperature field, spontaneous extension of the overriding plate associated with back arc basin development, slab dehydration and water transport above the slab associated with progressive mantle wedge hydration, fluid fluxed and decompression melting of the mantle wedge, melt extraction and volcanic crust growth (Gerya and Meilick, 2011).

(1) Plate rupture within an oceanic plate or at a passive margin (e.g., McKenzie, 1977).
(2) Polarity reversal of an existing subduction zone (e.g., Mitchell, 1984).
(3) Sediment or other topographic loading at continental/arc margins (e.g., Dewey, 1969; Cloetingh et al., 1982; Regenauer-Lieb et al., 2001).
(4) Conversion of oceanic transform faults/fracture zones into trenches by forced convergence (e.g., Uyeda and Ben-Avraham, 1972; Müeller and Phillips, 1991; Toth and Gurnis, 1998; Doin and Henry, 2001; Hall et al., 2003; Gurnis et al., 2004).
(5) Spontaneous initiation of retreating subduction due to a lateral thermal buoyancy contrast at oceanic fracture zones separating oceanic plates of contrasting ages (e.g., Gerya et al., 2008a; Nikolaeva et al., 2008; Zhu et al., 2009).
(6) Tensile decoupling of the continental and oceanic lithosphere due to rifting (Kemp and Stevenson, 1996).
(7) Rayleigh–Taylor instability growth due to a lateral thermal/compositional buoyancy contrast within the lithosphere (Matsumoto and Tomoda, 1983; Gurnis, 1992; Niu et al., 2003).
(8) Addition of water into the lithosphere (Regenauer-Lieb et al., 2001; Van der Lee et al., 2008).
(9) Spontaneous thrusting of the buoyant continental/arc crust over the oceanic plate (Mart et al., 2005; Goren et al., 2008; Nikolaeva et al., 2010, 2011).
(10) Small-scale convection in the sub-lithospheric mantle (Solomatov, 2004).
(11) Interaction of thermal–chemical plumes with the lithosphere (Ueda et al., 2008; Burov and Cloetingh, 2010).
(12) Large asteroid impacts (Hansen, 2007).
(13) Shear-heating induced localization along spontaneously forming lithospheric-scale fracture zones (Crameri and Kaus, 2010).

Indeed, only some of these hypotheses were tested numerically and ambiguity remains about physical consistency of some of the proposed mechanisms.

The first 2D numerical model of spontaneous subduction initiation (Matsumoto and Tomoda, 1983) attempted to predict the future crustal and lithospheric movement at a gigantic fracture zone in the Northeastern Pacific. This simple numerical simulation involved contact between two fluids with distinct viscosity and density values. From the standpoint of both bottom topography and lithospheric structure, their results suggested that the formation of a trench and a rudimentary slab will appear in several tens of millions years. Matsumoto and Tomoda (1983) also suggest that one typical example of such subduction initiation is given by the Nankai Trough. The interaction between the dense oceanic lithosphere of the Shikoku Basin and continental lithosphere of the Asian plate is speculated to have provided a sufficient gravitational instability to initiate formation of the Nankai trough and subsequent subduction.

Following the work of Matsumoto and Tomoda (1983), Gurnis (1992) developed a more complex buoyancy driven 2D models of subduction initiation using a pre-existing slab attached to the oceanic lithosphere to drive subduction. These models demonstrated that dynamic topography resulting from the initiation of slab subduction at an ocean-continent margin causes the continental lithosphere to subside rapidly. As subduction continues and the slab dip becomes shallower, a basin depocenter and forebulge migrate toward the continental interior. Finally, closure of the ocean basin leads to regional uplift. In certain cases, the dynamic subsidence rate exceeded 100 m per million years, which are similar to rates of sediment accumulation along convergent North American plate margins over the Phanerozoic (Gurnis, 1992).

Induced, subduction initiation across a pre-existing zone has been investigated in a number of numerical studies (Toth and Gurnis, 1998; Doin and Henry, 2001; Hall et al., 2003; Gurnis et al., 2004). In particular, Toth and Gurnis (1998) showed that a new subduction zone can initiate at a preexisting dipping fault zone with reasonable plate forces (on the order of 4×10^{12} N/m) and shear strength of the fault ($\leq$5 MPa), consistent with observations in the western Pacific. Doin and Henry (2001) further confirmed that a pre-existing weak brittle shear zone is the main requirement for subduction initiation under realistic plate forces. Hall et al. (2003) and Gurnis et al. (2004) demonstrated that an initial weak fracture zone could convert into a self-sustaining subduction zone

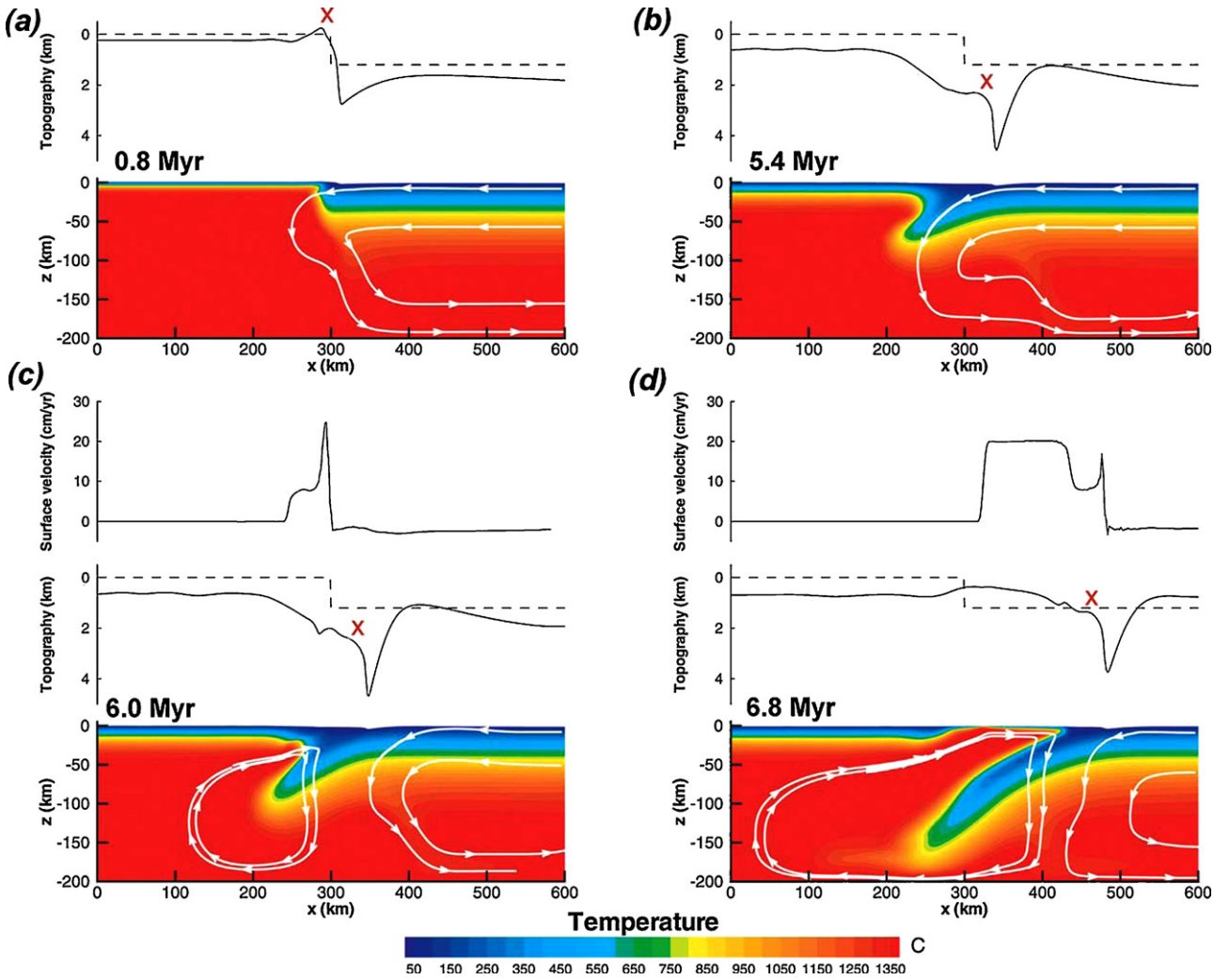

Fig. 2. Numerical model of induced subduction initiation across a pre-existing oceanic fracture zone (Hall et al., 2003). Each panel shows temperature (color code), instantaneous flow lines (white), and current (solid) and initial (dashed) topography. The red '*x*' shows the uplift and subsidence experienced by one unit of surface rocks. Panels (c) and (d) also show the horizontal component of surface velocity during the rapid extensional phase in the overriding plate.

(Fig. 2) after approximately 100–150 km of induced convergence with moderate plate forces ($2–3 \times 10^{12}$ N/m). Modeled initiation was accompanied by rapid extension of the overriding plate and explains the inferred catastrophic boninitic volcanism associated with Eocene initiation of the Izu–Bonin–Mariana (IBM) subduction zone (Hall et al., 2003; Gurnis et al., 2004). Indeed, it was shown later (Fig. 3a) that in the case of sufficiently wide and deep weak fracture zones subduction can also initiate in a retreating mode without any induced convergence (e.g., Gerya et al., 2008a; Nikolaeva et al., 2008; Zhu et al., 2009; Gerya, 2010). Recent experiments by Crameri and Kaus (2010) also demonstrate that self sustaining lithospheric weak zones may arise spontaneously in a homogeneous plate from shear-heating instabilities during induced convergence.

Regenauer-Lieb et al. (2001) examined spontaneous subduction initiation by sedimentary loading at passive continental margins with high-resolution 2D models and lithospheric rheologies taking into account the effects of water on rock strength. Prior work (e.g., Cloetingh et al., 1982) demonstrated that a solid–fluid thermomechanical instability driving a cold, stiff, and negatively buoyant lithosphere into the mantle can be triggered by sedimentary loading over a time span of 100 million years. Numerical results from Regenauer-Lieb et al. (2001) indicate that subduction initiation can proceed by a double feedback mechanism (thermoelastic and thermal–rheological) promoted by water lubrication. Later, Van der Lee et al. (2008) proposed that water introduced into the continental/oceanic lithospheric boundaries can be related to the past episodes of subduction due to hydrous mantle upwellings (thermal–chemical plumes) rising from deeply subducted slabs (e.g., Tamura, 1994; Gerya and Yuen, 2003; Richard and Bercovici, 2009). The effects of sedimentary loading on subduction initiation have also been studied recently by Nikolaeva et al. (2010) with the use of more complex passive margin geometries (Fig. 3b). Nikolaeva et al. (2010) found that in some cases sedimentary loading may actually preclude subduction initiation and promote horizontal overthrusting of continental crust over the oceanic plate.

Several numerical experiments outline spontaneous subduction initiation across a pre-existing oceanic fracture zone in both 2D (e.g., Gerya et al., 2008a; Nikolaeva et al., 2008; Gerya, 2010) and 3D (e.g., Zhu et al., 2009, 2011) without emphasis on the initiation process itself. Stable subduction initiation occurs for cases with a large cooling age contrasts between contacting plates (0.1–10 Myr vs. 40–90 Myr), combined with low strength (1–3 MPa) and large width and depth ($\geq$20 km $\times$ 20 km) of the pre-existing fracture zone (Fig. 3a). Development of self-sustaining one-sided subduction is marked by the beginning of down-dip slab motion, formation of the mantle wedge and appearance of the magmatic arc at 100–200 km distance from the retreating trench (Fig. 3a). The

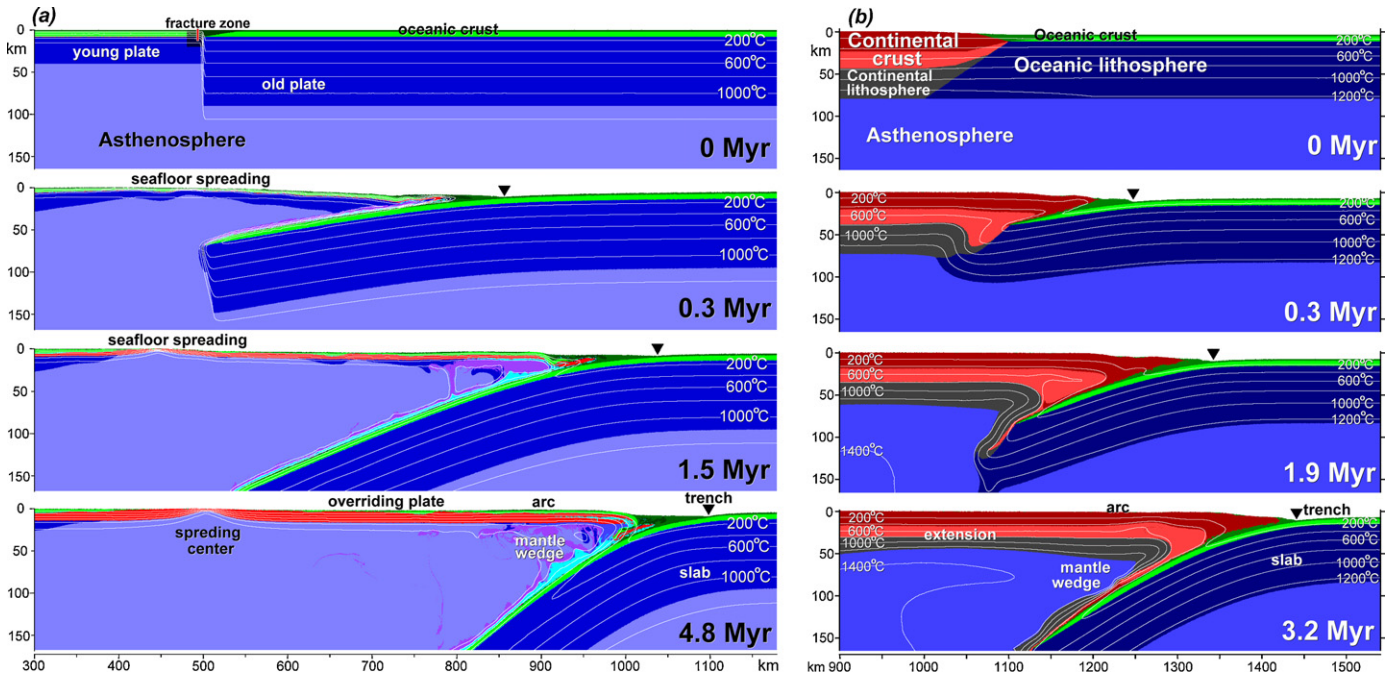

Fig. 3. Examples of numerical models for spontaneous initiation of subduction (a) at oceanic fracture zone (Gerya et al., 2008a) and (b) at a passive continental margin (Nikolaeva et al., 2010).

dynamics of subduction initiation agree well with previous theoretical and observation-based predictions (e.g., Hall et al., 2003; Stern, 2004 and references therein). The initiation process is associated with an increased subduction velocity and intense seafloor spreading and magma production (Fig. 3a, 0.3–1.5 Myr) (Nikolaeva et al., 2008; Zhu et al., 2009), as asthenosphere wells up to replace sunken lithosphere of the older plate. This is presumably the origin of most boninites and ophiolites (e.g., Hall et al., 2003; Stern, 2004 and references therein). Such an initiation process is assumed to have produced new subduction zones along the western edge of the Pacific plate during the Eocene (Stern, 2004 and references therein), although the short initial stage of subduction forcing has also been suggested for this region (e.g., Hall et al., 2003).

Passive continental/arc margin collapse (Fig. 3b) is driven by the geometry of the margin, where relatively thick (20–35 km) low density continental/arc crust is bounded laterally by significantly more dense oceanic lithosphere. During the margin evolution, when the forces generated from this lateral density contrast become large enough to overcome the continental/arc crust strength, the continental crust starts to creep over the oceanic crust (Fig. 3b, 0.3 Myr). This process causes deflection of the oceanic lithosphere (Fig. 3b, 0.3 Myr) and may actually lead to its delamination from the continental/arc lithosphere (Fig. 3b, 0.3–1.9 Myr), thus triggering a retreating subduction process (Fig. 3b, 1.9–3.2 Myr). This type of subduction nucleation has been systematically modeled with both analogue (Mart et al., 2005; Goren et al., 2008) and 2D numerical (Nikolaeva et al., 2010, 2011) techniques. With 2D models Nikolaeva et al. (2010) investigated the factors controlling passive margins' stability and showed that three subsequent tectonic regimes can develop at a passive margin: (1) stable margin, (2) overthrusting, and (3) subduction. The transition from a stable margin to the overthrusting regime is mainly controlled by the ductile strength of the lower continental crust. The transition from overthrusting to the subduction regime is governed by the ductile strength of the sub-continental lithospheric mantle and its chemical density contrast with the sub-oceanic lithospheric mantle. Nikolaeva et al. (2010) also demonstrated that in contrast to previous assumptions (e.g., Vlaar and Wortel, 1976; Davies, 1999), the age of the oceanic plate is a factor of secondary importance for subduction initiation. Rather, favorable conditions for subduction initiation correspond to passive margins where chemically buoyant (depleted) continental lithosphere becomes thin and hot (Moho temperature >660 °C). This situation can only arise when external processes such as rifting and/or thermo-chemical plume activity (e.g., Van der Lee et al., 2008) are imposed on the region of future subduction initiation.

The problem of subduction initiation at passive margins thus remains among the long-standing and controversial problems in plate tectonics. Although such initiation features in the classical Willson Cycle description, interestingly there is no irrefutable natural example of such subduction initiation. However, a number of regions may provide clues to subduction initiation at passive margins including subduction/overthrusting initiation at the southern Brasilian Atlantic margin (Marques et al., 2008; Nikolaeva et al., 2011) and the former initiation of the presently active Lesser–Antilles and the South Sandwich subduction systems (Goren et al., 2008). The numerical experiments of Nikolaeva et al. (2010, 2011) suggest that a typical passive margin, with a rifted continental crust thinner than 30–35 km, could transform into an active margin only if its lithosphere is unusually thin (<65–75 km). Combining this conclusion with the finding from Nikolaeva et al. (2010) that the subduction initiation process is indifferent to the age of the oceanic lithosphere past 20 Ma, one can conclude (Sobolev, personal communication) that passive margins can most easily convert to the active shortly (within some 20 Myr) after break-up, when its lithosphere is still thin and hot. If subduction initiation does not happen during this stage it is unlikely to occur later due to the cooling and thickening of the lithosphere along the margin wand. This sequence of events explains why mature passive margins are typically very stable (e.g., Nikolaeva et al., 2011).

The issue of induced versus spontaneous subduction initiation also remains partially controversial in both nature and within numerical models. As summarized by Gurnis et al. (2004), nearly half of all active subduction zones initiated during the Cenozoic. Furthermore, all subduction zones associated with active back arc extension have initiated since the Eocene, hinting that back arc

extension may be intimately associated with an interval (several tens of Myr) following subduction initiation Gurnis et al. (2004). That such a large proportion of subduction zones are young indicates that subduction initiation is a continuous process during the normal evolution of moving plates (Gurnis et al., 2004). This eludes to the fact that induced subduction initiation should play a dominant role (e.g., Hall et al., 2003; Gurnis et al., 2004), and would be difficult to avoid if tectonic plates remain dynamic. Although they occur within different tectonic settings, four known subduction initiation events (Izu–Bonin–Mariana along a fracture zone, Tonga-Kermadec along an extinct subduction boundary, New Hebrides within a back arc, and Puysegur-Fiordland along a spreading center) were typified by rapid uplift within the forearc, followed by sudden subsidence (Gurnis et al., 2004). This correlates well with the results of 2D numerical experiments that explored incipient compression across a pre-existing plate boundary, and found that the formation of a through-going fault is associated with rapid uplift on the hanging wall and subsidence on the footwall (e.g., Hall et al., 2003; Gurnis et al., 2004). On the other hand, a number of other thermo-mechanical models (e.g., Gerya et al., 2008a,b; Nikolaeva et al., 2008; Zhu et al., 2009; Gerya, 2010) suggest that an initial stage of compression is not a prerequisite for the initiation of self-sustaining, retreating subduction, given a sufficient age contrast between plates and width of the weak plate boundary. Further complications may come from three-dimensional aspects of the plate structure near pre-existing fracture zones such as transform faults. To date all subduction initiation experiments consider either 2D models (e.g., Hall et al., 2003; Gurnis et al., 2004; Nikolaeva et al., 2008, 2010), or laterally uniform plate boundary in 3D models (Zhu et al., 2009, 2011). In contrast, oceanic transform faults are characterized by notable lateral variations in the thermal and rheological structure and the buoyancy of the contacting plates, which could strongly affect likelihood and dynamics of subduction initiation in this geodynamic setting.

The record of deformation left on the overriding plates can potentially distinguish spontaneous and induced subduction. Induced nucleation begins with strong compression and uplift, whereas a spontaneous nucleation begins with rifting and seafloor spreading (Stern, 2004). However, a lack of known locations for active subduction initiations provides a major obstacle to directly investigating subduction initiation by observation of overriding plate deformation. According to numerical experiments (e.g., Nikolaeva et al., 2010, 2011) subduction initiation at passive continental margins is a long-term process and often has a "hidden" phase of initial slow movements (overthrusting), which are not expressed in typical subduction features such as a pronounced trench and magmatic arc. The main future challenge is, therefore, to identify possible subduction initiation localities worldwide by numerically evaluating the probability of subduction initiation at various passive margins and oceanic plate boundaries based on local lithospheric structures and acting tectonic forces (Nikolaeva et al., 2011). Simulated dynamics of unstable margins and plate boundaries can then be analyzed in order to understand and constrain the key natural observables which should be monitored. In particular, an interesting question concerning subduction initiation is what mechanism can lead to subduction of the Atlantic oceanic lithosphere. Possible scenarios may include a collapse of the South American passive margin (e.g., Marques et al., 2008; Nikolaeva et al., 2011) and outboard propagation of subduction zones from the Pacific (such as Lesser-Antilles and/or South Sandwich, Sobolev, personal communication). Considering potential links between subduction initiation and lithospheric thinning (Nikolaeva et al., 2010, 2011), additional study areas may also include (Sobolev, personal communication) the East African margin, which has been strongly affected by the recent Afar plume activity (e.g., Pérez-Gussinyé et al., 2009). Future technical advances will likely be directed toward modeling of subduction initiation in 3D with realistic high-resolution global (e.g., Stadler et al., 2010) and regional (e.g., Zhu et al., 2009, 2011) models, including free plate surfaces that can take into account actual plate configurations, the geometry of passive margin, oceanic transform/fracture zones and the distribution of continental/oceanic topography.

3. Fluid and melt transport in subduction zones

Subduction zones are one of the major sites of volcanism on Earth, yet the mechanisms of melt generation are still debated. It is widely accepted that a significant amount of H_2O is expelled from the subducting slab and contributes to melt generation in the hot portions of the mantle wedge (e.g., Peacock, 1990a,b). The introduction of H_2O lowers the melting temperature of rocks (i.e., 'flux melting'), which can produce significant amounts of melt even in a relatively cool environment above a subducting slab. Presently, water transport and melting are often implemented in numerical models of subduction (Fig. 4) using kinematic (e.g., Gerya et al., 2002, 2006, 2008a; Arcay et al., 2005), porous flow (e.g., Iwamori, 1998, 2000, 2007; Cagnioncle et al., 2007; Faccenda et al., 2009; Hebert et al., 2009) and water diffusion (Richard et al., 2006; Richard and Bercovici, 2009) approaches.

Peacock (1990a,b, 1993, 1996) analyzed fluid release and melting in subduction zones based on 2D thermal-kinematic models. In these models, fluids were released by continuous and discontinuous end-members of three different dehydration models: pressure-sensitive, temperature-sensitive, and amphibole (negative dP/dT) dehydration. Subduction zone P–T–time paths predicted by these models intersected the wet basaltic solidus only at the initiation of subduction. In mature subduction zones, and in the absence of significant frictional heating and induced mantle convection, P–T–time paths encountered subsolidus conditions at depths of 100–150 km beneath magmatic arcs, suggesting that slab dehydration reactions play an important role in arc magma genesis (Peacock, 1990a). In this respect, the blueschist to eclogite transition was regarded to be one of the crucial reactions for fluid flux induced melting (Peacock, 1993). At the depth of this transition, partial melting appeared to occur primarily in the overlying mantle wedge as a result of fluid infiltration (Peacock, 1990b). In both the temperature and amphibole dehydration models, the fluid production region moved to greater depths over time as the subduction zone cooled. Within the oceanic crust, fluid production starts at the top of the crust and migrates downward in the temperature and amphibole dehydration models. Peacock (1990a) further estimated fluid fluxes out of the subducting slab: for a convergence rate of 3 cm/yr, average fluid fluxes ranged from ~0.1 kg fluid/(m^2 yr) for the continuous reaction models, to >1 kg fluid/(m^2 yr) for the discontinuous pressure and amphibole dehydration models. It was further concluded (Peacock, 1990a) that vertical fluid fluxes on the order of 1 kg fluid/(m^2 yr) can substantially perturb the thermal structure of overlying rocks and can cause large-scale hydration and metasomatism of the overlying mantle wedge. In contrast, the thermal effect of fluid flow parallel to the subduction thrust zone were estimated to be insignificant compared to the thermal effect of the subducting oceanic lithosphere (Peacock, 1990a).

The influential work of Davies and Stevenson (1992) was one of the first numerical studies of subduction to elucidate the significance of water propagation in the mantle wedge beneath volcanic arcs. In this study, the steady state thermal field is evaluated for a model subduction zone where the plates are prescribed by kinematic boundary conditions, such that the subducting slab induces a flow in the mantle wedge. It was proposed that the combination of vertical motion of water as a free phase and the transport of hydrous phases (e.g., amphiboles) by the slab-induced mantle wedge flow,

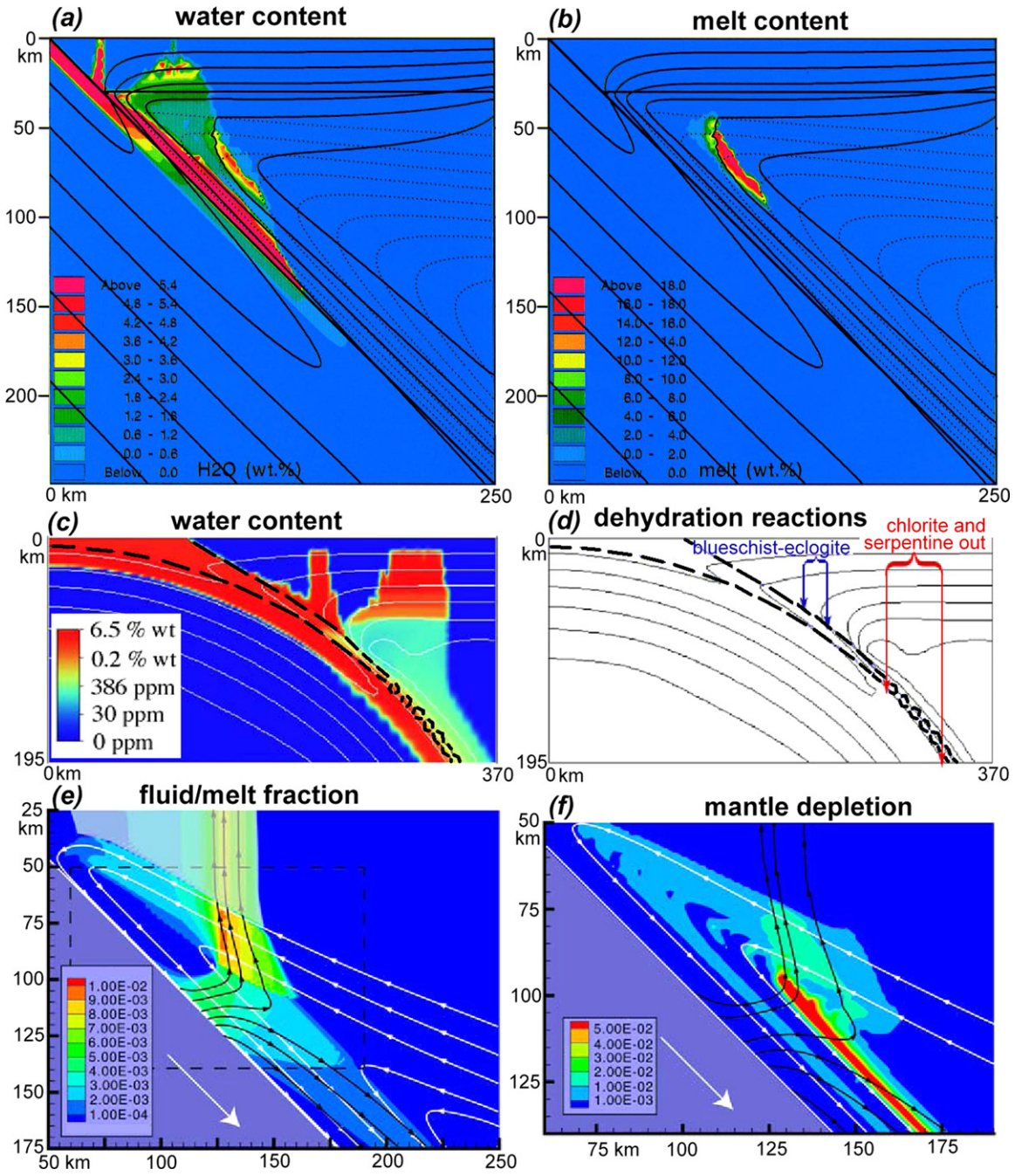

Fig. 4. Examples of numerical models for hydration and melting above a subducting slab. (a, b) Model of Iwamori (1998), the dotted lines in the mantle wedge indicate the stream lines, the solid lines indicate the isothermal contours with a 200 °C interval. (c, d) Model of Arcay et al. (2005), isotherms (solid lines) are plotted every 200 °C, the dashed line limits crustal rocks in the medium. (e, f) Model of Cagnioncle et al. (2007), fluid flow lines are shown in black, and solid flow lines are shown in white.

lead to the net transport of water being horizontal, across the mantle wedge from the slab. Provided the subducting oceanic crust enters the asthenosphere at a velocity >6(±2) cm/yr, the mantle wedge will be hot enough at the limit of the lateral water transport mechanism to generate melting at the amphibole-buffered solidus.

Iwamori (1998, 2000, 2004, 2007) was the first to create a self-consistent numerical model of subduction that included slab dehydration, water transport, mantle hydration and melting of the mantle wedge (Fig. 4a). In this numerical model the aqueous fluid migrates by porous flow and interacts chemically (including melting reactions) with the convecting solid. The calculations suggested (Iwamori, 1998, 2007) that: (i) an aqueous fluid released from the subducting oceanic crust forms a serpentinite + chlorite layer in the mantle wedge just above the subducting slab, maintaining a condition close to equilibrium in terms of hydration–dehydration reactions during aqueous fluid migration and (ii) most of the H_2O is subducted to a depth where serpentine and chlorite in the serpentinite layer break down. This depth (up to 150 km) depends on the thermal structure of the slab, and is greater for the older plates. As a consequence, aqueous fluids and melt, in general, do not migrate directly upwards to the volcanic front. This result correlates well with qualitative prediction of Davies and Stevenson (1992) and is rather different from the conventional view of fluid migration in subduction zones. Iwamori (2000) also demonstrated that slower thermal recovery of the subducting plate can shift the dehydration reactions to greater depths along the plate, which in

turn deflects the magmatic front (as e.g., in central Japan near the triple junction of the Pacific, Philippine Sea and North American plates). The low geothermal gradient along the subducting plate also implies that a considerable amount of H_2O is carried further down by the high-pressure hydrous mantle phase (phase A), which is formed just above the subducting plate, without being released for magmatism (Iwamori, 2000).

Later studies by several researchers investigated a number of geodynamic consequences of water release and propagation above slabs based on various models of water transport and melting:

- Formation of low-viscosity serpentinized channels with internal circulation above the subducting slab where high-pressure rocks are formed and exhumed (Gerya et al., 2002);
- Triggering of Rayleigh–Taylor instabilities and propagation of thermal–chemical plumes from the hydrated layer above slab (Gerya and Yuen, 2003; Gerya et al., 2004a; Manea et al., 2005; Zhu et al., 2009);
- Formation of a low-viscosity wedge, low-viscosity channel and overriding plate thinning by hydration from the slab (Arcay et al., 2005, 2006; Hebert et al., 2009);
- Influence of mantle hydration dynamics on viscosity structure above slabs and the degree of rheological coupling between plates and its geodynamic regimes of subduction (e.g., Gorczyk et al., 2007a; Hebert et al., 2009; Gerya and Meilick, 2011);
- Effect of solid flow on water distribution and melting above a subducting slab at convergent plate boundaries (Cagnioncle et al., 2007).
- Development of asymmetric one-sided terrestrial-style subduction by water-related weakening of plate interfaces (Gerya et al., 2008a);
- Seismic velocity structures associated with hydration and melting in the mantle wedge (e.g., Gerya et al., 2006; Nikolaeva et al., 2008; Gerya and Meilick, 2011);
- Magmatic productivity above slabs and the dynamics of crustal growth in volcanic arcs driven by water and melt transport (Gorczyk et al., 2007a,b; Nikolaeva et al., 2008; Zhu et al., 2009, 2011; Gerya and Meilick, 2011);
- Slab dehydration and water-induced convection in the Earth's mantle transition zone (Richard et al., 2006; Richard and Bercovici, 2009);
- Deep slab hydration induced by bending related variations in tectonic pressure (Faccenda et al., 2009).

In particular, Cagnioncle et al. (2007) investigated the distribution of hydrous fluid and subsequent melt in the wedge using 2D models that included solid mantle flow and associated the temperature distributions, buoyant fluid migration and melting (Fig. 4e). The results demonstrate that solid mantle flow deflects hydrous fluid from their buoyant vertical migration through the wedge. As a result, melting does not occur directly above the region where hydrous fluids are released from the slab, which a number of previous studies also concluded (Iwamori, 1998, 2000, 2004). Rather, a melting front develops where hydrous fluids first encounter mantle material hot enough to melt. Wet melting is influenced by solid flow through the advection of fertile mantle material into the wet melting region and the removal of depleted material. The region of maximum melting occurs where the maximum flux of water from slab mineral dehydration reaches the wet melting region. The extent of melting, and melt production rates, increases with increasing convergence rate and grain size due to increased temperatures along the melting front and increased fractions of water reaching the melting front, respectively. The position of isotherms above the wet solidus varies with increasing slab dip and thereby also influences the extent of melting and melts production rates.

Gerya et al. (2008a) investigated the asymmetric nature of subduction at convergent plate boundaries, where the subducted slab sinks downward and the overriding plate moves horizontally (one-sided subduction). In contrast, global mantle convection models (except for recent work of Tackley et al., 2010) generally predict downwelling of both plates at convergent margins (two-sided subduction, Tackley, 2000). Gerya et al. (2008a) studied two-dimensional (2D) visco-elasto-plastic numerical models for retreating oceanic subduction with a free surface and kinematic water transport above the slab to elucidate the cause of one-sided subduction. It was demonstrated that the stability, intensity, and mode of subduction mainly depends on slab strength and the amount of weak hydrated rocks created above the slab by fluid infiltration. Two-sided subduction occurs at low slab strength ($\sin[\phi] < 0.15$, where ϕ is the effective internal friction angle), regardless of the extent of hydration. In contrast, steady-state one-sided subduction requires a weak hydrated slab interface and high slab strength ($\sin[\phi] > 0.15$). The weak interface is maintained by the release of fluids from the subducted oceanic crust as a consequence of metamorphism. The resulting weak inter-plate zone localizes deformation at the interface and decouples the strong plates, facilitating asymmetric plate movement. Gerya et al. (2008a) concluded that high plate strength and the presence of water on the Earth are thus major factors controlling the style of terrestrial plate tectonics driven by self-sustaining one-sided subduction processes.

Recently, investigatations by Faccenda et al. (2009) revealed the critical role of ocean plate bending in deep slab hydrations. Slab bending at subduction zones results in extension and widespread normal faulting in the upper, brittle region of the slab. Detailed seismic surveys at trenches reveal that this part of the oceanic plate can be pervasively hydrated for several kilometers below the crust–mantle boundary (e.g., Ranero and Sallares, 2004). Based on 2D numerical experiments (Fig. 5) with coupled solid and fluid flow, Faccenda et al. (2009) found that bending of oceanic plates near trenches produces subhydrostatic or even negative pressure gradients along normal faults (Fig. 5c), favoring downward pumping of fluids deep into the oceanic lithosphere. The fluids then react with the crust and mantle surrounding the faults and are stored in the form of hydrous minerals. These results have implications for the transport of water into the deeper parts of the mantle (e.g., Iwamori, 1998; Ohtani et al., 2004; Richard et al., 2006), and for the seismic anisotropy in subduction zones (e.g., Long and Silver, 2008; Faccenda et al., 2008a).

At present, the subduction modeling community is working toward developing more realistic thermo-mechanical models including fluid and melt transport above slabs by porous (e.g., Connolly and Podladchikov, 1998; Schmeling, 2000; Miller et al., 2004; Rozhko et al., 2007) and reactive flows (Spiegelman et al., 2001) as well as by diffusion (Richard et al., 2006; Richard and Bercovici, 2009) and diapiric rise (e.g., Gerya and Yuen, 2003; Zhu et al., 2009). Such models would also contain feedbacks from rheological, thermal and compositional coupling between fluids and melts migration and the visco-(elasto)-plastic deformation of solids. The complex relationships between long-term deformation, fluid and melt transport, subduction zone seismicity and magmatic activity (e.g., Miller et al., 2004; Caricchi et al., 2007) will likely receive strong attention from the numerical modeling community in the future.

4. Subduction channel processes and the history of high-pressure rocks during subduction

Subduction channel development is an important component of subduction zone evolution (e.g., Hsu, 1971; Cloos, 1982). On one hand, processes taking place in the subduction channel leaves

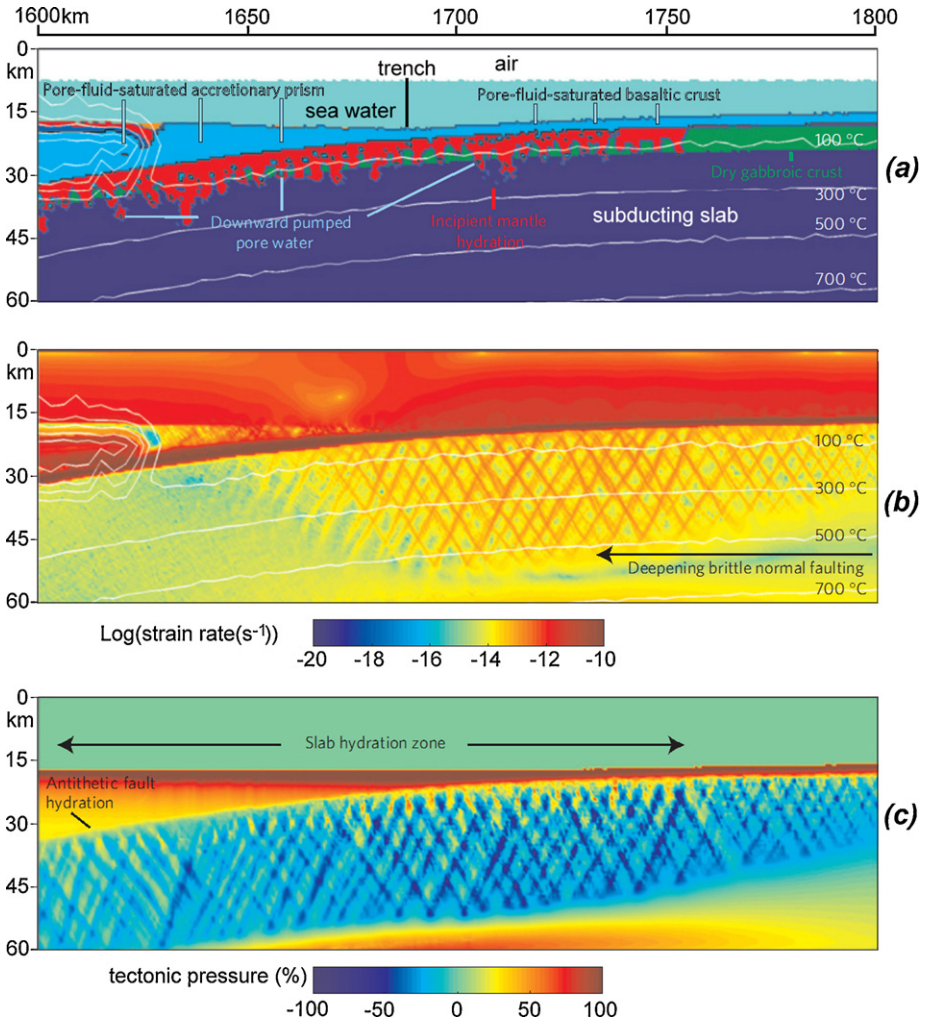

Fig. 5. Numerical model of deep slab hydration (Faccenda et al., 2009). (a) Compositional map of the trench area. (b) Strain-rate map. Fault activation due to the bending of the plate starts at shallow depths offshore of the trench and progressively deepens. (c) Tectonic pressure map (i.e., deviation of mean stress on solids from lithostatic pressure). Stress changes induced by the bending oceanic plate produce sub-hydrostatic or even negative pressure gradients along normal faults, favoring downward pumping of fluids.

notable and directly accessible records at the surface in the form of exhumed high-pressure (HP) and ultrahigh-pressure (UHP) rock complexes (e.g., Ernst, 1977; Cloos, 1982; Shreve and Cloos, 1986; Hermann et al., 2000; Federico et al., 2007; Krebs et al., 2008). Subduction channel processes may also contribute to a magmatic record through deep subduction and melting of hydrated rock mélanges formed in the channel (e.g., Gerya and Yuen, 2003; Gerya et al., 2006; Castro and Gerya, 2008; Castro et al., 2009, 2010; Zhu et al., 2009). It is widely accepted that the deep burial of high-pressure metamorphic rocks is due to subduction of these rocks with the downgoing slab. However, the mechanisms of their exhumation remain the subject of discussion and several models have been proposed (e.g., Cloos, 1982; Platt, 1993; Maruyama et al., 1996; Ring et al., 1999). According to the most popular corner flow model (Hsu, 1971; Cloos, 1982; Cloos and Shreve, 1988a,b; Shreve and Cloos, 1986; Gerya et al., 2002), exhumation of high-pressure metamorphic crustal slices, at rates on the order of the plate velocity, are driven by forced flow in a wedge-shaped subduction channel.

The first noteworthy analytical models of subduction channel flow with numerical integration of rock trajectories were presented by Cloos (1982), Shreve and Cloos (1986) and Cloos and Shreve (1988a,b). These models assumed that subducting sediment deforms approximately as a viscous material once it is dragged into a relatively thin shear zone, or subduction channel, between the downgoing and overriding plates. Model predictions of the movement patterns of sediment matrix and eclogite inclusions within the channel were able to explain many of the observed features at convergent plate margins, and quantified the processes of sediment subduction, offscraping, underplating and the formation of subduction mélanges (Cloos, 1982; Shreve and Cloos, 1986; Cloos and Shreve, 1988a,b). These models also demonstrated that variations in tectonic behavior depend mainly on the channel geometry, rate of subduction, the supply of sediment, the geometry of the descending plate and the topography and structure of the overriding block. The results of Cloos (1982) revealed that the thermal regime in a mature channel flow is such that the downward and upward *P*–*T* paths of rocks should almost coincide, which is in close agreement with natural observations (e.g., Ernst, 1977; Cloos, 1982).

The next series of influential 2D thermal-kinematic subduction models addressing the prograde history of metamorphic rocks was presented by Peacock (1987a, 1990a,b, 1993, 1996). The models focused on elucidating the *P*–*T*–time paths of high-pressure rocks associated with subduction and constraining the thermal conditions under which inverted metamorphic gradients, characteristic of high-pressure complexes, are created and preserved. Rapid subduction ($\sim$10 cm yr^{-1}) beneath young oceanic lithosphere (<10 Ma) results in rapid heat conduction downward from the hanging wall and the creation of inverted thermal gradients in excess of $-100\,^{\circ}$C km^{-1} in the top portion of the downgoing slab. In order

to be preserved in the geological record the inverted metamorphic gradient must accrete to the base of the hanging wall. Accretion of the upper portion of the subducting slab may occur due to declining temperatures that cause downward migration of the viscous slip zone and/or greenschist facies devolatilization reactions that weaken the descending slab (spontaneous accretion of subducted rocks was confirmed numerically by Gerya et al., 2002). The models predicted that (1) the high-grade metamorphic rocks in inverted metamorphic gradients form early in the subduction process and therefore effectively date the initiation of subduction, and (2) inverted metamorphic gradients mark sites of major plate convergence in excess of 1000 km.

Recently Syracuse et al. (2010) modeled 56 segments of subduction zones using kinematically defined slabs to obtain a comprehensive suite of thermal models for the global subduction system. Prograde *P–T* paths for subducted rocks were systematically investigated depending on their position relative to the top of the slab. Peculiar shapes of *P–T* paths with a pronounced near-isobaric heating stage were systematically documented for the top of the oceanic crust and sediments. The temperature of rocks during this stage increased from 300–400 °C to 700–800 °C, suggesting very intense dehydration in a very limited range of depths. These depths correspond to the relatively sharp transition from partial, to full coupling between subducted and overriding plates. In contrast, the interior of the oceanic crust and underlying mantle within the downgoing plate remained cold enough for hydrous phases to be stable beyond the arc in all but the hottest subduction zones, allowing water to be carried beyond the arc in the slab.

Gerya et al. (2002) used 2D models to investigate the self-organizing evolution of the accretionary wedge and the subduction channel during intra-oceanic subduction (Fig. 6). In this fully coupled thermo-mechanical subduction model, the geometry of the accretionary wedge and the subduction channel were neither prescribed nor assumed to represent a steady state. Instead, the system is free to evolve, starting from an imposed early stage of subduction and controlled by the progressive modification of the thermal, petrological, and rheological structure of the subduction zone. In this evolution, upward migration of the aqueous fluid released from the subducting slab and progressive hydration of the mantle wedge play a dominant role. The following conclusions have been made (Gerya et al., 2002):

- Burial and exhumation of high-pressure metamorphic rocks in subduction zones are likely affected by progressive hydration (serpentinization) of the fore-arc mantle lithosphere (e.g., Peacock, 1987b; Schmidt and Poli, 1998). This process controls the shape and internal circulation pattern of a subduction channel. Widening of the subduction channel due to hydration of the hanging wall mantle results in the onset of forced return flow in the subduction channel. This may explain why the association of high- and/or ultrahigh-pressure metamorphic rocks with more or less hydrated (serpentinized) mantle material is often characteristic for high-pressure metamorphic complexes (e.g., Cloos, 1982).
- The shape of the *P–T* path and the maximum *P–T* conditions achieved by an individual high-pressure metamorphic rock depend on the specific trajectory of circulation in the subduction channel (Fig. 6). Both clockwise and counterclockwise *P–T* paths are possible for fragments of oceanic crust that became involved in the circulation. Counterclockwise *P–T* paths are found for slices accreted to the hanging wall at an early stage of subduction (Fig. 6, 6.4 Myr), that are later set free by the progress of hydration and softening in a more evolved stage (Fig. 6, 19.4 Myr), and eventually returned toward the surface in a cooler environment. On the other hand, slices that were involved in continuous circulation, or that entered the subduction zone when a more stable, colder thermal structure was already achieved, reveal exclusively clockwise trajectories.

These conclusions, based on a relatively simple, low-viscosity serpentinized subduction channel model (Fig. 6), were recently supported by petrological studies of subduction related metamorphic complexes (e.g., Federico et al., 2007; Krebs et al., 2008; Blanco-Quintero et al., 2010) on the basis of *P–T*–time paths of high-, and ultrahigh-pressure rocks in serpentinite mélanges. One general conclusion that can be made on the basis of both numerical and petrological studies is that there is not any steady state in subduction zone evolution. This is mainly due to continuous water release from the slab and respective hydration of the overriding plate that always changes the thermal, rheological, and compositional structure of subduction zones through time (e.g., Gerya et al., 2002; Gerya and Yuen, 2003; Krebs et al., 2008; Blanco-Quintero et al., 2010; Gerya and Meilick, 2011). Consequently, thermo-mechanical steady states used in simple models of subduction (e.g., Peacock, 1987a, 1990a,b, 1993, 1996) may not be characteristic of real subduction zones.

It has also been shown recently that ultrahigh-pressure mantle rocks (garnet-bearing peridotites) can also be present in intra-oceanic subduction mélanges (e.g., in Greater Antilles in Hispaniola, Abbott et al., 2006). Gorczyk et al. (2007c) modeled this phenomenon numerically and concluded that exhumation of such garnet-bearing peridotites can be related to fore-arc extension during subduction of an oceanic plate formed at a slow spreading ridge and characterized by serpentinite-rich crust. In this case, the subduction channel contains both serpentinites accreted from the subducting plate crust and progressively serpentinized fore-arc mantle. Intense rheological weakening of the mantle wedge takes place due to its strong hydration during subduction of a water-rich, slow spreading ridge. This weakening triggers upwelling of the hydrated peridotites and partially molten peridotites followed by an upwelling of the hot asthenosphere and subsequent retreat of the subducting slab. According to their numerical modeling of *P–T* paths, this process can explain the exhumation of UHP rocks in an intra-oceanic setting from depths of up to 120 km (4 GPa).

Several 2D numerical thermo-mechanical studies were also conducted for simulating the evolution of high- and ultrahigh-pressure complexes in oceanic-continental subduction (e.g., Stoeckhert and Gerya, 2005; Gerya and Stoeckhert, 2006; Yamato et al., 2007; Babeyko and Sobolev, 2008). Stoeckhert and Gerya (2005) and Gerya and Stoeckhert (2006) studied the evolution of a serpentinized subduction channel and orogenic wedge for an active continental margin, with *P–T* paths being displayed for representative rock units. Stoeckhert and Gerya (2005) demonstrated that four metamorphic zones should develop in such a tectonic setting from the trench into the forearc: (A) an accretionary complex of low grade metamorphic sedimentary material, (B) a wedge of nappes with alternating upper and lower crustal provenance, and minor interleaving of oceanic, or hydrated mantle material, (C) a megascale mélange composed of HP and UHP metamorphic rocks extruded from the subduction channel, and (D) the upward tilted frontal part of the remaining lid. It was also shown (Gerya and Stoeckhert, 2006) that the exhumation rates for ultrahigh-pressure rocks can exceed subduction and burial rates by a factor of 1.5–3, when forced return flow in the hanging wall portion of the self-organizing subduction channel is focused due to a non-linear temperature-dependent rheology. This may explain very rapid exhumation rates recorded for some of the natural subduction complexes (Rubatto and Hermann, 2001). Yamato et al. (2007) analyzed the dynamic processes leading to the exhumation of high-pressure, low-temperature rocks at accretionary margins with application to the well studied Schistes Lustrés complex (Western Alps). After a transition period of 3–5 Ma the modeled accretionary wedge

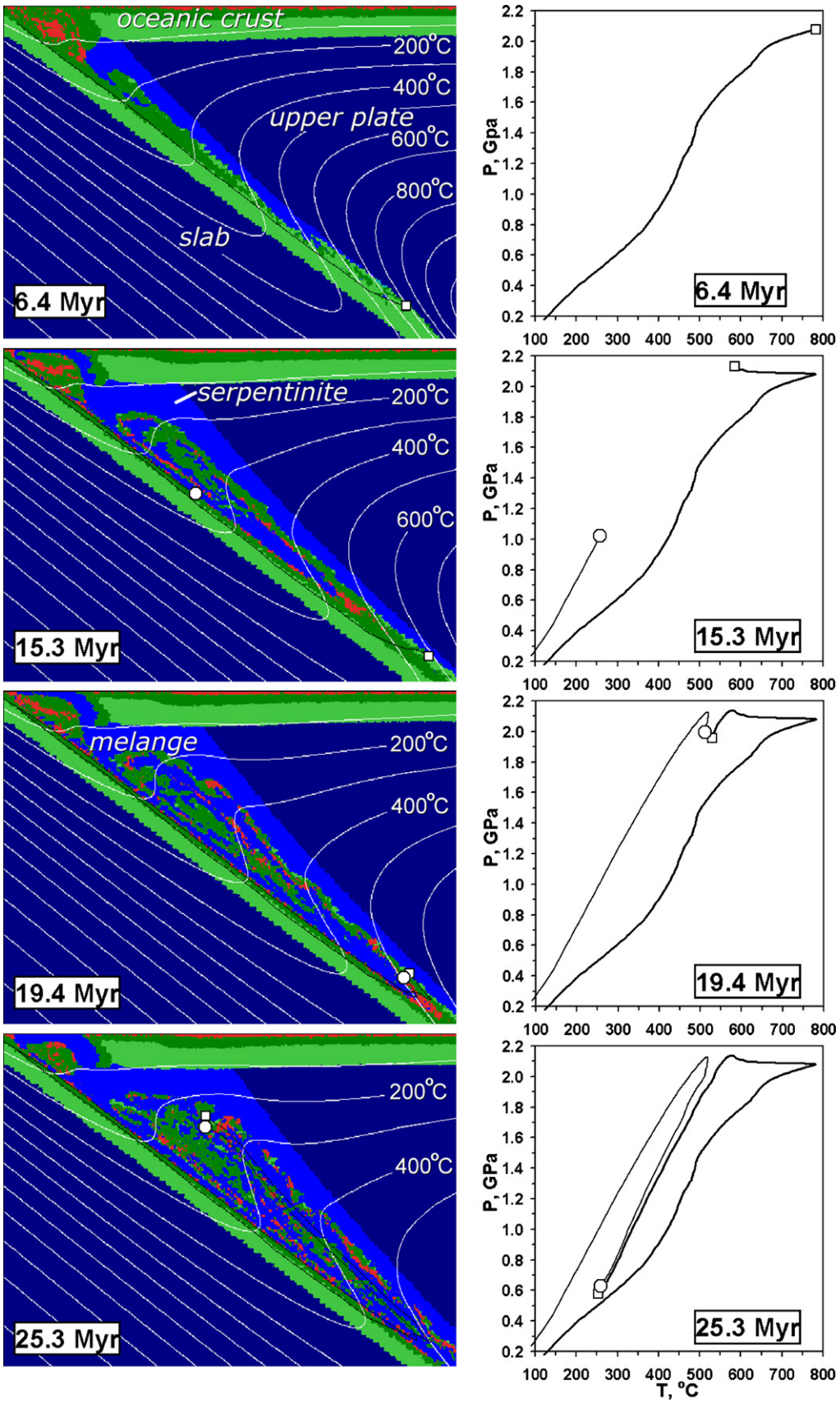

Fig. 6. Numerical model for spontaneous development of weak serpentinized subduction channel during intra-oceanic subduction (Gerya et al., 2002). Left column – development of the lithological field and isotherms (white lines, °C). Right column – development of *P*–*T* paths for two rock fragments (see open circle and open rectangle in the left column).

reaches a steady state which lasts over 20 Ma with *P*–*T* conditions (15–20 kbar; 350–450 °C) and exhumation rates (<6 mm yr^{-1}) typical of the modeled Schistes Lustrés complex. Babeyko and Sobolev (2008) investigated the stress state of the slab and its influence on *P*–*T* paths of subducted rocks at the Andean-type margins. For shallow-dipping slabs, the dominant stress (1–1.5 GPa) is an unbending stress occurring at 50–100 km depth. Unbending creates two (5–10 km distance between maximums) compression zones in the upper part of the slab and a zone of extension some 20–30 km below. Pressure in these zones differs from the lithostatic pressure by as much as ±0.8 GPa, which is enough to notably affect the *P*–*T*–time trajectories of subducted rocks. On the other hand, overpressure in the subduction channel in all models did not exceed 100 MPa. Large over- and under-pressures in the slab do not, however, lead to significant (more than 10 km) offsets of the main dehydration reactions in the crustal and mantle sections of the slab.

Finally, many recent numerical modeling studies have focused on explaining the histories of HP and UHP rocks (Chopin, 2003; Liou et al., 2004) formed during the transition from subduction to collision (e.g., Burov et al., 2001; Gerya et al., 2008b; Warren et al., 2008). Growing evidences from Phanerozoic collision belts has revealed the burial of crustal rocks to depths on the order of 150–200 km and of subsequent exhumation from such depths (e.g., Chopin, 2003 and references therein) within the time scale of shortly before or during the early continental collision (e.g., Liou et al., 2004 and references therein). Burov et al. (2001) presented the first 2D thermo-mechanical numerical model for the formation and exhumation of HP-UHP rocks during continental subduction using an initial setup with pre-subducted continental crust. These models demonstrated that the exhumation of HP and UHP rocks is a complex multi-level process that involves both buoyancy driven flow and forced circulation of rocks at the interface between two colliding plates. Using similar thermo-mechanical models coupled to phase transformation and *P*–*T* paths modeling, Yamato et al. (2008) demonstrated the potential application to the processes of HP-UHP rock exhumation in the Western Alps. Indeed, lowered peak metamorphic temperatures of UHP rocks on the order of 100–150 °C were documented along synthetic *P*–*T* paths compared to natural data (Yamato et al., 2008). Additional 2D models addressed the initiation of continental collision starting from subduction of an intermediate oceanic plate located between two continents (e.g., Faccenda et al., 2008b; Warren et al., 2008; Gerya et al., 2008b; Li and Gerya, 2009). In particular, two contrasting tectonic styles of early continental subduction were identified (Faccenda et al., 2008b; Warren et al., 2008) which are mainly controlled by the degree of rheological coupling between plates (Faccenda et al., 2008b): one-sided subduction (overriding plate does not subduct) (e.g., Burov et al., 2001) and ablative (two-sided) subduction (both plates subduct together) (e.g., Tao and O'Connell, 1992; Pope and Willett, 1998). Significantly, only the one-sided continental subduction was able to produce significant syntectonic UHP rock exhumation (Warren et al., 2008). Warren et al. (2008) subdivided ablative subduction into two regimes (Fig. 7a): double subduction associated with backthrusting of the retro-continental margin (symmetrical ablative subduction, in the case of rheologically weak retro-continental crust) and subduction of the retro-continental margin (asymmetrical ablative subduction, in the case of strong retro-continental crust). For one-sided subduction buoyant uplift, driven cavity flow circulation and plunger-driven expulsion were identified as the major mechanisms of UHP rock exhumation (Warren et al., 2008) (Fig. 7b). Similar to Yamato et al. (2008), lowered peak metamorphic temperatures of UHP rocks (by 100–150 °C) were documented along synthetic *P*–*T* paths compared to natural data (Fig. 7b, left column).

Gerya et al. (2008b) addressed problem of high peak metamorphic temperatures of UHP rocks and demonstrated that this phenomenon may be explained by a transient "hot channel effect" taking place during the transition from subduction to collision. Anomalous high temperatures are caused by intense radiogenic and shear heating in the forming crustal channel, which is composed of deeply subducted radiogenic upper-crustal rocks (especially, sediments of passive margin origin) and mantle rocks. Heating is associated with partial melting of crustal rocks due to pervasive flow of aqueous fluids. The fluids are released by rapid dehydration (deserpentinization) from the overriding mantle lithosphere, which was hydrated during earlier subduction stages. The channel penetrates the plate interface to the bottom of the overriding plate lithosphere (150–200 km) and is characterized by metamorphic temperatures reaching 700–900 °C. The hot channel exists only during early collision, but rapidly produces large amounts of ultrahigh-pressure and high-temperature rocks. Further collision closes the channel by squeezing rheologically weak, partially molten, buoyant rocks between the strong lithospheric mantles of the two colliding plates. Assemblages of complicated *P*–*T* paths with repetitive loops characterize exhumation of ultrahigh-pressure rocks in the convoluted flow pattern of the hot channel. Li and Gerya (2009) demonstrated that sub-lithospheric crustal plume formation may also produce high-temperature UHP rocks and identified an inherent periodicity of rock exhumation during the early continental subduction process. Numerical models suggested that subducted UHP rocks which are positively buoyant compared to the mantle, may detach from the slab, forming a flattened plume underplating the overriding lithosphere (Fig. 7b, middle column). This sub-lithospheric plume may persist for several million years as it is heated to 800–900 °C by the surrounding hot mantle. At a later stage, upward extrusion of hot partially molten rocks from the plume may exhume high-temperature (HT) UHP complexes toward the surface. Crustal structures created by such UHP plumes were identified from geological and petrological record (Li and Gerya, 2009; Beaumont et al., 2009). The influence of non-lithostatic pressure on *P*–*T* paths of HP-UHP rocks in continental subduction/collision zones was also modeled numerically (Burov and Yamato, 2008; Gerya et al., 2008b; Li et al., 2010).

Future studies of metamorphic rock histories in subduction zones are likely to be directed toward testing numerical models with natural data (e.g., Federico et al., 2007; Yamato et al., 2007; Krebs et al., 2008) and conducting "modeling-inspired" observational studies related to the non-trivial and somewhat counter-intuitive predictions generated by numerical models (e.g., repetitive *P*–*T* loops of subducted rocks in internally convecting subduction channels, Gerya and Stoeckhert, 2006; Blanco-Quintero et al., 2010). Methodological advances will likely include development of high-resolution regional 3D models with realistically implemented surface processes (e.g., Braun and Yamato, 2010) which will be able to address the lateral variability of subduction related metamorphic rock complexes.

5. Small-scale convection and thermal–chemical plumes in the mantle wedge

It is commonly accepted that dehydration of subducting slabs and hydration of the overlying mantle wedges are the key processes controlling magmatic activity and consequently crustal growth above subduction zones (e.g., Stern, 2002; van Keken et al., 2002; Van Keken and King, 2005). Mantle wedge processes have been investigated from geophysical (e.g., Zhao et al., 2002; Tamura et al., 2002), numerical (e.g., Davies and Stevenson, 1992; Iwamori, 1998; Kelemen et al., 2004; Arcay et al., 2005; Gerya et al., 2006; Nikolaeva et al., 2008), experimental (e.g., Poli and Schmidt, 1995, 2002; Schmidt and Poli, 1998), and geochemical (e.g., Ito and Stern, 1986; Sajona et al., 1996, 2000; Kelley et al., 2006; Kimura et al., 2009)

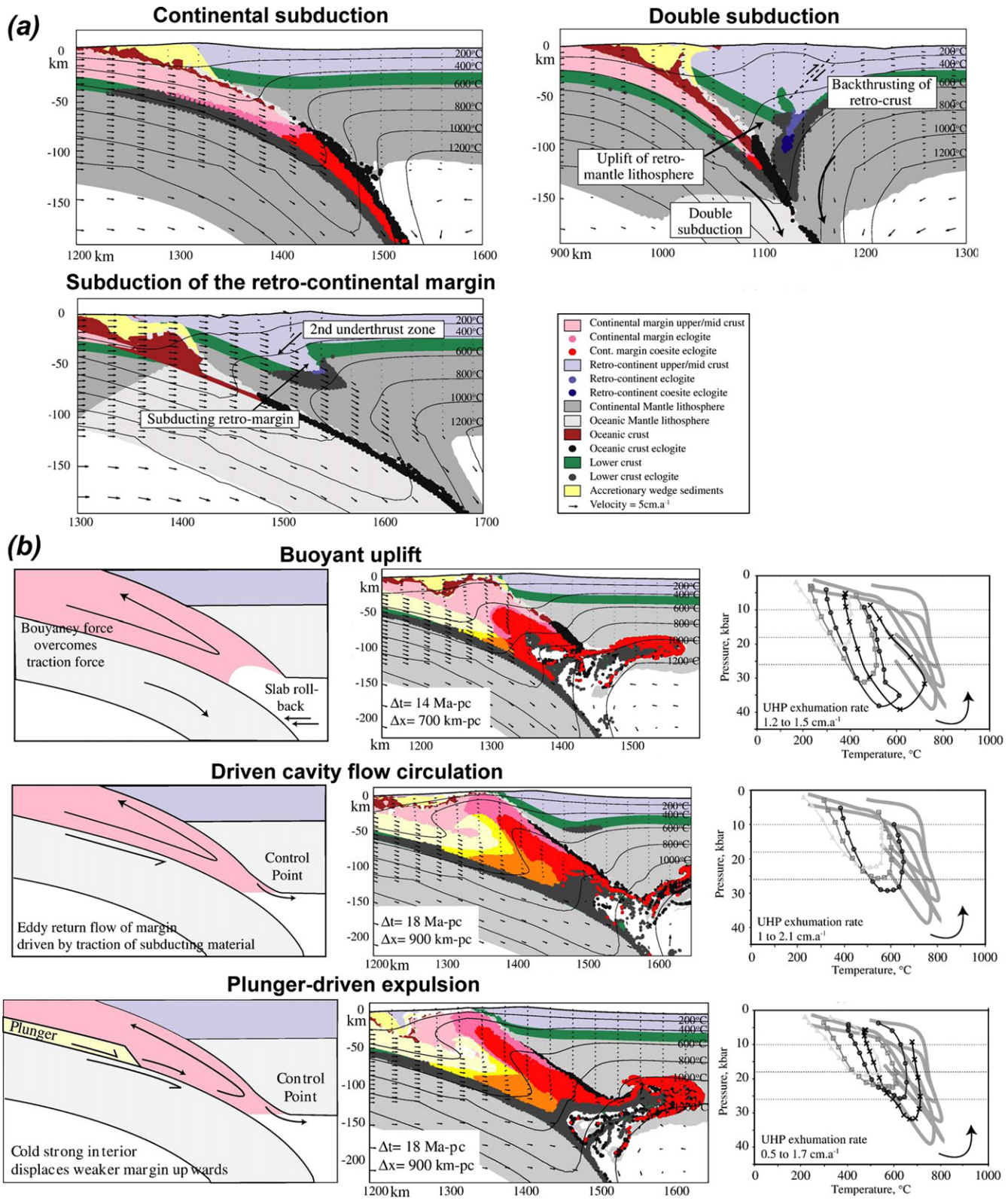

Fig. 7. Numerical models for post-subduction continental collision (Warren et al., 2008). (a) Three geodynamic regimes of collision identified in numerical experiments: continental subduction (one-sided subduction), subduction of retro-continental margin (asymmetrical ablative subduction) and double subduction (symmetrical ablative subduction). (b) Three major mechanisms of rock exhumation during the one-sided subduction regime (left and middle columns) and computed *P*–*T* paths for UHP rocks (right column, lines with symbols) compared to natural data (thick grey lines without symbols). Δt and Δx in the middle column of (b) are the time lag and amount of convergence "post-collision" (pc), defined as the time at which the leading edge of the continental margin first enters the collision zone. Horizontal lines at 10, 18 and 26 kbar in the right column of (b) indicate the pressures at amphibolite, eclogite and coesite–eclogite facies conditions, respectively.

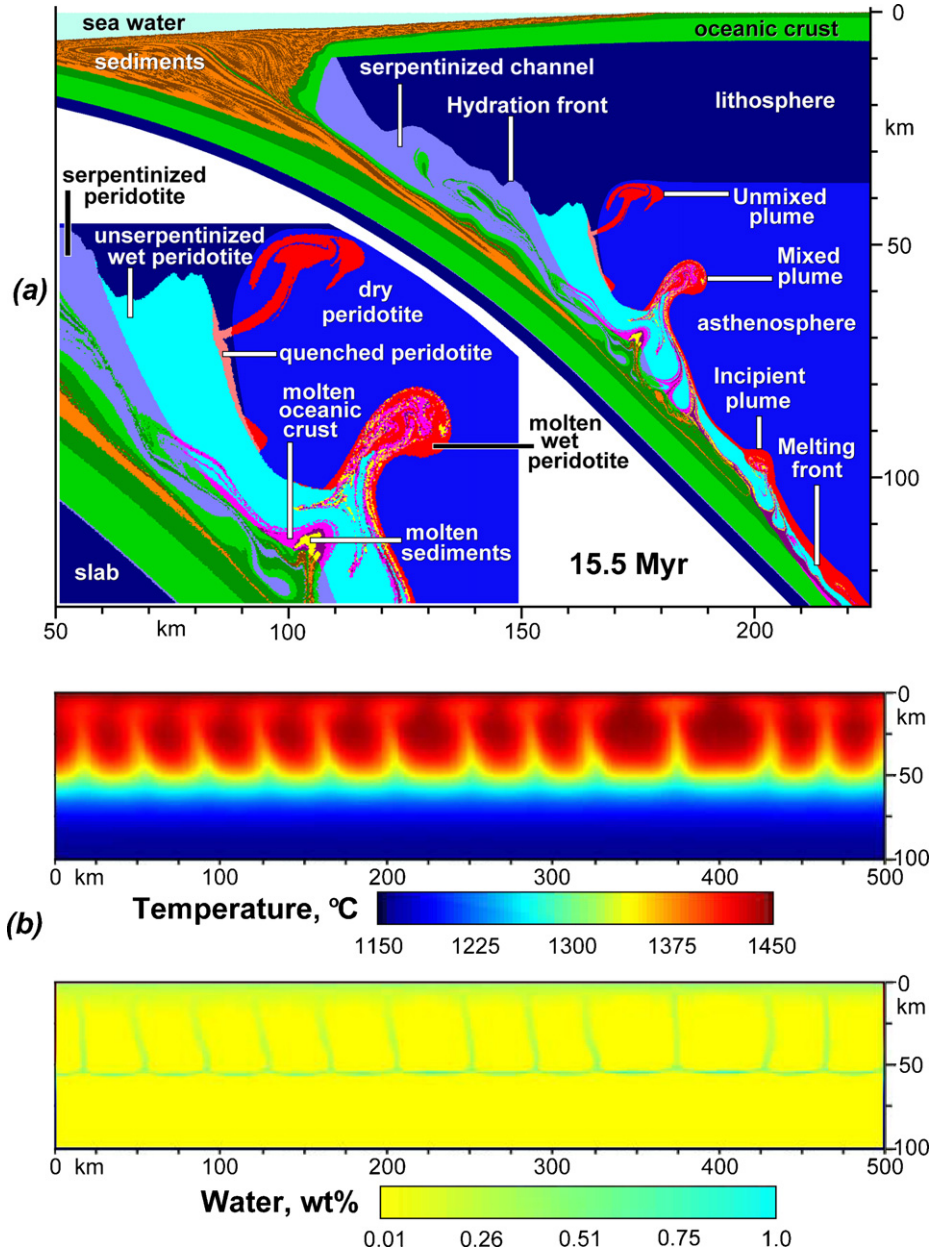

Fig. 8. Examples of 2D numerical models of thermal-chemical plumes rising from subducting slabs. (a) Model by Gerya et al. (2006), two types of plumes develop from the slab: (i) unmixed plumes composed of hydrated partially molten mantle and (ii) mixed plumes composed of tectonic mélange from partially molten hydrated crustal and mantle rocks. (b) Model by Richard and Bercovici (2009), section across the floating slab in the transition zone is modeled, note negative temperature anomaly associated with chemically buoyant water-rich plumes rising from the slab.

perspectives. However, the detailed circulation patterns, thermal structure and melt production distribution above slabs remains puzzling. Particularly, the relative importance of slab melting (e.g., Kelemen et al., 2004; Nikolaeva et al., 2008; Syracuse et al., 2010) versus melting induced by simple thermal convection (Honda et al., 2002; Honda and Saito, 2003; Honda et al., 2007) and/or thermal–chemical plumes (Figs. 8 and 9) (e.g., Tamura, 1994; Hall and Kincaid, 2001; Obata and Takazawa, 2004; Gerya and Yuen, 2003; Manea et al., 2005; Gerya et al., 2006; Gorczyk et al., 2007b; Zhu et al., 2009) to melt production in volcanic arcs is not fully understood.

Several authors (e.g., Tamura et al., 2002; Honda et al., 2007; Zhu et al., 2009; van Stiphout et al., 2009) analyzed the spatial distribution of volcanism in Japan and Alaska and concluded that several clusters of volcanism can be distinguished in space and time. The typical spatial periodicity of such volcanic clusters is 50–100 km, while their life extent corresponds to 2–7 Myr. Two trench-parallel lines of volcanic density maxima can also be distinguished for some periods of arc evolution. Spatial and temporal clustering of volcanic activity is also associated with a strongly variable crustal thickness distribution along arcs (e.g., Kodaira et al., 2006, 2007) and lateral seismic velocity anomalies changes in the mantle wedges under volcanic arcs (e.g., Zhao et al., 1992, 2002; Zhao, 2001; Tamura et al., 2002; Nakajima and Hasegawa, 2003a,b; van Stiphout et al., 2009). This further points toward a relationship between the mantle wedge processes and crustal growth in intra-oceanic arcs.

Davies and Stevenson (1992) pioneered modeling of thermal–chemical convection in the mantle wedge by using a relatively simple model with a kinematically prescribed slab and an imposed localized source of positive buoyancy (melt, residue, etc.) in the mantle wedge. Estimates of the buoyancy sources and appropriate viscosity in the wedge suggested that only a weak

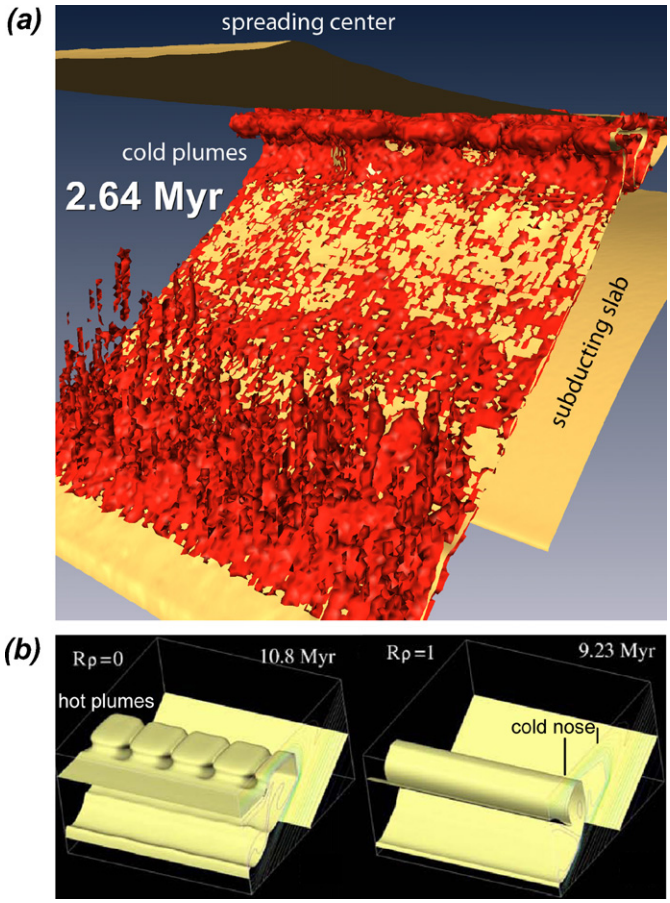

Fig. 9. Examples of 3D numerical models of plumes in the mantle wedge. (a) Model by Zhu et al. (2009), the 1077 °C isosurface of temperature (yellow) with partially molten hydrated rocks (red), which are responsible for plume buoyancy, note two trench-parallel lines of plumes that develop from the slab at different depths. (b) Model by Honda et al. (2010), finger-like (left) and sheet-like (right) patterns of convection in the mantle wedge depending on the chemical/thermal buoyancy ratio ($R\rho$), the 1000 °C isosurface of temperature (yellow) is shown).

modulation of the slab-induced flow is likely unless the slab and wedge are locally decoupled, for instance by shear heating, the presence of water or dehydration/hydration reactions. If there is decoupling, then it is possible for there to be an appreciable reversal of the slab-induced flow. Such an appreciable reversal of flow, if it persists, leads to cooling of the mantle wedge. Hence flow reversal cannot be a steady state mechanism. Instead it would lead to melting cycle with a period of O (1 Myr). The time dependence of a model with appreciable flow reversal would be reinforced by the need to clear the wedge of infertile material.

Based on 3D numerical models Honda and co-workers (Honda et al., 2002, 2007; Honda and Saito, 2003; Honda and Yoshida, 2005) proposed the development of small-scale thermally driven convection in the uppermost corner of the mantle wedge with lowered viscosity (low viscosity wedge, LVW, Billen and Gurnis, 2001; Conder and Wiens, 2007; Honda and Saito, 2003; Honda et al., 2002; Honda and Yoshida, 2005; Arcay et al., 2005) and suggested that a roll (finger)-like pattern of hot (upwellings) and cold (downwellings) thermal anomalies emerges in the mantle wedge above the subducting slab (Fig. 9b, left), contributing to clustering of magmatic activity at the arc surface. These purely thermal mantle wedge convection models, however, neglected chemical buoyancy effects coming from hydration and melting atop the subducting slab, which are known to lead to thermal–chemical convection and diapirism (e.g., Tamura, 1994; Davies and Stevenson, 1992; Hall and Kincaid, 2001; Gerya and Yuen, 2003).

Gerya and Yuen (2003) developed a 2D thermo-mechanical model of thermal–chemical convection in the mantle wedge taking into account spontaneous mantle hydration and melting due to fluid propagation from the slab. It was demonstrated that hydration and partial melting along the slab creates a situation where Rayleigh–Taylor instabilities can develop at the top of a cold subducting slab. This resulted in rather paradoxical thermo-mechanical phenomenon, in which rising diapiric structures, colder than the asthenosphere by 300–400 °C, are driven upward by compositional buoyancy (Fig. 8). These "cold plumes" with a compositional, hydrous origin, launched from asthenospheric depths, remained lubricated by viscous heating and maintained an upward velocity in excess of 10 cm/yr. On account of this upward velocity, the "cold plumes" are able to penetrate the relatively hot asthenosphere in the mantle wedge within a couple of million years and thus can cool the surrounding material. These "cold plumes" are fueled by partial melting of the hydrated mantle and subducted oceanic crust due to fluid released from dehydration reactions within the slab, including the decomposition of serpentine. Later, Gerya et al. (2004a) also identified another type of similar thermo-mechanical phenomena—"cold waves", which are wave-like structures propagating upward along descending slabs and consisting of compositionally buoyant, hydrated and partially molten subducted crustal and mantle material. These wave structures are 300–500 °C colder than the mantle wedge and may have an upward velocity of >1 m/yr due to the reduced viscosity of hydrated zone along the top of the slab.

Recently, chemical buoyancy aspects have further been studied numerically based on 2D (Fig. 8) and 3D (Fig. 9) thermo-mechanical models including water transport and melting. These models predicted

(i) Spontaneous formation of a low viscosity wedge by hydration of the mantle atop the slab (Arcay et al., 2005; Zhu et al., 2009).
(ii) The presence of two distinct chemical types of plumes (Fig. 8a) in the mantle wedge (Gerya et al., 2006): (A) mixed plumes consisting of partially molten mantle, recycled oceanic crust and sediments and (B) unmixed plumes made of hydrated partially molten mantle.
(iii) Underplating of the overriding plate by sedimentary plumes, which is controlled by the thickness and rheology of the sedimentary layer subducted atop the slab (Currie et al., 2007).
(iv) Broad variations in the 3D geometry of thermal chemical plumes atop slabs: (A) finger-like plumes that form sheet-like structure parallel to the trench (Fig. 9a); (B) ridge-like structures perpendicular to the trench; (C) flattened wave-like instabilities propagating upwards along the upper surface of the slab and forming zig-zag patterns subparallel to the trench (Zhu et al., 2009, 2011).
(v) Large-scale rigid body rotation phenomena in subduction zones due to inhomogeneous hydration and cooling of the mantle wedge (Gorczyk et al., 2006; Nikolaeva et al., 2008).
(vi) Broad variations in seismic velocity beneath intraoceanic arcs due to hydration and melting (Gerya et al., 2006; Gorczyk et al., 2006; Nikolaeva et al., 2008).
(vii) Variations in melt production and crustal growth processes caused by propagation of hydrated plumes in the mantle wedge (Gorczyk et al., 2007b; Nikolaeva et al., 2008; Zhu et al., 2009).
(viii) Suppression of 3D thermal instabilities in the mantle wedge by low density chemical anomalies originating from downgoing slabs slab (e.g., due to hydration) and instead stabilization of thermal–chemical plumes and/or an internally convecting chemically buoyant "cold nose" (Fig. 9b, right) in the upper corner of the mantle wedge (Honda et al., 2010).

Richard and Bercovici (2009) have recently investigated the consequences of deep dehydration of subducted slabs for mantle convection based on 2D thermo-mechanical models including water diffusion (Fig. 8b). The consequences of water exchange between a floating slab and the transition zone were investigated, with a particular focus on the possible onset of small-scale thermal–chemical convection, despite the adverse thermal gradient (i.e., mantle is cooled from below by the slab). The competition between thermal and hydrous effects on the density and thus on the convective stability of the top layer of the slab were examined numerically, including water-dependent density and viscosity and temperature-dependent water solubility. It was concluded that for plausible initial water content in a slab ($\geq$0.5 wt%), an episode of convection is likely to occur after a relatively short time delay (5–20 Ma) after the slab enters the transition zone. However, water induced rheological weakening is seen to be a controlling parameter for the onset time of convection. Moreover, small-scale thermal–chemical convection above a stagnant slab greatly enhances the rate of slab dehydration. This small-scale convection also facilitates heating of the slab, which in itself may prolong the residence time of the slab in the transition zone.

Further investigations of thermal–chemical, mantle wedge convection will likely involve broadening the 3D modeling approaches and theoretical understanding of the variability of modeled plume morphologies in the mantle wedge (e.g., Zhu et al., 2009, 2011; Honda et al., 2010). Further progress in understanding the relative significance of thermal and chemical components of mantle wedge convection will likely require the implementation of more sophisticated fluid and melt transport algorithms (e.g., Iwamori, 1998, 2007; Connolly and Podladchikov, 1998; Rozhko et al., 2007) that may help to better quantifying the actual magnitude of chemical buoyancy present above slabs in nature.

6. Crustal growth and magmatic arc development

Reymer and Schubert (1984) estimated crustal generation rates of 20–40 km^3/km/Myr for the western Pacific region during intra-oceanic subduction based on the total arc crust volume divided by the oldest known igneous age. More recent estimates for the same area by (Stern and Bloomer, 1992) (early stage of IBM development), Taira et al. (1998) (Izu-Bonin island arc), Holbrook et al. (1999) (Aleutian island arc), and Dimalanta et al. (2002) (Tonga, New Hebrides, Marianas, Southern and Northern Izu-Bonin, Aleutian island arcs) are much higher and range from 40–95 km^3/km/Myr to 120–180 km^3/km/Myr. These values are average rates of crust production, calculated by dividing the estimated total volume of generated crust by the time in which it was produced and by the length of the arc.

Numerical modeling of crustal growth in the arc is relatively rare. Nikolaeva et al. (2008) investigated crustal growth processes on the basis of a 2D coupled petrological-thermo-mechanical numerical model of retreating intra-oceanic subduction (Fig. 10). The model included spontaneous slab retreat and bending, subducted crust dehydration, aqueous fluid transport, mantle wedge melting, and melt extraction resulting in crustal growth. From the numerical experiments, the rate of crust formation was found to be strongly variable in time and positively correlated with the subduction rate (Fig. 10, bottom diagram). Modeled average rates of crustal growth (30–50 km^3/km/Ma, without effects of dry decompression melting) are close to the lower edge of the observed range of rates for real intra-oceanic arcs (40–180 km^3/km/Ma). The composition of new crust depends strongly on the evolution of subduction. Four major magmatic sources can contribute to the formation of the crust: (1) hydrated partially molten peridotite from the mantle wedge, (2) melted subducted sediments, (3) melted subducted basalts, (4) melted subducted gabbro. Crust produced from the first source is always predominant and typically comprises more than 95% of the growing arc crust (Nikolaeva et al., 2008). In all studied cases, this source appears shortly after beginning of subduction and is a persistent component while subduction remains active. Significant amounts of crust produced from the other three sources appear; (1) in the beginning of subduction due to the melting of the slab "nose" and (2), at later stages when subduction velocity is low (<1 cm/a), which leads to the thermal relaxation of the slab. Both the intensity of melt extraction and the age of the subducted plate affect the volume of generated crust. On a long time scale the greatest volume of magmatic arc crust is formed with an intermediate melt extraction threshold (2–6%) and medium subducted plate ages (70–100 Ma) (Nikolaeva et al., 2008).

Zhu et al. (2009, 2011) examined 3D thermal–chemical mantle wedge convection and related melt production dynamics during intra-oceanic subduction. These numerical experiments focused on the geometries and patterns of hydrous thermal–chemical upwellings ("cold plumes") formed above the slab (Fig. 9a) and their consequences for melt production. The computed spatial and temporal patterns of melt generation (i.e., crust production) intensity above the slab appear to be strongly controlled by the hydrous plume activities. Peaks of the melt production projected to the arc surface at different times always indicate individual thermal–chemical plumes growing at the same time. Such peaks often form a linear structure close to the trench and another line of peaks in a linear pattern approximately 200 km away from the trench (Fig. 9a). The peaks close to the trench are from depths of 50–70 km and the second peaks are from depths of 140–170 km. The plume-like structures are reflected by distinct melt productivity maxima that are bounded in both time and space. Each maximum corresponds to the activity of a distinct plume that; (1) increases the melt productivity during the early stage when the growing melt production is related to decompressing and heating of the rising plume material and (2), decreases the melt productivity during the later stage when the temperature, pressure and the degree of melting stabilize inside the horizontally spreading and thermally relaxing plume. The modeled wavelength (25–100 km) and the growth time (2–7 Myr) of the thermal–chemical plumes are comparable to spatial periodicity (50–100 km) and the life extent (2–7 Myr) of volcanic clusters, and to the spatial periodicity (50–100 km) of crustal thickness variations in intra-oceanic arcs (e.g., Zhu et al., 2009; Kodaira et al., 2006, 2007). The existence of two contemporaneous trench-parallel lines of melt productivity (Fig. 9a) is also similar to natural observations (e.g., Wyss et al., 2001; Kimura and Yoshida, 2006; Zhu et al., 2009).

Gerya and Meilick (2011) analyzed 2D crustal growth at active continental margins (Fig. 1b) by including volcanic additions from both fluid flux and decompression melting and by analyzing subduction accretion/erosion processes. In these models the volcanic crustal growth rates are strongly variable in time and depend on the presence/absence of back-arc spreading. Rates of crust accumulation in models without back-arc spreading typically vary from 0 to 60 km^3/km/Myr, where the main magmatic addition is given by flux melting products (hydrated mantle and subducted crust). This estimate is comparable to the results of Nikolaeva et al. (2008), who did not take into account decompression melting. In contrast, in the case of back-arc spreading center formation, crustal growth rates may reach 200 km^3/km/Myr. This is mainly due to a strong contribution from decompression melting of dry mantle which creates new oceanic crust around the forming back-arc spreading center. The average crustal production rate calculated for the model with back-arc spreading was 97.5 km^3/km/Myr, which includes decompression melting products (MORB-type crust) formed in the new spreading center. Thus, the crustal addition rate is rather overestimated since the production of new oceanic floor is typically not

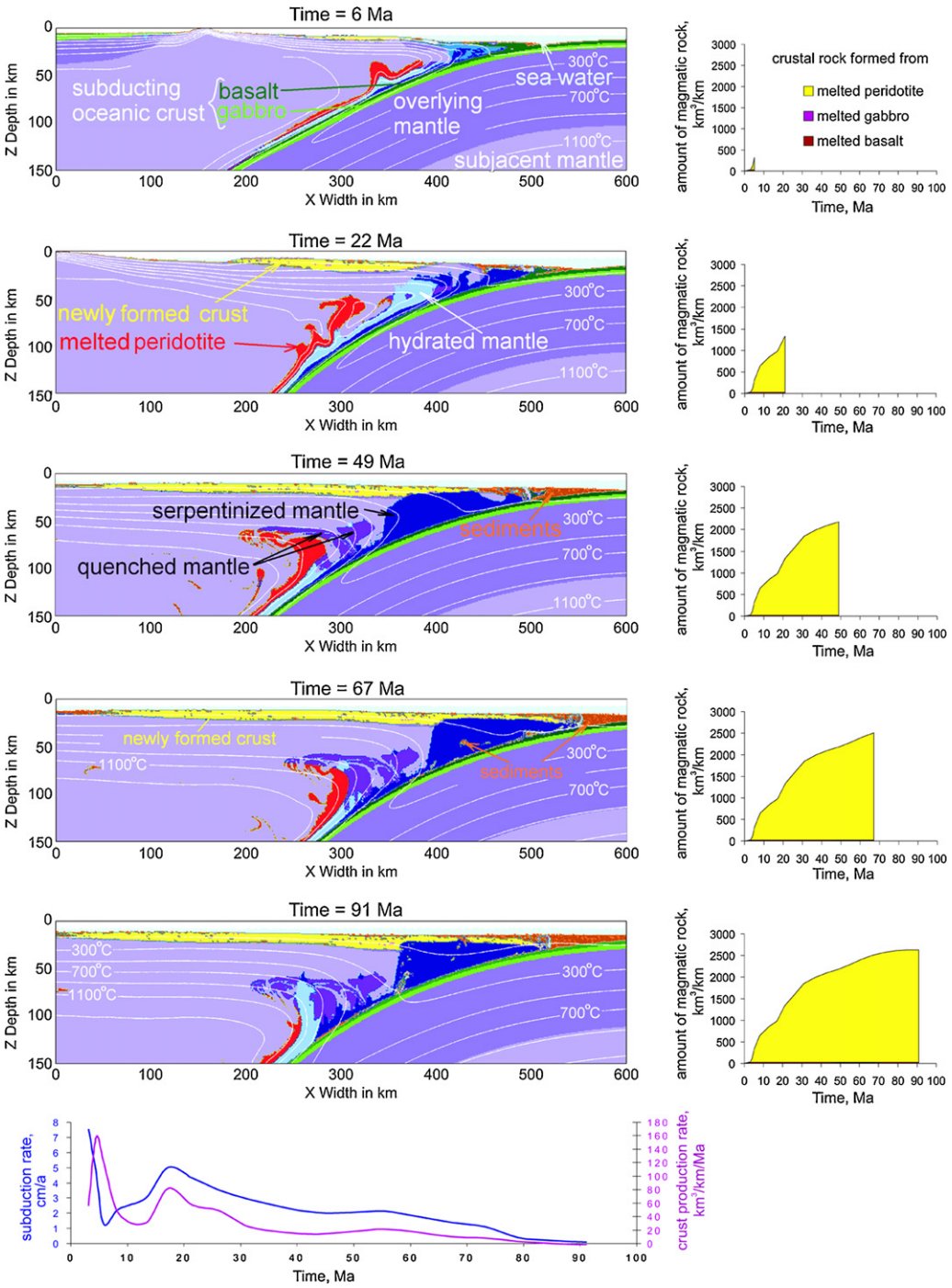

Fig. 10. Numerical model for intra-oceanic arc development (Nikolaeva et al., 2008). Dynamics of a pure retreating intra-oceanic subduction (left column) and associated magmatic crust growth (right column). Spontaneous changes in subduction rate and crust accumulation rate with time are depicted below. Decompression melting of dry mantle was neglected in this model.

included in calculations of crustal production rates in natural volcanic arcs. If the crust produced by dry melting is fully excluded, an average crust production rate of 45.9 km^3/km/Myr is obtained in the model with back-arc spreading. Indeed, dry decompression melting in nature also contributes to the formation of magmatic arcs close to the back-arc region where the amount of water in the source region is considerably smaller (e.g., Kelley et al., 2006). In this model, the region was represented by the inter-layered flux melting and decompression melting products. Therefore, the actual value of crustal growth rate in these models is in between two marginal estimates of 97.5 and 45.9 km^3/km/Ma, and is thus quite comparable to nature (e.g., Dimalanta et al., 2002). In the same series of 2D experiments, the amount of subduction accretion and erosion was mainly dependent on fluid-related rheological weakening of the forearc. Larger fluid weakening effects result in weaker sediments that tend to decouple from the plate, stack up and remain at the surface, rather than be subducted with the slab. In contrast, smaller fluid weakening effects favor a higher rheological strength of sediments, which enhances subduction erosion and reduces the size of the accretion wedge. In general, three regimes of sedimentary wedge dynamics were found in the models: (1) subduction accretion regime (strong weakening of the forearc by fluids)—sediment

accretion dominates and a large accretionary wedge is built with time; (2) balanced accretion/erosion regime (moderate weakening by fluids)—accretion and erosion of sediments tend to compensate each other and the accretionary wedge size remains stable; (3) subduction erosion regime (small/no weakening by fluids)—sediments are eroded by the subducting slab and the sedimentary wedge gradually disappears.

Recently, Kimura et al. (2009) incorporated results from thermo-mechanical subduction models that simulate the geochemical variability of primitive magmas across an intra-oceanic arc. The geochemical variability arises from partitioning of incompatible elements and Sr–Nd–Pb isotopic compositions in slab-derived fluids and in arc basaltic magma generated by an open system fluid-fluxed melting of mantle wedge peridotite. Based on these simulations, contrasting geochemical behavior has been shown between arcs along the Western and Eastern Pacific rims. Arc magmatism due to slab-derived fluids is proposed for the Western Pacific arcs, including the Kurile, NE Japan, and the Izu–Bonin–Mariana arcs. In contrast, slab melting better explains the origin of high-MgO intermediate lavas in the Eastern Pacific, although the role of slab fluids remains an important factor in some of the arcs.

Another key issue of the crustal growth processes is the composition of the forming continental crust. The Earth's continents are mostly composed of igneous and meta-igneous rocks, that on average, yield an andesite composition (e.g., Taylor and McLennan, 1985; Rudnick and Gao, 2003) that is not in equilibrium with the underlying peridotite mantle (Rudnick, 1995). The broadly accepted hypothesis (Ringwood and Green, 1966; Herzberg et al., 1983) suggests that igneous processes can lead to crustal differentiation by lower crustal foundering. This foundering hypothesis contends that mantle-derived basaltic magma intrudes into the crust and forms a buoyant differentiate that is retained in the crust, plus a dense, olivine- and pyroxene-rich residue that sinks into the mantle. However, a less popular alternative model also exists, based on the arrival of an already-fractionated magma of andesitic composition (Taylor, 1967). Recently, this model was supported by a combination of numerical modeling of subduction with high-pressure laboratory experiments, suggesting that melting of subducted mélanges in rising thermo-chemical plumes and hybridization with the mantle peridotite may form voluminous silicic magmas atop subducting slabs (Castro and Gerya, 2008; Castro et al., 2010). These magmas are added to the bottom of magmatic arcs in the form of large batholitic intrusions that are subjected to magmatic fractionation processes (Castro and Gerya, 2008; Castro et al., 2010; Gerya and Meilick, 2011). A somewhat similar idea of continental crust differentiation by relamination was recently developed by Hacker et al. (2011). According to this hypothesis, subducted mafic rocks may sink into the mantle after converting into eclogite, whereas more silica-rich rocks are transformed into felsic gneisses that are less dense than peridotite but more dense than the upper crust. These more felsic rocks rise buoyantly, undergo decompression melting and melt extraction, and are relaminated to the base of the crust. As a result of this process, such felsic rocks could form much of the lower crust (Hacker et al., 2011). Indeed, the processes of magmatic fractionation of various magmas in arcs are not yet well addressed in numerical models and thus their inclusion represents one of the most challenging tasks for the future work.

It is expected in the future that crustal growth processes in magmatic arcs will attract a more systematic effort from the numerical modeling community. The progress in this direction will likely depend on the development of more sophisticated crustal growth models including subduction accretion and erosion, fluid fluxed and decompression melting in the wedge (e.g., Gerya and Meilick, 2011) and plutonic and volcanic addition of melts to the arc crust subjected to magmatic differentiation processes. Modeling predictions will be validated against the growing volume of geophysical, geochemical and geological data on the spatial and temporal variations in magmatic arc structure. Coupled geochemical-thermo-mechanical modeling will be developed in order to correlate (e.g., Kimura et al., 2009) crustal growth processes with the abundant amount of geochemical data available for magmatic arc crust.

7. Overriding plate dynamics

Natural observations demonstrate the complex dynamics of overriding plates, which involve both extension and shortening episodes that significantly affect the topography and geometry of subduction zones worldwide (e.g., Leat and Larter, 2003; Stern, 2002; Sobolev and Babeyko, 2005). In particular, the development and evolution of back-arc basins represents a fundamental process of plate tectonics, many aspects of which remain unexplained. Part of the enigmatic nature of back-arc basins is that while they form at convergent plate boundaries, they represent extensional processes, in contrast to the overall pattern of convergence. Even after extensional stresses generated from trench rollback (and retrograde migration of their associated slabs) were identified as the likely origin of back-arc basins (Dvorkin et al., 1993; Faccenna et al., 1996; Jolivet et al., 1994), the exact mechanism controlling back-arc rifting is still not apparent. In addition, a recent kinematic synthesis of the evolution back-arc basins in the Pacific Ocean during the past 60 Myr (Sdrolias and Müller, 2006) revealed a large amount of periodicity. The distribution of sea-floor ages in this study suggests that extension alternates with phases of tectonic quiescence or compression. Similar arguments can be made for observations related to orogenesis, that the state of mountain building is determined by the trench velocity, and whether it is advancing toward the overriding plate or retreating from it (Lister et al., 2001).

Several numerical studies have been performed to address the influence of overriding plate dynamics on subduction process (e.g., Van Hunen et al., 2000, 2004; Sobolev and Babeyko, 2005; Clark et al., 2008; Gerya and Meilick, 2011). An early prominent study (Van Hunen et al., 2000, 2004) demonstrated that active horizontal movement of the overriding plate toward the subducting slab (i.e., obduction) notably flattens the subducting slab angle (Fig. 11a) at shallow depths (as observed today under parts of the west coast of North and South America) and can also explain the subduction of young oceanic lithosphere. This influence is clearly expressed by the ratio of the subduction velocity to the overriding plate velocity. Another important, regional numerical modeling study by Sobolev and Babeyko (2005) investigated the factors controlling the intensity of tectonic shortening of the overriding South American plate, in relation to the Andean orogeny (Fig. 11b). A coupled thermo-mechanical numerical modeling technique was used to identify that the most important factors were (i) accelerated westward drift of the South American plate toward the subducting Nazca plate, (ii) crustal structure of the overriding plate and (iii) degree of shear coupling at the plate interface (Sobolev and Babeyko, 2005). Models with a thick (40–45 km at 30 Ma) South American crust and relatively high friction coefficient (0.05) at the Nazca–South American interface generate around 300 km of tectonic shortening during 30–35 Myr and replicate the crustal structure and evolution of the high central Andes. On the other hand, models with an initially thinner (~40 km) continental crust and lower friction coefficient (~0.015) results in only ~40 km of South American plate shortening, replicating the situation in the Southern Andes.

Arcay et al. (2005) investigated thermal–chemical thinning of the overriding plate caused by water release from the subducting slab (Fig. 4b). In subduction zones, many observations indicate

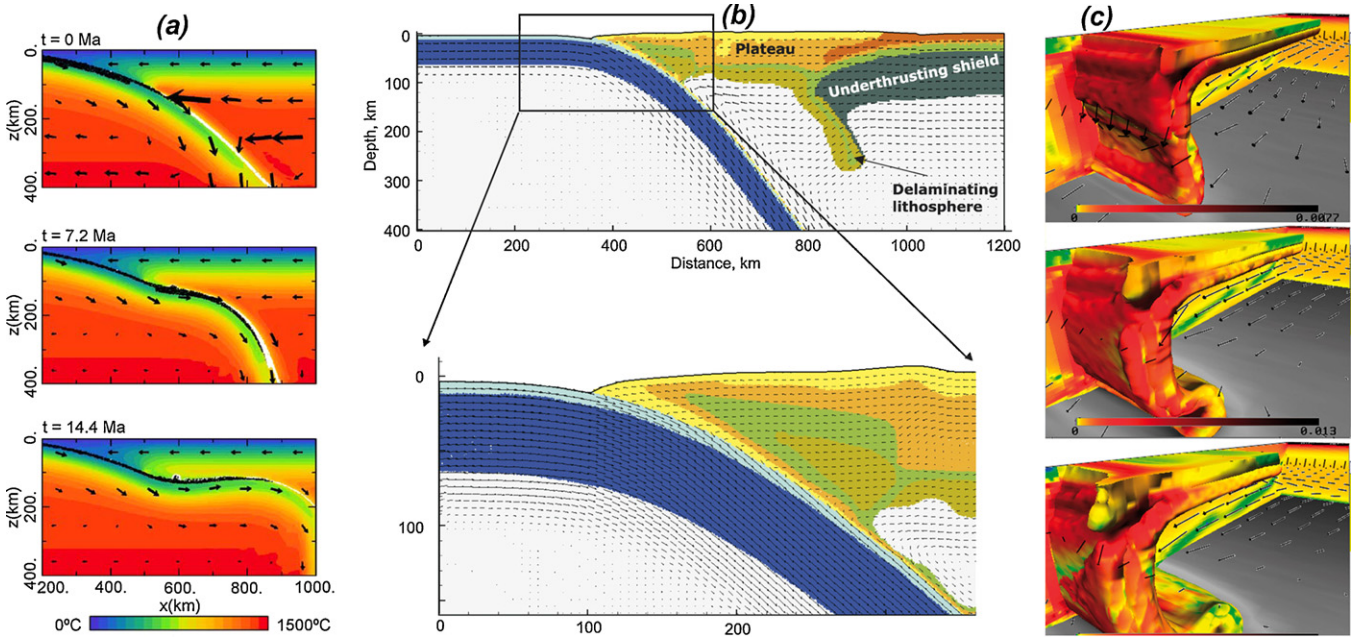

Fig. 11. Examples of numerical models used for investigation of dynamics of the overriding plate. (a) 2D model by Van Hunen et al. (2004) for flat subduction caused by active horizontal movement of the overriding plate toward the slab. (b) 2D model by Sobolev and Babeyko (2005) and Babeyko and Sobolev (2008) for tectonic shortening of the overriding plate during Andean subduction and orogeny. (c) 3D model by Clark et al. (2008) for hyper-episodic regime of subduction (the combination of advancing and retreating trench motions).

that the back-arc thermal state is particularly hot and that the upper lithosphere is thin, even if no recent period of extension has occurred. Based on 2D experiments, Arcay et al. (2005) suggested that this might result from free thermal convection favored by low viscosities in the hydrated mantle wedge. For low strength reductions associated to water content, the upper plate is locally thinned by enhanced corner flow. For larger strength reductions, small convection cells rapidly thin the upper plate (in less than 15 Myr) in the region of the overriding lithosphere hydrated by slab-derived water fluxes. As a result, the thinned region location depends on the subducting plate thermal state, which increases with high convergence rates and low subduction dip angles. The experiments also showed that the thinning process is not influenced by the corner flow. The lithospheric erosion mechanism identified in these simulations explained the characteristic duration of erosion as a function of the hydrous strength reduction. It was found that the presence of amphibole in the upper lithosphere in significant proportions is required down to a temperature of about 980 °C (corresponding to an initial depth of 70 km) to strongly decrease the strength of the base of the lithosphere and trigger rapid erosion (<15 Myr). Recently, Arcay et al. (2008) also applied their thermal–chemical erosion model to investigations of back-arc strain in subduction zones. Their modeling confirmed a statistical, kinematic relationship based on natural observations (Lallemand et al., 2008) between the subducting and overriding plate velocities, which describes the transition from extensional to compressive stresses in the arc lithosphere. Furthermore, high overriding plate velocities toward the trench promoted shallow flat subduction, which was also the case in the experiments of Van Hunen et al. (2000, 2004). However, it remains arguable whether or not the hydration-related erosion of the overriding plate predicted by Arcay et al. (2006, 2008) will be precluded by high temperatures (>1000 °C) within the convecting portion of the mantle wedge (Fig. 4b), where water supplied from the slab will be consumed by mantle-derived melts at the fluid flux melting front (e.g., Iwamori, 1998; Gerya et al., 2006; Cagnioncle et al., 2007), rather than propagate freely toward the bottom of the lithosphere. Rheological weakening of the overriding plate by magmatic processes was also proposed by several studies (e.g., Ueda et al., 2008; Sizova et al., 2010), which may cause effective thinning of the overriding plate by trench retreat and extension (e.g., Gerya and Meilick, 2011).

Gorczyk et al. (2007a) investigated the influence of effective water propagation velocities from the slab on fore-arc extension processes at Pacific-type convergent margins with a coupled petrological-thermo-mechanical model of subduction. They found that the degree of plate coupling strongly depends on the dimensionless ratio (R_{H_2O}) between the plate convergence rate and the water propagation velocity. Fore-arc extension and delamination of the slab from the overriding plate followed by trench retreat (that finally results in a growth of young overriding plate and a back-arc spreading center formation) was common for models with slower convergence rate/higher water velocity ($R_{H_2O} < 4$). In contrast, higher convergence rate/lower water velocity ($R_{H_2O} > 4$) resulted in continuous plate coupling. Two fundamentally different regimes of melt productivity were observed in numerical experiments and correlated with natural observations. Firstly, during continuous convergence with coupled plates (i.e., Late Paleozoic margin of central Chile) the largest melt productivity occurred at the onset of subduction due to temporary steepening of the slab. This stage is followed by rapidly decaying productivity with time due to flattening of the slab inclination angle, thereby precluding further formation of partially molten mantle wedge plumes. Secondly, the highest melt productivity is obtained in simulations associated with slab delamination and trench retreat. As a result, extension occurs with a decoupling of the plates, which finally leads to the formation of a pronounced back-arc basin similar to the Mesozoic margin of southernmost Chile. In this case melt production increases with time due to a stabilization of the slab inclination associated with upward asthenospheric mantle flow toward the spreading center, thereby favoring the generation of hydrous partially molten plumes from the slab.

Clark et al. (2008) examined episodicity in back-arc tectonic regimes by using 3D, time-dependent numerical models of subduction with an overriding plate. The authors defined three types

of episodicity (pseudo-, quasi- and hyper-episodicity) and found evidence of these in nature. Quasi-episodicity, in which the back-arc shifts between phases of rifting, spreading and quiescence, is presently the dominant form of episodic back-arc development (e.g., Izu-Bonin Trench, the Mariana Trench, the Japan Trench, the Java-Sunda Trench and the central portion of the Peru–Chile Trench). This type of episodicity was found in models for which the subducting plate's velocity was determined by the sinking slabs' buoyancy (i.e., the system is dynamically consistent). Hyper-episodicity (Fig. 11c) corresponds to the combination of advancing and retreating trench motions. Quasi- and hyper-episodicity are only found in subduction zones with relatively high subducting plate velocities, between 6 and 9 cm/year. On the other hand, subduction zones with slow subducting plate velocities (e.g., Mediterranean, Scotia Sea) experience only pseudo-episodicity, where the spreading moves linearly toward the trench but often does so in discrete ridge-jump events.

Recently, geodynamic scenarios of oceanic-continental subduction including overriding plate dynamics were analyzed with a coupled 2D petrological-thermo-mechanical model (Fig. 1b) (Gerya and Meilick, 2011). The model included a free erosion/sedimentation surface, spontaneous slab bending, dehydration of the subducted crust, aqueous fluid transport, partial melting of both crustal and mantle rocks as well as melt extraction processes resulting in magmatic arc crust growth by volcanic addition. The following five geodynamic regimes of overriding plate dynamics were identified: (1) stable subduction with no back-arc spreading center and without plumes in the mantle wedge, (2) retreating subduction with a focused back-arc spreading center and without plumes, (3) retreating subduction with distributed intra-arc extension and trans-lithospheric sedimentary plumes, (4) advancing subduction with underplating (laterally extending) sub-lithospheric plumes and (5) stable to advancing subduction with stationary (laterally limited) sub-lithospheric plumes. Transitions between these different regimes are mainly caused by the concurrence of rheological weakening effects of (1) aqueous fluids percolating from the subducting slab into the mantle wedge and (2) melts propagating from the partially molten areas formed in the mantle wedge toward the surface. The aqueous fluids mainly affect the forearc region. Strong fluid-related weakening promotes plate decoupling and reduces subduction drag, and thus results in stacking of sediments in the accretionary prism. In contrast, reduced fluid weakening results in strong coupling of the plates and leads to advancing collision-like subduction with enhanced subduction erosion. This behavior promotes thickening of the overriding plate and large sedimentary plumes in the mantle wedge. In contrast, melts extracted from the hot regions above the slab rheologically weaken the lithosphere below the arc, which controls extension and shortening of the overriding plate. Strong rheological weakening by melts in combination with weak plate coupling triggers retreating subduction with a pronounced back-arc spreading center. Also, weakening of the continental lithosphere by melts extracted from trans-lithospheric sedimentary plumes generates a weak channel through which these structures may be emplaced into subarc crust. If there is insufficient melt-related weakening, plumes are unable to ascend but rather extend horizontally and thus underplate the lithosphere (Gerya and Meilick, 2011).

Recent directions in modeling overriding plate dynamics include elaboration of realistic self-consistent 3D numerical setups (Clark et al., 2008) with a free surface (Zhu et al., 2009, 2011), in which the subducting slab and overriding plate dynamics are not prescribed and the system is free to evolve spontaneously. Such setups are appropriate for studying laterally variable and episodic overriding plate processes including topography development, back-arc spreading dynamics and arc extension/rifting processes.

8. Deep subduction and slab bending processes

High-resolution seismic tomographic models (e.g., van der Hilst et al., 1991, 1997; van der Hilst, 1995; Grand, 1994; Widiyantoro et al., 1999) suggest various scenarios of deep slab behavior and slab interaction with the transition zone. While in some subduction zones slabs are observed to penetrate through the upper-lower mantle boundary at a depth of 670 km without any significant deformation (e.g., Kermadec, Java, central America), in others slabs are horizontally deflected by the boundary and seem to be at least temporarily trapped in the transition zone (Tonga, Izu-Bonin). Seismic tomography also revealed that slabs tend to thicken during penetration into the lower mantle (e.g., Wortel and Spakman, 2000; Li et al., 2008).

Using a finite element model of time-dependent convection, Christensen and Yuen (1984) were the first to determine the conditions for a vertical penetration of a subducted plate into the lower mantle. A temperature-dependent and non-Newtonian rheology was applied to achieve plate-like behavior of the upper plate sinking along one of the lateral model boundaries. The upper-lower mantle discontinuity was taken as either a chemical or phase boundary, or as a combination of both. It was found that when the compositional density contrast is greater than about 5%, the vertically descending slab is deflected sideward's at the boundary and two-layer convection prevails. A resulting depression of the boundary was in the range of 50–200 km. A compositional density difference less than 5%, resulted in the slab plunging several hundred kilometers into the lower mantle. With a pure phase change boundary, a negative Clapeyron slope of about −6 MPa/K (−60 bar/K) was required to establish a type of "leaky" double-layer convection. A more moderate slope would aid a small compositional density difference to prevent slab penetration into the lower mantle.

Some 10 years later Gaherty and Hager (1994) formulated a 2D Cartesian finite element models which explored the deformation of a vertical, compositionally layered slab as it encounters a viscosity increase at the boundary between the upper and lower mantle. They observed that approximately a factor of two thickening occurs via pure shear just above the discontinuity, with additional enhancement due to slab folding by over a factor of two. Comparison with models in which compositional buoyancy was explicitly ignored indicated that the thermal buoyancy largely controls slab evolution. Recently, Behounkova and Čížková (2008) re-analyzed slab buckling and thickening process with a more realistic mantle rheology, including diffusion creep, dislocation creep and a power–law stress limiter. Thickening, or the buckling of the plate was observed in models with relatively low yield stress (0.1 GPa) for the stress-limiting mechanism and with a viscosity increase at the 670 km discontinuity. It was also demonstrated that both the major mantle phase transitions and the strength of the crustal layer have significant consequences for the development of buckling instabilities, which contributes to thickening of slabs in the lower mantle.

Christensen (1996) used a Cartesian two-dimensional numerical convection model to systematically study the ability of an inclined subducted slab to penetrate the endothermic phase boundary at 660 km depth. The transient subduction history of an oceanic plate was modeled by imposing plate and trench motion at the surface. A variety of styles of slab behavior was observed, depending predominantly on the trench velocity. When trench retreat was faster than 2–4 cm/a, the descending slab flattened above the phase boundary. At slower rates, it penetrated straight into the lower mantle, although flattening in the transition zone sometimes occurred at a later stage, leading to complex slab morphology. Slab buckle was also observed to be independent of penetration or flattening at the phase boundary, but significantly

more likely when there was a localized increase in viscosity at the phase boundary. Flattened slabs were only temporarily arrested in the transition zone and sunk ultimately into the lower mantle.

Cížková et al. (2002) presented a parametric study of slab behavior in the transition zone and upper part of the lower mantle using more sophisticated visco-plastic models of deep subduction (Fig. 12a), which included diffusion creep, dislocation creep, Peierls stress limit as well as rheological weakening due to grain size reduction. The results showed that in the absence of grain size weakening, the subducting slab is rigid and has a strong tendency to penetrate into the lower mantle which is not significantly affected by trench retreat. In contrast, in the presence of grain size weakening, the subducting slab is more flexible and its penetration through the upper–lower mantle boundary is strongly dependent on the trench retreat rate, similarly to the previous study of Christensen (1996).

Mishin et al. (2008) used 2D visco-plastic models with a free surface and mineralogical phase transformations in the mantle and subducted crust to simulate slab dynamics and investigate their tomographic signature in the deep mantle. Double subduction processes were modeled by forcing two plates to follow each other and subduct contemporaneously (as e.g., in the modern Izu–Bonin–Marianas and Ryukyu arcs and ancient West Himalaya collision zone). It was found that in case of multiple slabs, subduction dynamics is more complex and involves several tectonic processes that were unknown in simple subduction models, such as (i) eduction (i.e., slab "un-subduction" from depths), (ii) subduction re-initiation, (iii) subduction flips and (iv) up-side-down, turn-over of a detached slab in the transition zone. Simulated tomographic structures related to slab propagation account for both penetration and non-penetration of the 660 km discontinuity. In accordance with previous results (e.g., Christensen, 1996; Cížková et al., 2002) non-penetration is favored by (i) low convergence rate, (ii) faster relative movement of the overriding plate, (iii) a young subducting slab age and (iv) up-side-down, turn-over of a detached slab.

Thickening of slabs penetrating the upper–lower mantle boundary (e.g., Wortel and Spakman, 2000; Li et al., 2008) has traditionally been interpreted as evidence for the buckling and piling of slabs at this boundary, where a strong contrast in viscosity may exist and cause resistance to slab penetration into the lower mantle (e.g., Gaherty and Hager, 1994; Ribe et al., 2007; Behounkova and Cížková, 2008). In contrast, Loiselet et al. (2010) argued recently, based on 3D numerical models, that such phenomena can also be explained by the internal deformation of propagating slabs due to their relatively low viscosity contrast (1–100) with the surrounding mantle. They showed that the shape of such low viscosity slabs evolves toward an inverted plume, or "jellyfish" shape. A parametric study revealed that low viscosity subducting slabs may achieve a variety of shapes that are in good agreement with the diversity of natural slab shapes imaged by seismic tomography. Further 3D modeling of deforming slab geometries interacting with a mid mantle discontinuity was recently conducted by Morra et al. (2010) based on the boundary element method. The models showed that a plate may or may not penetrate into the lowermost mantle and in some cases may stall in the mid-lower mantle for long periods, depending on the radial profiles of density and viscosity. Morra et al. (2010) proposed a scenario in which the accumulation of depleted slabs in the mid mantle over long time periods would give rise to a partially chemically stratified mantle. Recently, self-consistent models of deep subduction with realistic visco-elasto-plastic rheology of the slab were used to constrain viscosity structure of the mantle (Quinteros et al., 2010). Subduction velocity, slab shape and slab penetration (or not) into the lower mantle appeared to be a strong indicator for assessing the viscosity distribution in the mantle transition zone and lower mantle. It was found, in particular, that a viscosity jump of ~5 times from the transition zone to the lower mantle gives the most reasonable results comparable to nature. Estimated optimal values of viscosity in the transition zone were in the range of 3×10^{20}–10^{21} Pa s (Quinteros et al., 2010).

A subject of intense debate is whether the forces associated with the downgoing plate, the overriding plate, passive or active mantle flow are dominant in controlling the trajectory of plates descending into the deep mantle. Capitanio et al. (2007) used a 2D viscoplastic free surface model to investigate the dynamics and energetics of a free subduction system with an overriding plate, driven solely by downgoing plate buoyancy and sinking into a passive unbounded mantle represented by drag forces (Fig. 12b). It was demonstrated that such a single, free plate achieves subduction mainly through trench retreat. Most of the energy dissipation occurs in driving the passive mantle response, while the contribution of slab bending is minor. As a result, the slab's sinking velocity is the Stokes velocity which is determined by lithospheric buoyancy and mantle viscosity. Furthermore, Goes et al. (2008) identified lower-mantle slab penetration events by comparing Cenozoic plate motions at the Earth's main subduction zones with motions predicted by these fully dynamic visco-elastic models of subduction. It was demonstrated that whereas subduction of older, intrinsically denser, lithosphere occurs at rates consistent with the model, younger lithosphere (of ages less than about 60 Myr) often subducts up to two times faster, while trench motions are very low. Goes et al. (2008) concluded that the most likely explanation is that older lithosphere, subducting under significant trench retreat, tends to lay down flat above the transition to the high-viscosity lower mantle, whereas younger lithosphere, which is less able to drive trench retreat and deforms more readily, buckles and thickens. Slab thickening enhances buoyancy (volume times density) and thereby Stokes sinking velocity, thus facilitating fast lower mantle penetration. The stress distribution related to the bending of penetrating and non-penetrating slabs has also been analyzed recently (Capitanio et al., 2007; Čížková et al., 2007).

Stegman et al. (2010) used 3D models to analyze distinct styles of subduction (as distinguished by a characteristic slab morphology) for spontaneously subducting finite slabs with no overriding plate. Five distinct subduction regimes (modes) were discriminated on the basis of systematic numerical experiments (Fig. 13): (I) viscous beam mode, (II) advance-fold-retreat mode, (III) advancing mode, (IV) retreating mode, (V) folding mode. It was found that only a very restrictive range of plates ("strong" plates with smaller buoyancy) tend to favor modes of subduction which are exclusively advancing. In contrast, plates with greater negative buoyancy tend to develop a retreating subduction style. Stegman et al. (2010) demonstrated that the flexural strength and buoyancy of the plate determines the subduction style and controls several subduction characteristics including the partitioning between slab rollback and plate advance, the trench curvature, and the slab's radius of curvature. "Weak" plates (80–100 km thick with slab/mantle viscosity contrast of 100–300) exhibited slab geometry with several recumbent folds atop the more viscous lower mantle. This regime of weak plates with their associated slab morphologies (predominant folding) was argued to be most similar to slabs on Earth based on the presence of folded slab piles in Earth's upper mantle (Stegman et al., 2010).

Recently, Tackley (2011) performed remarkable 3D simulations of a compositionally-stratified basalt-harzburgite slab reaching the core-mantle boundary (CMB) (Fig. 14). It was shown that compositional stratification of the slab results in a strong torque due to the relatively high density of basalt and low density of harzburgite, which tends to rotate the slab such that the basalt side faces down. This slab–CMB interaction is characterized by heating of the slab followed by separation of the basalt and harzburgite layers, with harzburgite rising in vigorous plumes. Plumes form at the edges and sides of slabs at the CMB as well as in their interiors

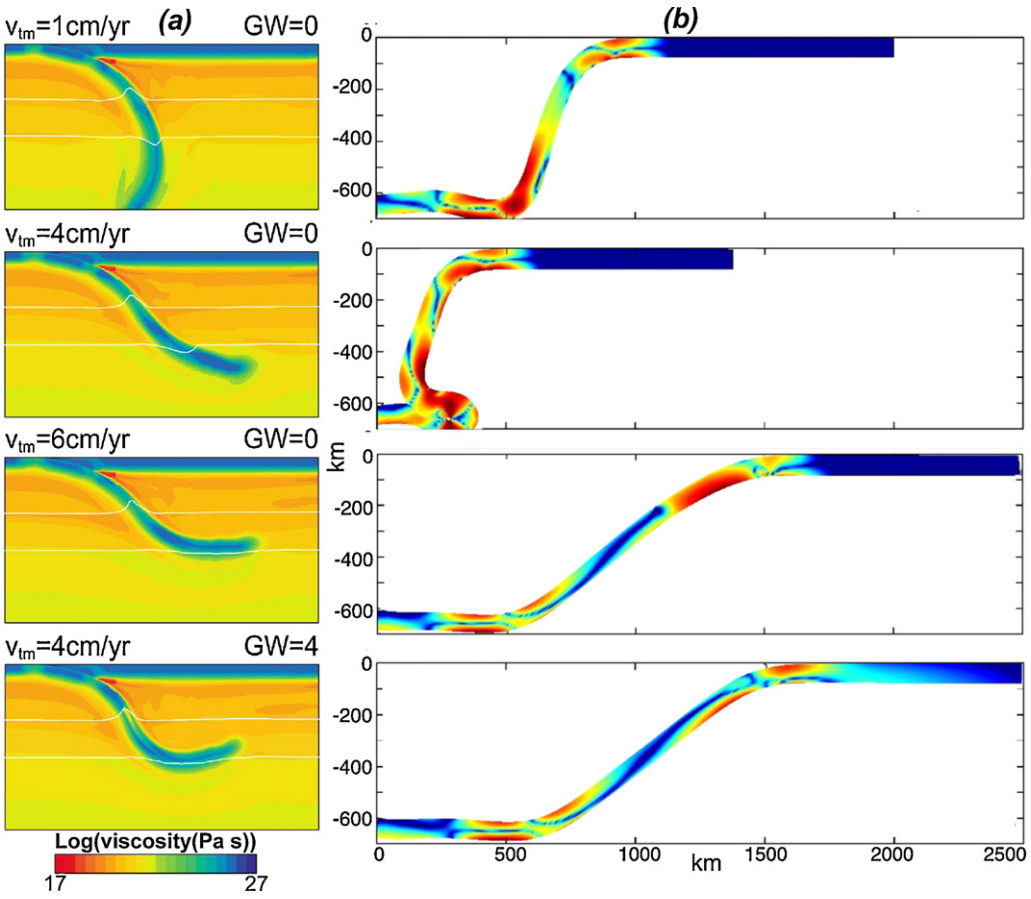

Fig. 12. Examples of 2D numerical models for morphology of deeply subducted slabs. (a) Models by Cížková et al. (2002) showing dependence of slab penetration into the lower mantle from trench retreat velocity (v_{tm}) and rheological weakening (GW) due to grain size reduction. Model size 2000 km × 1000 km. White lines indicate the positions of the major phase transition boundaries at the depths of 400 km and 670 km. (b) Models of Capitanio et al. (2007) showing variability of morphology and energy dissipation (color code) for deeply subducted viscoelastic slabs.

with plume heads dominated by depleted harzburgitic material, while plume tails entrain basaltic material. Segregation of basalt depends strongly on the presence or absence of a preexisting dense layer at the CMB and by dimensionality. A pre-existing dense layer greatly increases the fraction of basalt that segregates from the slab. In 3D this fraction is in the range 0.5–0.7 with a layer present compared to 0.25–0.45 with no preexisting layer. Two modes of basalt segregation are observed for slabs that land basalt side-up (i) hot harzburgite extruding from the sides and edges and (ii) hot, harzburgite-rich plumes bursting through the basalt layer, whereas for a slab that lands basalt side down (iii) hot basalt can peel off from its underside, displaying fingering instabilities in 3D (Tackley, 2011). It is also demonstrated that 2D simulations give a good first-order guide to the dynamics obtained in fully 3D geometry, but inherently 3D structures are missed (plumes versus sheets, fingering) and there is a quantitative difference in the fraction of basalt segregated (Tackley, 2011).

Further efforts in numerical modeling of deep slab dynamics are currently directed toward 3D regional (e.g., Stegman et al., 2010; Loiselet et al., 2010; Morra et al., 2010; Tackley, 2011) and global (e.g., Stadler et al., 2010) approaches accounting for complex slab rheology (e.g., Čížková et al., 2007; Capitanio et al., 2007) and mantle mineralogy (e.g., Mishin et al., 2008).

9. Termination of subduction and slab break-off

Termination of subduction in any subduction zone is an unavoidable consequence of terrestrial plate tectonics where positively buoyant continents, magmatic arcs, oceanic plateaus, ridges and seamounts chains may collide with active subduction zones. Slab break-off, or slab detachment, is often referred to as an early collisional process during which a part of the subducted slab detaches from the subducting plate. Such a rupture would cause the detached slab to sink down into the Earth's mantle and cause a major thermo-mechanical re-equilibration at the lithospheric-upper mantle scale. The concept of slab break-off originally comes from the analysis of gaps in hypocentral distributions and tomographic images of subducted slabs (e.g., Isacks and Molnar, 1969; Barazangi et al., 1973; Pascal et al., 1973; Wortel and Spakman, 2000). Many other observations suggest the possibility of slab detachment in subduction–collision settings such as seismicity patterns in subduction zones (e.g., Chen and Brudzinski, 2001; Sperner et al., 2001), magmatic geochemistry and the surface expression of volcanism (Keskin, 2003; Ferrari, 2004; Qin et al., 2008), uplift data analysis (e.g., Rogers et al., 2002; Wilmsen et al., 2009) and interpretation of structural and petrological data for exhumation of UHP rocks (e.g., Andersen et al., 1991).

Davies and von Blanckenburg (1995) published the first comprehensive analytical work on slab detachment processes, whereas initial numerical analyses were presented by Yoshioka et al. (1994) and Yoshioka and Wortel (1995). Davies and von Blanckenburg (1995) analyzed a post-subduction continental collision scenario in which negatively buoyant oceanic lithosphere detaches from positively buoyant continental lithosphere that attempts to subduct. The authors quantitatively evaluated an upper bound for the

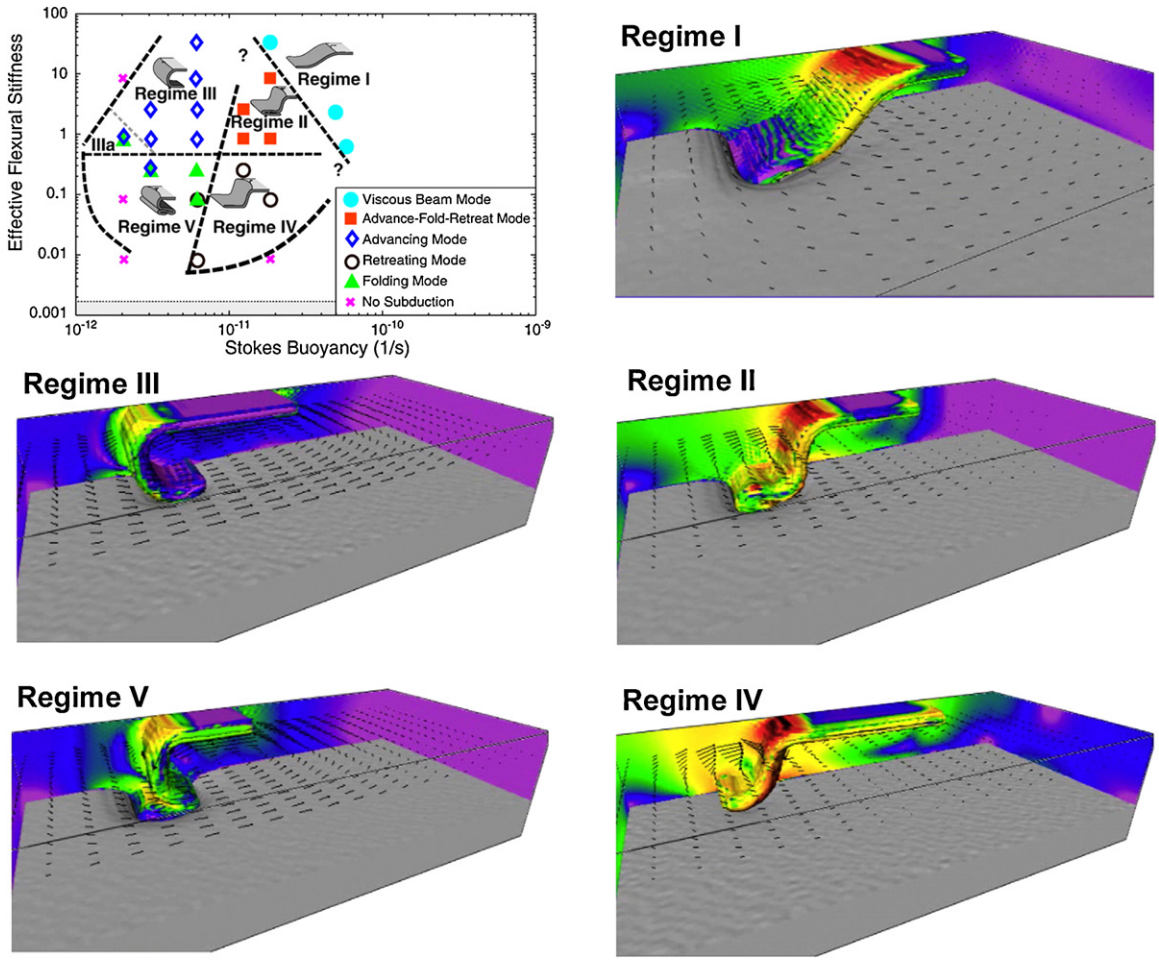

Fig. 13. Five major regimes of subduction characteristic for single viscous slab embedded in low-viscosity mantle (Stegman et al., 2010). Color code shows second invariant of the strain rate. Arrows show velocity field.

strength of the lithosphere, and compared it with the change in buoyancy force during continental subduction. It was found that whether break-off will occur, as well as the depth at which it will occur, is a strong function of temperature and hence the subduction velocity. For a subduction velocity of 1 cm/yr break-off occurred at depths of between 50 and 120 km, while at higher velocities break-off is still likely to occur, but at deeper depths. It was also demonstrated that as a result of the slab rifting during break-off, the asthenosphere upwells into the narrow rift and impinges on the mechanical lithosphere of the overriding plate. The resulting conducted thermal perturbation leads to melting of the metasomatised overriding mantle lithosphere, producing magmatism. Dry asthenospheric mantle will melt only if break-off occurs at a depth shallower than ca. 50 km. Yoshioka et al. (1994) and Yoshioka and Wortel (1995) investigated the physical mechanism of the slab detachment based on a visco-elastic 3D purely mechanical finite element model with a small initial tear from one side of the slab. Their results showed that an area of high shear stress concentration of the order of several hundred MPa forms near the tip of the tear inside the slab, thus causing further lateral migration of the tear. It was also concluded (Yoshioka and Wortel, 1995) that favorable conditions for slab detachment are characterized by a high inter-plate frictional force and a low convergence rate, which generates in-plate tensional stress at intermediate depths. Furthermore, Yoshioka et al. (1994) used a 2D thermo-mechanical model to demonstrate the influence of nonlinear stress-dependent rheology and shear heating on local slab weakening that can lead to slab detachment process.

Until recently, numerical modeling studies of slab break-off concentrated on relatively static scenarios involving the evolution of an already subducted slab (Wong et al., 1997; van de Zedde and Wortel, 2001; Buiter et al., 2002; Cloetingh et al., 2004; Gerya et al., 2004b; Toussaint et al., 2004; Macera et al., 2008; Andrews and Billen, 2009). In particular, Buiter et al. (2002) quantified the surface deformation generated by slab detachment by with a 2D mechanical model and determined a maximum surface uplift of 2–6 km related to slab detachment. Cloetingh et al. (2004) and Toussaint et al. (2004) numerically reproduced slab detachment scenarios associated with deep continental subduction (e.g., Andersen et al., 1991) based on 2D visco-elasto-plastic thermo-mechanical models with a pre-subducted oceanic slab. Gerya et al. (2004b) presented systematic 2D experiments for thermo-mechanical controls of slab break-off and showed that this process can be initiated in the form of slab necking by a prolonged (8–30 My) period of slab weakening due to thermal diffusion (<20 °C/My) after cessation of active subduction. Following the period of weakening, rapid slab detachment takes place over a few million years and is accelerated by non-Newtonian strain-rate softening and focused thermal erosion (>60 °C/Myr) due to strong positive thermal feedback from shear heating. Detached slab fragments sink rapidly with a tendency for coherent rotation. Andrews and Billen (2009) investigated the significance of plastic yielding for the detachment process and demonstrated two major modes of detachment: (1) slow and deep viscous detachment of strong slabs (500 MPa or greater maximum yield strength) controlled by heating of the slab, and (2) fast and shallow detachment of weaker slabs (300 MPa) controlled by

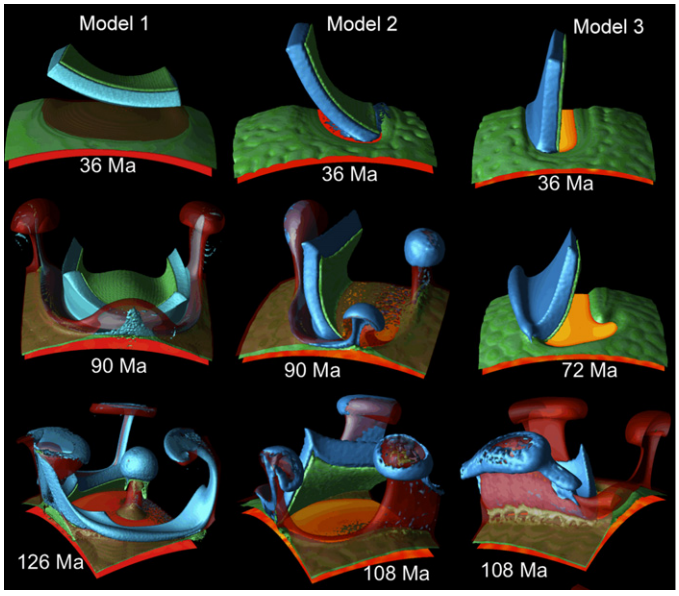

Fig. 14. The interaction of a compositionally-stratified basalt-harzburgite slab with a 150 km thick layer above the core-mantle boundary (CMB), for three different initial slab dips (Tackley, 2011). Plotted are isosurfaces of composition = 0.25 (blue, showing depleted material), composition = 0.5 (green, showing basalt) and temperature = 3000 K (red semi-transparent). Times are as labeled.

yielding within the slab interior. For slabs with a maximum yield strength of 500 MPa, the time to detachment increases with slab age (for ages ranging from 40 to 120 My), indicating that the detachment time is controlled by the integrated stiffness of the slab, which limits the sinking rate. However, the detachment time for weaker slabs (300 MPa) is independent of age.

The first fully dynamic models for spontaneous slab break-off associated with continental collision were presented by Faccenda et al. (2008a) and examined a range of behaviors characteristic of a post-subduction collisional orogeny. In their 2D thermo-mechanical models the subducting oceanic plate was attached to an incoming continental margin. After some period of forced convergence the system was left free to evolve spontaneously where a continental collision stage was driven by the negative buoyancy of the subducted slab. This approach was recently used by Baumann et al. (2010) and Duretz et al. (2011) who investigated the influences of mantle phase transformations as well as a brittle-plastic and Peierls rheology on spontaneous slab break-off process. In particular, Baumann et al. (2010) delineated five tectonic phases typically associated with spontaneous subduction termination and viscous slab detachment: (1) oceanic slab subduction and bending; (2) continental collision initiation followed by spontaneous slab blocking, thermal relaxation and unbending (in the case of old oceanic plates in this phase slab roll-back occurs); (3) slab stretching and necking; (4) slab break-off and accelerated sinking; (5) post-break-off relaxation. By varying the oceanic slab age and initial plate convergence rate Duretz et al. (2011) found four different end-members of spontaneous slab break-off process differing in depth and dominating rheological mechanisms. In this parameter space, the break-off depth ranges from 40 to 400 km and each break-off modes displayed complex rheological behavior during break-off. Peierls creep in olivine turns out to be a key mechanism for slab break-off, generally causing slabs to break earlier and at shallower depths. It was also demonstrated that models involving different depths of break-off are subject to different topographic evolution, but always display a sharp break-off signal (Fig. 15). Post break-off uplift rates in foreland and hinterland basins correlate negatively with the break-off depth and range between 0.1 km/My for deep detachment (Fig. 15b) and 0.8 km/Myr for shallow detachment (Fig. 15a). Continental crust subduction was observed in spontaneous break-off experiments involving oceanic lithosphere older than 30 Myr (Fig. 15b). Different exhumation processes such as slab retreat and eduction occurred according to the break-off depth.

Another fully dynamic model of spontaneous slab detachment related to ridge–trench collision was recently represented by Burkett and Billen (2009, 2010), where the approach of a buoyant spreading ridge to a subduction zone was tested as a mechanism for slab detachment. This process was invoked as an explanation for observed ridge abandonment and slab window related magmatism (e.g., in Baja California, Michaud et al., 2006). Burkett and Billen (2009) used dynamic 2D models including a non-Newtonian rheology to study the approach of a trench-parallel spreading ridge to a subduction zone. They found that before the ridge approaches within 100 km of the trench, detachment of the subducted slab occurs due to the combined effects of increased buoyancy and reduced strength of the lithosphere with ridge proximity. The following key features were also found in these experiments: (1) a decrease in subduction velocity as the ridge approaches the trench, (2) a shrinking surface plate that maintains a uniform plate-like subduction velocity, (3) ridge abandonment distances 100–275 km from the trench, and (4) slab gap distances 195–285 km from the trench. These results are consistent with observations in Baja California, where detachment of the Cocos slab may explain abandonment of observed segments of the East Pacific Rise 50–200 km outboard of the trench and the presence of non-arc related magmatism located 100–250 km inboard of the trench.

Burkett and Billen (2010) presented the first fully-dynamic, 3D thermo-mechanical numerical models for the ridge–trench collision process and demonstrated that for a finite laterally symmetric slab, the 3D detachment process occurs nearly simultaneously along strike by way of boudinage-type necking and opening of holes central to the slab (Fig. 16a). For a case involving the two offset ridge segments approaching a trench, slab tearing occurs in the form of (1) a vertical propagating separation along the age offset boundary within the slab that was previously weakened by a transform weak zone, and (2) a horizontal propagating detachment controlled by the lateral transfer of slab pull to adjacent surface plate segments (Fig. 16b). However, lateral decoupling between offset adjacent plate segments and the propagating nature of the vertical and horizontal tearing are dependent upon fracture zones remaining weak through the subduction zone. Whether detachment occurs simultaneously along strike, or propagates laterally, the process is controlled by plastic yielding of the slab interior when young lithosphere entering the trench can no longer support slab pull.

Recently, van Hunen and Allen (2011) used 3D models to analyze the conditions and dynamics of a subduction–collision system and subsequent slab break-off and slab tear propagation (Fig. 16c and d). Model results indicate that collision after the subduction of an old, strong subducting oceanic slab leads to slab break-off at 20–25 Myr after the onset of continental collision, and subsequently a slab tear migrates more or less horizontally through the slab with a propagation speed of 100–150 mm/yr. In contrast, young and weak oceanic slabs show the first break-off at 10 Myr after continental collision and experience tear migration rates up to 800 mm/yr. Slab strength plays a more important role in the timing of slab break-off and the speed of a propagating slab tear than (negative) slab buoyancy does. Slab break-off is viable even for slabs that are supported by the viscosity jump and phase change between the upper and lower mantle. The density of the oceanic slab and the subducting continental block is important for the amount of continental subduction and the depth of slab break-off.

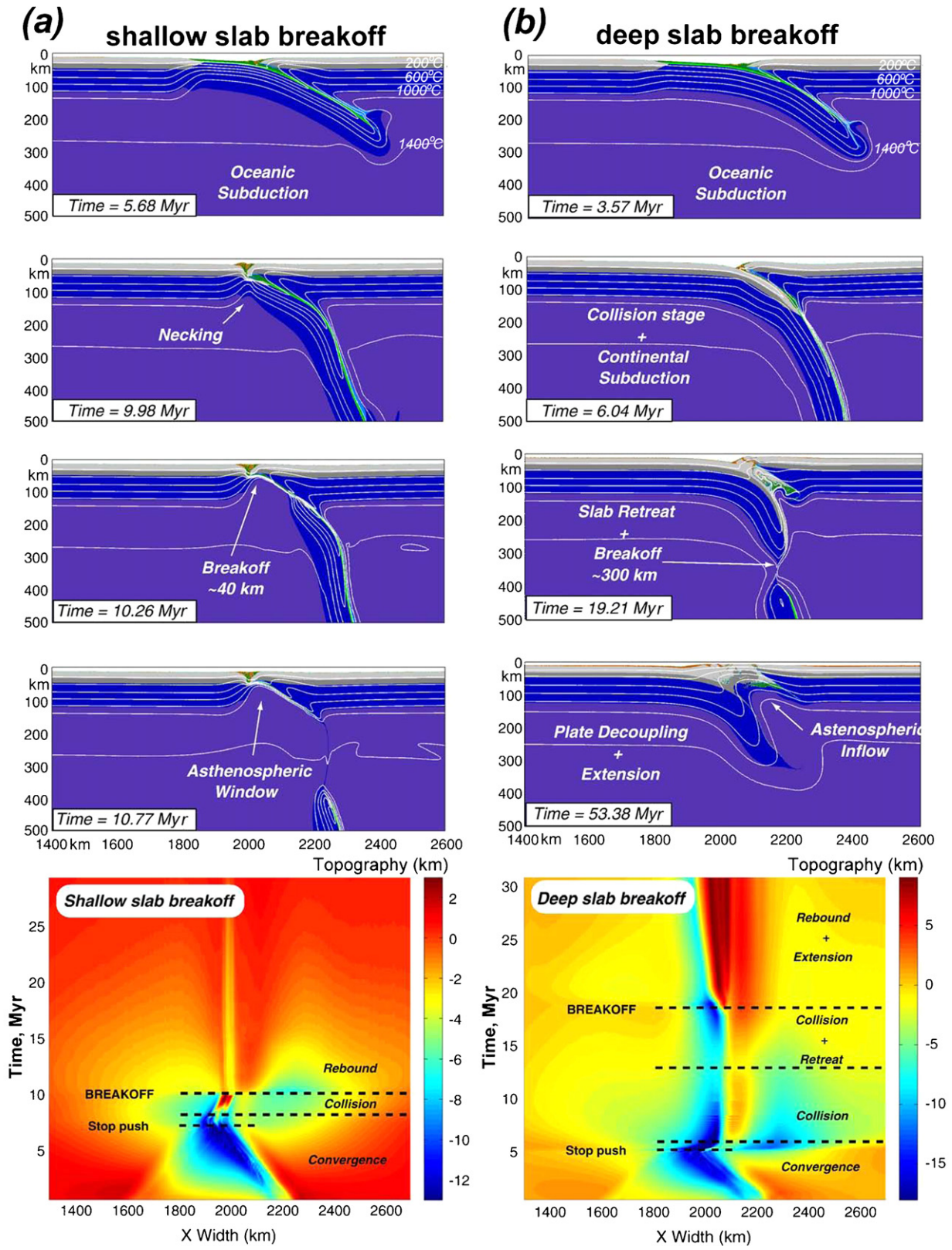

Fig. 15. Examples of 2D numerical models of spontaneous slab break-off during continental collision (Duretz et al., 2011). (a) Four stages (top diagrams) of model evolution for the shallow slab break-off regime and associated surface topography development (bottom diagram). During slab necking and break-off, the subducted crust deforms in a brittle manner and the mantle lithosphere deforms viscously. (b) Four stages (top diagrams) of model evolution for the deep slab break-off regime and associated surface topography development (bottom diagram). During slab necking and break-off, the subducted crust deforms viscously and the mantle lithosphere deforms both viscously and by Peierls mechanism.

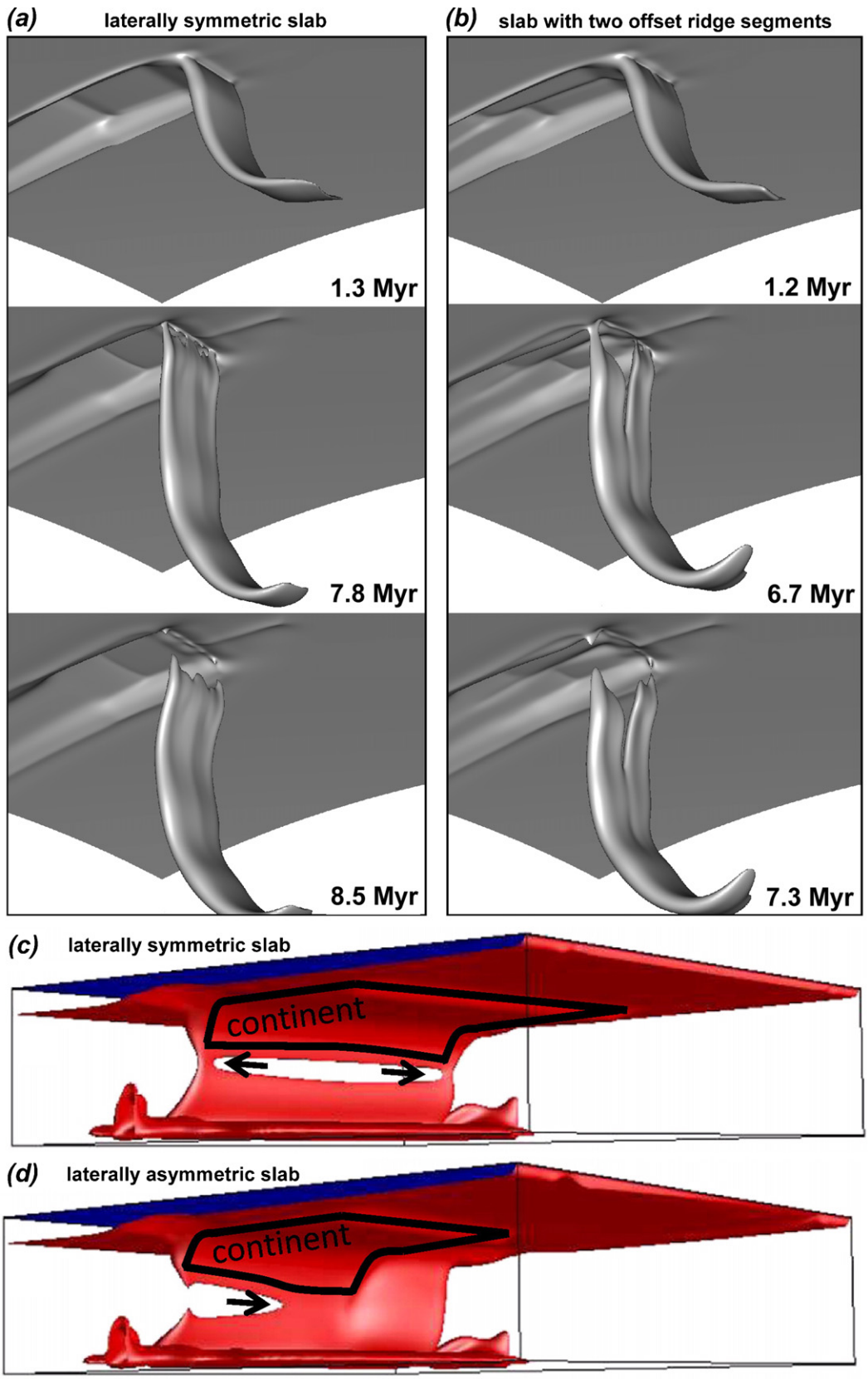

Fig. 16. 3D numerical models of slab break-off due to ridge–trench collision (a, b) (Burkett and Billen, 2010) and continental collision (c, d) (van Hunen and Allen (2011). (a, c) Detachment of laterally symmetric slabs. (b, d) Detachment of laterally asymmetric slabs: (b) slab with two offset ridge segments separated by weak fracture zone, (d) only part of the slab has a continental block. Slab width is 300 km in (a, b) and 2000 km in (c, d). The 1050 °C isosurface is shown in (a, b) and 945 °C in (c, d).

A 40-km thick continental crust can be buried to depths greater than 200 km, although this maximum depth is significantly less for younger or very weak slabs, or thicker continental crust. In the 3D models performed slab break-off typically started at a depth of 300 km, mostly independent of mantle rheology, but, like continental crustal burial, can be shallower for young or buoyant plates. In agreement with previous models (Burkett and Billen, 2010), the 3D numerical experiments of van Hunen and Allen (2011) suggest that break-off has an intrinsic small preference to start as a slab window within the slab's interior, rather than as a slab tear at the slab edge (Fig. 16c). Any significant asymmetry in the collision setting such as earlier collision at one end of the subduction zone, however, usually overrides this tendency and leads to slab tearing starting near one edge of the slab (Fig. 16d) (van Hunen and Allen, 2011).

Future progress in numerical modeling of subduction termination and slab detachment processes will likely be directed toward creating fully-dynamic, self-consistent 3D models that account for spontaneous plate movements (Burkett and Billen, 2010; van Hunen and Allen, 2011) and phase transformations including melting and free erosion-sedimentation surface (e.g., Zhu et al., 2009; Duretz et al., 2011). Of particular interest is the lateral variability of magmatic, metamorphic and topographic processes (e.g., Duretz et al., 2011) related to various geodynamic modes of slab break-off and identification and quantification of these modes in nature.

10. Subduction in the early Earth

Two fundamental questions regarding the styles of Precambrian subduction have been the subject of much debate during the past decades (e.g., Davies, 1992, 2006; Hamilton, 1998; de Wit, 1998; Griffin et al., 2003; Brown, 2006, 2007; Stern, 2007; O'Neill et al., 2007a,b; van Hunen and van den Berg, 2008). First, what was the reason that the Earth developed a plate tectonics regime and, second, what was the timing of the transition to the plate tectonics regime on Earth? The main arguments about the timing of plate tectonic initiation have been based on the interpretation of geological, petrological and geochemical observations (Benn et al., 2005; Condie and Pease, 2008). To date, the interpretation of geological observations has not achieved a consensus about the style of the tectonic regime in the Precambrian. On the one hand, there is a variety of evidence for Archean, particularly Mesoarchean-to-Neoarchean, plate tectonics and subduction settings (e.g., de Wit, 1998; Brown, 2006; Condie and Pease, 2008), but some authors argue that the modern style of subduction has only been active since the appearance of ophiolites in the Proterozoic and ultrahigh-pressure metamorphism in the late Neoproterozoic (Hamilton, 1998; Stern, 2005, 2007). Recently, thermo-mechanical numerical modeling experiments have been used to investigate the development and timing of plate tectonics (e.g., Davies, 2006; O'Neill et al., 2007a,b; Sleep, 2007; van Hunen and van den Berg, 2008) in order to resolve these con-

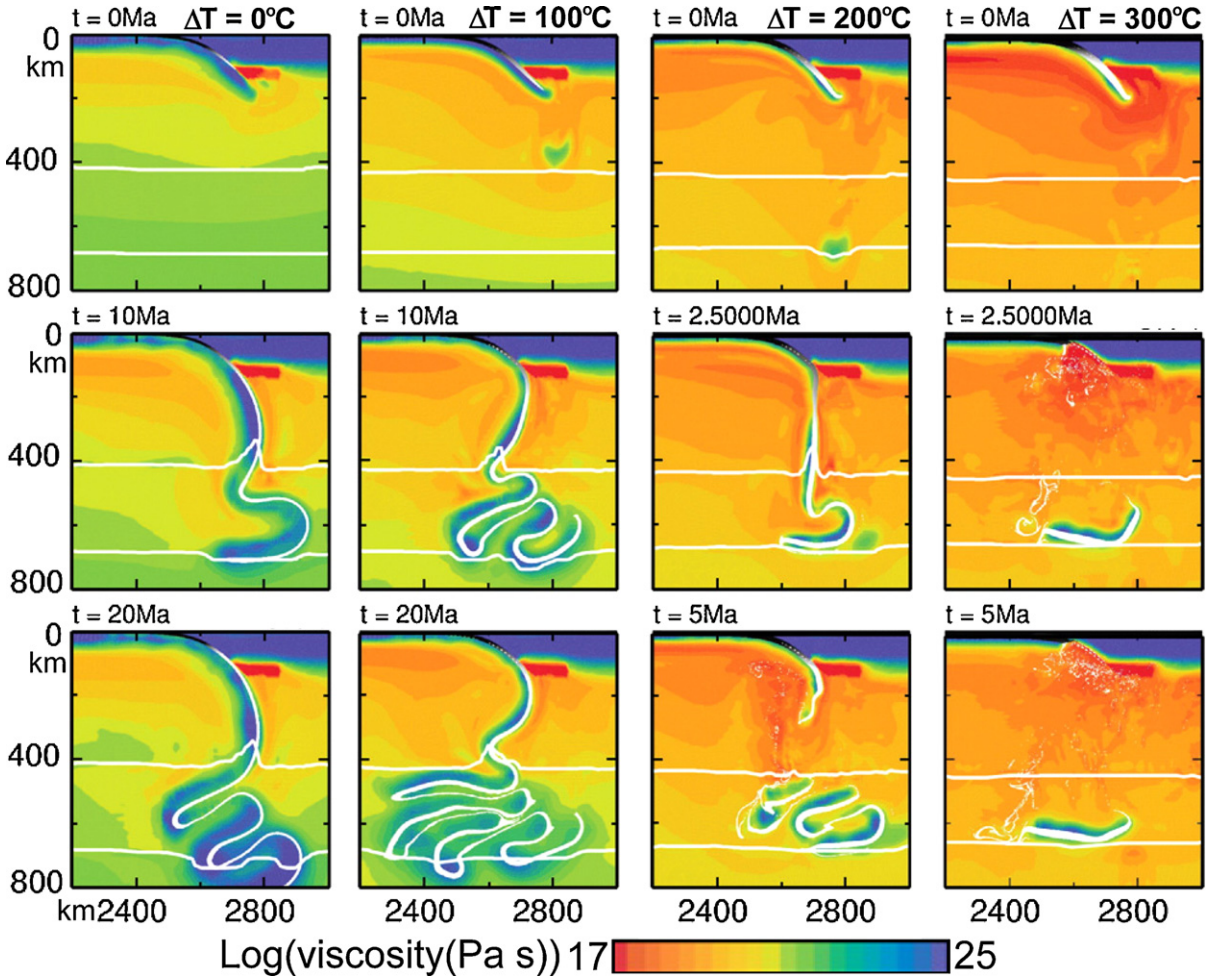

Fig. 17. Variations in tectonic style of subduction with changing mantle temperature (van Hunen and van den Berg, 2008). Four columns show time evolution (t) for cases with various mantle temperature difference (ΔT) above present day values. The olivine–spinel and perovskite transitions are denoted by the thin white lines, crustal material by black areas, and eclogite by white areas.

trasting interpretations of the geological evidence for early plate tectonics.

Numerical models of Precambrian plate tectonics and possible styles of subduction in a hotter, early Earth are still relatively rare. Modeling by Davies (1992, 2006) with kinematically prescribed motion of oceanic plates takes into account early depletion of the upper mantle, which led him to suggest that the oceanic crust might have been thinner than modern oceanic crust (<3 km on average), and that the thermal boundary layer might also have been overall thinner. The thinner oceanic crust estimated from the models would substantially improve the viability of subduction, and hence of plate tectonics, in the earliest Earth. However, the numerical modeling suggests spatial and temporal variability in crustal thicknesses might have allowed some plates to subduct whereas other plates might have been blocked and forced to form proto-continental crust.

In an alternative scenario without early depletion of the upper mantle, modeling by van Hunen and van den Berg (2008) suggests that the lower viscosity and higher degree of melting for a hotter, fertile mantle might have led to both a thicker crust and a thicker depleted harzburgite layer making up the oceanic lithosphere. A thicker lithosphere might have been a serious limitation to the initiation of subduction, and a different mode of downwelling (Davies, 1992) or "sub-lithospheric" subduction (van Hunen and van den Berg, 2008) might have characterized Earth in the Precambrian, although the conversion of basalt to eclogite may significantly relax this limitation (e.g., van Thienen et al., 2004; Ueda et al., 2008). The intrinsic lower viscosity of the oceanic lithosphere on a hotter Earth would also lead to more frequent slab break-off (Fig. 17), and in some cases crustal separation from the mantle lithosphere. Therefore, lithospheric weakness could be the principal limitation on the viability of modern-style plate tectonics on a hotter Earth.

Sizova et al. (2010) performed a series of experiments using a 2D petrological-thermo-mechanical numerical model of oceanic-continental subduction and systematically investigated the dependence of tectono-metamorphic and magmatic regimes at an active plate margin on upper-mantle temperature, crustal radiogenic heat production and degree of lithospheric weakening by fluids and melts. From these experiments the authors identified a first-order transition from a "no-subduction" tectonic regime to a "pre-subduction" tectonic regime and finally to the modern style of subduction (Fig. 18). The first transition is gradual and occurs at upper-mantle temperatures between 250 and 200 °C above the present-day values, whereas the second transition is more abrupt and occurs at 175–160 °C. The link between geological observations and model results suggests that the transition to the modern plate tectonic regime might have occurred during the Mesoarchean–Neoarchean time (ca. 3.2–2.5 Ga). In the case of the "pre-subduction" tectonic regime (upper-mantle temperature 175–250 °C above the present), the plates are weakened by intense percolation of melts derived from the underlying hot melt-bearing sub-lithospheric mantle. In such cases, convergence does not produce self-sustaining one-sided subduction, but rather results in shallow underthrusting of the oceanic plate under the continental plate. A further increase in the upper-mantle temperature (>250 °C above the present) causes a transition to a "no-subduction" regime, where horizontal movements of small deformable plate fragments are accommodated by internal strain, where even shallow underthrusts do not form under the imposed convergence. Thus, based on the results of the numerical modeling, it was suggested that the crucial parameter controlling the tectonic regime is the degree of lithospheric weakening induced by emplacement of sub-lithospheric melts into the lithosphere. A lower melt flux at upper-mantle temperatures <175–160 °C results in a lesser degree of melt-related weakening and stronger plates, which stabilizes the

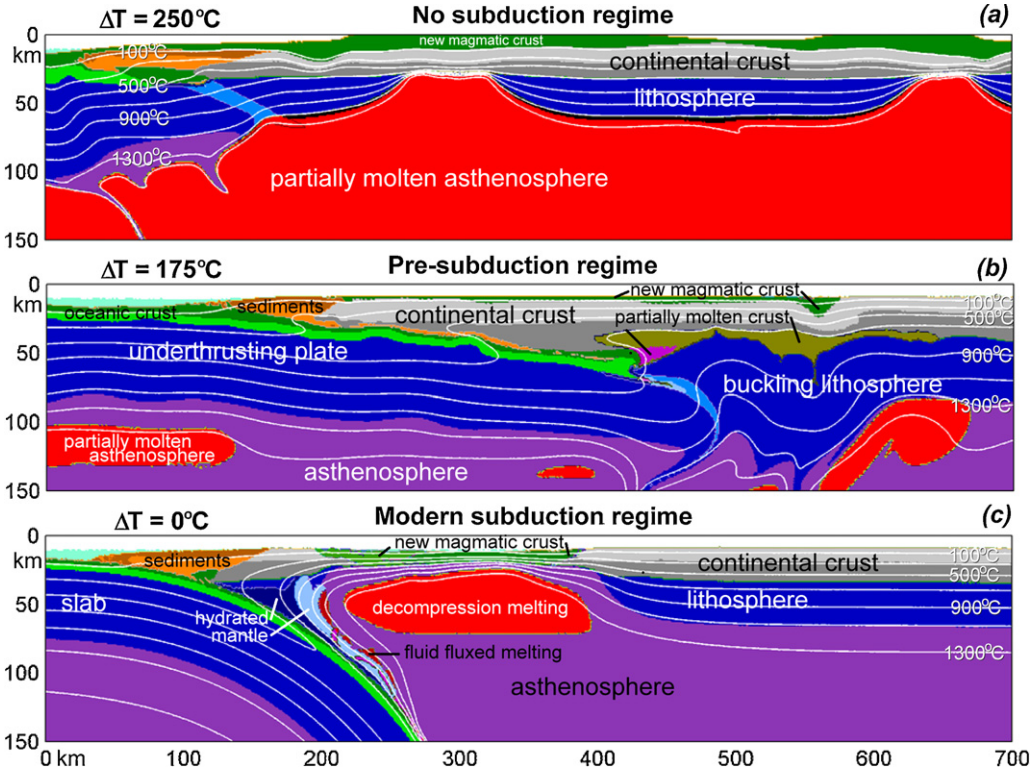

Fig. 18. High-resolution numerical models of an active continental margin evolution for various mantle temperature difference (ΔT) above present day values (Sizova et al., 2010). Models predict a first-order transition from a "no-subduction" tectonic regime (a) through a "pre-subduction" tectonic regime (b) to the modern style of subduction (c).

modern subduction style even at high mantle temperatures (Sizova et al., 2010).

Ueda et al. (2008) examined subduction initiation related to thermo-chemical plumes, which has implications to Archean tectonics. Numerical testing of this hypothesis has been conducted in 2D with a thermo-mechanical code accounting for phase transitions and a viscoplastic model of a thin oceanic lithosphere, impacted by a partially molten, thermo-chemical or purely thermal plume. It was demonstrated that a mantle plume can break the lithosphere and initiate self-sustaining subduction, provided the plume causes a critical local weakening of the lithospheric material above it due to percolation of melts extracted from the plume toward the surface. The intensity of the required weakening depends on the plume volume, plume buoyancy and the thickness of the lithosphere. The weakening is the greatest for the least buoyant, purely thermal plumes. Another necessary condition is the presence of high-pressure fluids at the slabs' upper interface, which reduces the effective friction coefficient to very low values. Based on numerical results, it was suggested that sheet-like instabilities during Archean mantle convection could have initiated subduction on Earth where an ocean was already present in less stable tectonic settings, provided that mantle plumes (sheets) at that time were rich in water and melt, which could drastically reduce the effective friction coefficient in the lithosphere above the plume (Ueda et al., 2008).

Plate tectonics and subduction initiation in the early Earth will likely receive more attention from modelers in the near future, as these topics have not yet been explored systematically. Future work in this area will likely focus on the development of self-consistent 2D and 3D models taking into account peculiar exogenic and endogenic conditions of the early Earth: higher crustal and mantle temperature, increased radiogenic heat production, frequent large asteroid impacts (Hansen, 2007), low surface elevation (e.g., Rey and Coltice, 2008) and other relevant features. Progress will also depend on the continued development of self-consistent global mantle convection and plate tectonics models for present day conditions.

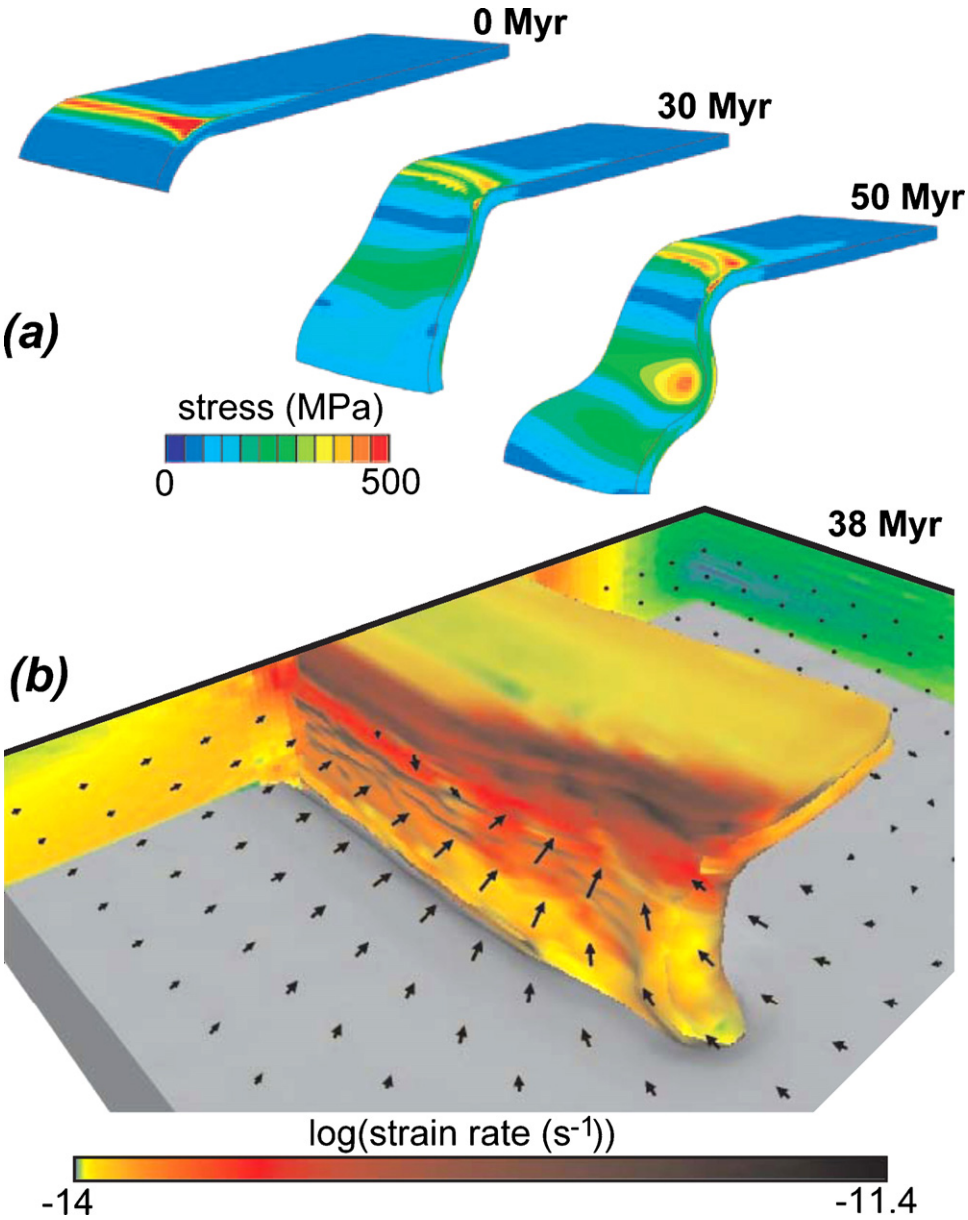

Fig. 19. Examples of numerical models of spontaneously curved slabs embedded in a viscous mantle. (a) Model of Morra et al. (2006). (b) Model of Schellart et al. (2007).

11. Lateral variability of subduction processes in 3D

Subduction zones and their associated slabs are limited in lateral extent (250–7400 km), their three-dimensional geometry evolves over time (e.g., Schellart et al., 2007) and can often be quite complex (e.g., Jadamec and Billen, 2010). In addition, complicated patterns of mantle circulation can develop above slabs (e.g., Honda and Saito, 2003; Zhu et al., 2009). This lateral variability unavoidably calls for the utilization of 3D numerical modeling approaches. 3D modeling of subduction is still far from routine and much of the efforts of the modeling community are currently directed toward creating robust tools for performing high-resolution subduction simulations in three dimensions. Certain 3D numerical modeling studies have already been discussed in relation to specific topics. Here I will concentrate on a number of additional studies that aimed to address the lateral variability of subduction processes.

The first 3D subduction modeling studies were developed in the broader context of whole mantle convection simulations that aimed to investigate specific convection regimes with plate-like behavior of the model upper surface (e.g., Tackley, 1998, 2000; Trompert and Hansen, 1998). Trompert and Hansen (1998) and Tackley (1998, 2000) presented three-dimensional convection models that spontaneously generated plates through the use of a temperature-(strain-rate)-dependent viscosity combined with a yield stress. Their 3D models produced a style of convection that exhibited some important features of plate tectonics, such as subduction of the stiff upper layer and plate-like motions on the surface. However, Tackley (1998, 2000) noted that subduction in these models was double-sided (i.e., unrealistic for the Earth) so that plates were subducting from two sides along spontaneously forming convergence zones. This non-terrestrial style of subduction was attributed to insufficient resolution, simplified rheology and the absence of continents in the models (Tackley, 1998, 2000). Recently, it was also suggested that realistic spontaneous single-sided subduction is strongly promoted by high plate strength and water-related lubrication of plate interfaces (Gerya et al., 2008a) as well as by a free-surface condition on the upper boundary (Tackley et al., 2010). Honda and Saito (2003) developed the first simple 3D regional subduction model, where a kinematically prescribed inclined slab was used to study mantle wedge dynamics. This approach has been used by a number of additional studies to investigate 3D thermal, compositional and flow structures around descending slabs (e.g., Honda and Yoshida, 2005; Honda, 2009; Honda et al., 2010). Zhu et al. (2009, 2011) also developed complex thermal–chemical–mineralogical regional 3D subduction models with a free-surface, high-resolution mesh and spontaneously bending slabs (Zhu et al., 2009, 2011).

Morra et al. (2006) used a novel combination of finite-element and boundary element modeling for simulating the 3D dynamical evolution of a single slab interacting with the surrounding mantle in order to assess the origins of arc curvature (Fig. 19a). The possible physical mechanisms were grouped into two classes: (1) external feedbacks between the migrating lithosphere and secondary induced mantle flow and (2) internal heterogeneities within the lithosphere resulting from different plate cooling ages at the trench. It was suggested based on a statistical analysis that almost all arcs on the Earth can be described by these two general mechanisms (Morra et al., 2006). The issue of lateral plate curvature was also investigated by Stegman et al. (2006) and Schellart et al. (2007) by analyzing the 3D morphology (Fig. 19b) of single spontaneously subducting slabs of variable width. It was found that the slab width controls two first-order features of plate tectonics: the curvature of subduction zones and their tendency to retreat backwards with time, which is actually in good agreement with the first mechanism of Morra et al. (2006). Schellart et al. (2007) demonstrated that the trench migration rate is inversely related to slab width and depends on the proximity to a lateral slab edge. These results are consistent with trench retreat velocities observed globally, with maximum velocities (6–16 cm/yr) only observed close to slab edges (<1200 km), whereas far from slab

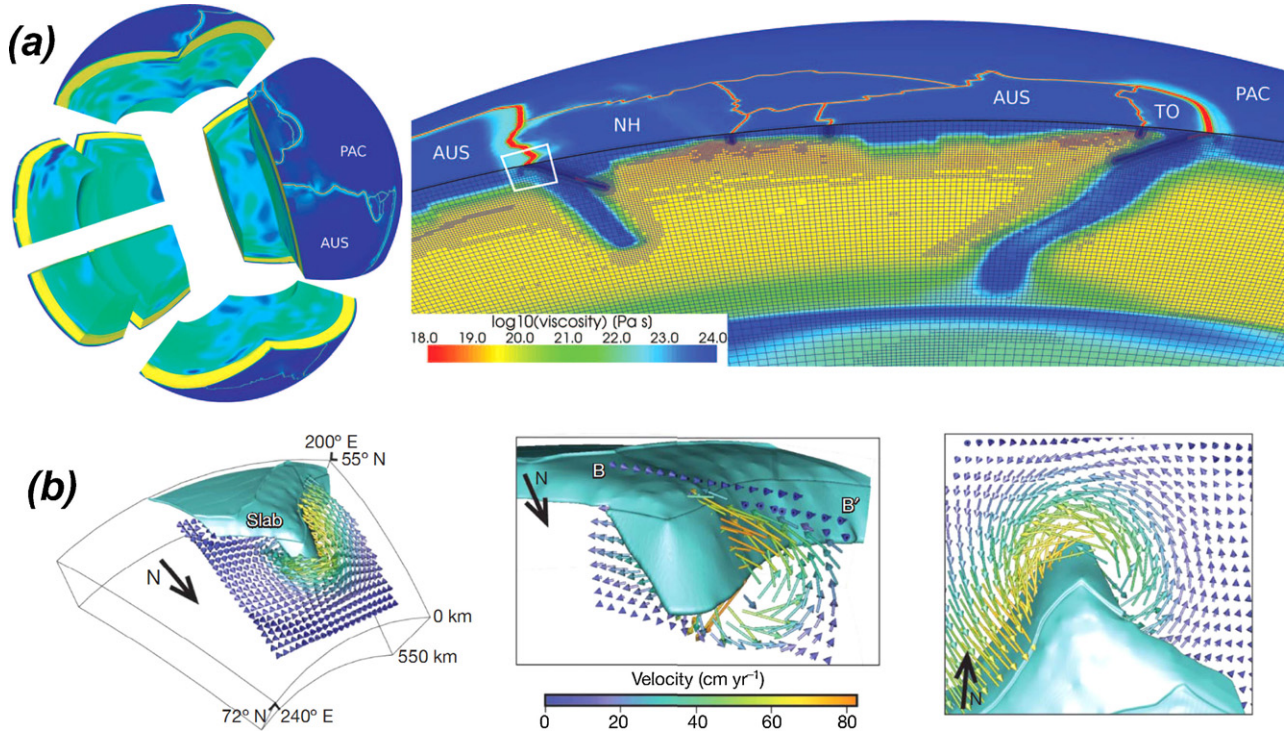

Fig. 20. Examples of high-resolution 3D "snapshot models" of existing subduction zones. (a) Model of Stadler et al. (2010) for the global system of tectonic plates driven by buoyancy of subducted slabs. Grid in the right panel shows the adaptively refined mesh with a finest resolution of about 1 km. (b) Model of Jadamec and Billen (2010) for buoyancy-driven deformation of the Alaska subduction–transform system. Slab geometry is shown by isosurface of viscosity. Arrows show velocity field.

edges (>2000 km), retreat velocities are always slow (2.0 cm/yr). Models with narrow slabs (≤1500 km) retreat quickly and develop a curved geometry, concave toward the mantle wedge side. Models with intermediate-width slabs (2000–3000 km) are sub-linear and retreat more slowly. Models with wide slabs (≥4000 km) are nearly stationary in the center and develop a convex geometry, whereas trench retreat increases toward concave-shaped edges. Additionally, Schellart et al. (2007) identified periods (5–10 Myr) of slow trench advance at the center of wide slabs. It was argued that such transient trench advance may explain, in particular, mountain building in the central Andes, which is located far from slab edges (Schellart et al., 2007).

A significant effort has also been directed toward constructing realistic high-resolution "snapshot models" (i.e., a single present moment of time is modeled) of subduction and plate tectonics based on the density and viscosity distribution in the Earth's mantle as constrained by geophysical data (e.g., Jadamec and Billen, 2010; Stadler et al., 2010). Stadler et al. (2010) constrained a non-evolutionary high-resolution 3D buoyancy-driven model of global plate tectonics (Fig. 20a) using adaptive mesh refinement algorithms on parallel computers. Global plate motions were correctly simulated, with individual plate margins (including subduction zones) resolved down to a scale of 1 kilometer. Back-arc extension and slab rollback were found to be emergent consequences of slab descent in the upper mantle. Cold thermal anomalies within the lower mantle couple into oceanic plates through narrow high-viscosity slabs, altering the velocity of oceanic plates. It was also concluded that viscous dissipation within the bending lithosphere at trenches is minor (5–20%) compared to the total dissipation through the entire lithosphere and mantle; this agree well with previous conclusions coming from regional 2D subduction models (Capitanio et al., 2007). Jadamec and Billen (2010) presented non-evolutionary regional 3D numerical models of buoyancy-driven deformation with realistic slab geometry for the Alaska subduction–transform system (Fig. 20b). They found that near a subduction zone edge mantle flow velocities can have magnitudes of more than ten times the surface plate motions, whereas surface plate velocities are consistent with plate motions and the complex mantle flow field is consistent with observations from seismic anisotropy. The seismic anisotropy observations constrain the shape of the eastern slab edge and require a non-Newtonian mantle rheology. The incorporation of the non-Newtonian viscosity results in low mantle viscosities (10^{17}–10^{18} Pa s) in regions of high strain rate, and this low viscosity enables the mantle flow field to partially decouple from surface plate motion. These results also imply local rapid transport of geochemical signatures through subduction zones and that the internal deformation of slabs decreases the slab-pull force available to drive subducting plates.

Further advances in 3D subduction modeling are directed toward making this currently technically challenging type of high-resolution, physically complex simulation (e.g., OzBench et al., 2008; Zhu et al., 2009; Burkett and Billen, 2010; Stadler et al., 2010; Tackley, 2011; van Hunen and Allen, 2011) a standard tool for geodynamicists studying regional and global aspects of subduction-driven plate tectonics.

12. Conclusions: short summary of future directions

Future directions in subduction modeling will primarily target a number of unresolved issues that have been outlined in the preceding chapters. The following issues are of first order importance:

(1) Resolving the controversy of subduction initiation. Deciphering major physical mechanisms responsible for this process. Identifying examples of modern subduction initiation in nature by numerically testing the stability of existing plate boundaries. Establishing key natural observables to be monitored for testing various subduction initiation scenarios.
(2) Constraining high-resolution global and regional models of terrestrial plate tectonics employing realistic rock rheologies, free surface boundary conditions and spontaneously forming convergent, divergent and transform plate boundaries. This will unavoidably require creating more realistic global mantle convection models involving spontaneous asymmetric (one-sided) subduction and transform faults.
(3) Understanding deep slab processes in the upper mantle, down to the core-mantle boundary. Automated mutual coupling of global tomography models with global high-resolution thermo-mechanical simulations will be needed to incorporate limitations from flow modeling and phase changes into seismic tomography interpretations.
(4) Constraining crustal growth and differentiation in magmatic arc with models including various mechanisms of crustal growth (volcanic and plutonic addition, magmatic differentiation, plume accretion, lithospheric delamination, subduction accretion/erosion, surface processes, etc.). Combining numerical predictions with natural observations to decipher deep arc crustal and lithospheric compositions as well as the physical controls for spatial and temporal periodicity of crustal growth.
(5) Robust modeling of fluid and melt transport in subduction zones. A new generation of thermo-mechanical codes will be needed to address various transport mechanisms (porous and reactive flows, diffusion, diapiric transport, etc.) in a self-consistent manner. These new codes will be crucial for modeling and understanding the deep structure of magmatic arcs and mantle wedges, as well as for understanding the physical controls of magmatic processes and associated crustal growth in arcs.
(6) Realistic modeling of high- and ultrahigh-pressure rocks histories in subduction/collision zones with 3D geometries, surface processes, metamorphic phase transformations (including dehydration/hydration reactions and melting) and pressure–temperature–time path simulations tested against natural data from subduction-related metamorphic complexes.
(7) Coupled geochemical–mineralogical thermo-mechanical modeling of subduction zones. Evolution of geochemical signatures should be predicted for different realistic thermo-mechanical subduction scenarios. These types of models are needed to properly interpret the abundant amount of geochemical data available for natural subduction systems and will be particularly crucial for understanding the complex fluid and melts processes in the mantle wedge under magmatic arcs. Progress in this area will be strongly tied to progress in fluid and melt transport modeling.
(8) Coupling of realistic, multiple-scale geodynamic models of subduction with volcanic and seismic risk assessment in subduction zones. Understanding the relationship between long-term deformation, fluid/melt transport and short-term processes such as seismic rupture and volcanic events. Development of multiple-scale (in both time and space), high-resolution numerical tools will be needed.
(9) Understanding the onset of plate tectonics on Earth with robust numerical models of plate tectonic development and constraining the key observables to monitor in nature for testing various plate tectonics initiation scenarios.

This list is obviously non-exclusive and progress in subduction modeling will also require strong input from other disciplines (rheology, phase petrology, seismic tomography, geochemistry, numerical analysis, etc.). Indeed, due to the intrinsic complexity of terrestrial subduction processes, the role of numerical model-

ing approaches will inevitably grow, providing an integrative basis for conducting quantitative cross-disciplinary subduction studies combining natural observations, laboratory experiments, and modeling.

Acknowledgements

This work was supported by ETH Research Grants ETH-0807-2, ETH-0807-3, ETH-0609-2, SNF Research Grants 200020-126832, 200020-129487, Crystal2Plate program, SNF ProDoc program 4-D-Adamello and TopoEurope Program. Constructive reviews of Stephan Sobolev and an anonymous reviewer are appreciated. David May and John Naliboff are thanked for valuable suggestions to the paper.

References

Abbott, R.N., Draper, G., Broman, B.N., 2006. *P–T* path for ultrahighpressure garnet ultramafic rocks of the Cuaba Gneiss, Rio San Juan complex, Dominican Republic. Int. Geol. Rev. 48, 778–790.

Andersen, T.B., Jamtveit, B., Dewey, J.F., 1991. Subduction and eduction of continental crust: major mechanisms during continent–continent collision and orogenic extensional collapse, a model based on the south Norwegian Caledonides. Terra Nova 3, 303–310.

Andrews, E.R., Billen, M.I., 2009. Rheologic controls on the dynamics of slab detachment. Tectonophysics 464, 60–69.

Arcay, D., Tric, E., Doin, M.P., 2005. Numerical simulations of subduction zones: effect of slab dehydration on the mantle wedge dynamics. Phys. Earth Planet. Inter. 149, 133–153.

Arcay, D., Doin, M.P., Tric, E., Bousquet, R., de Capitani, C., 2006. Overriding plate thinning in subduction zones: localized convection induced by slab dehydration. Geochem. Geophys. Geosyst. 7, Q02007.

Arcay, D., Lallemand, S., Doin, M.-P., 2008. Back-arc strain in subduction zones: statistical observations versus numerical modeling. Geochem. Geophys. Geosyst. 9, Q05015.

Beaumont, C., Jamieson, R.A., Butler, J.P., Warren, C.J., 2009. Crustal structure: a key constraint on the mechanism of ultra-high-pressure rock exhumation. Earth Planet. Sci. Lett. 287, 116–129.

Babeyko, A.Y., Sobolev, S.V., 2008. High-resolution numerical modeling of stress distribution in visco-elasto-plastic subducting slabs. Lithos 103, 205–216.

Barazangi, M., Isacks, B.L., Oliver, J., Dubois, J., Pascal, G., 1973. Descent of lithosphere beneath New Hebrides, Tonga–Fiji and New Zealand: evidence for detached slabs. Nature 242, 98–101.

Baumann, C., Gerya, T., Connolly, J.A.D., 2010. Numerical modeling of spontaneous slab break-off dynamics during continental collision. In: Spalla, M.I., Marotta, A.M., Gosso, G. (Eds.), Advances in Interpretation of Geological Processes, vol. 332. Geological Society, London, pp. 99–114 (Special Publications).

Behounkova, M., Čížková, H., 2008. Long-wavelength character of subducted slabs in the lower mantle. Earth Planet. Sci. Lett. 275, 43–53.

Benn, K., Mareschal, J.-C., Condie, K., 2005. Archean geodynamics and environments. Geophysical Union. Geophysical Monograph Series 64, 320.

Billen, M., Gurnis, M., 2001. A low viscosity wedge in subduction zones. Earth Planet. Sci. Lett. 193, 227–236.

Blanco-Quintero, I.F., García-Casco, A., Gerya, T.V., 2010. Tectonic blocks in serpentinite mélange (eastern Cuba) reveal large-scale convective flow of the subduction channel. Geology 39, 79–82.

Braun, J., Yamato, P., 2010. Structural evolution of a three-dimensional, finite-width crustal wedge. Tectonophysics 484, 181–192.

Brown, M., 2006. Duality of thermal regimes is the distinctive characteristic of plate tectonics since the Neoarchean. Geology 34, 961–964.

Brown, M., 2007. Metamorphic conditions in orogenic belts: a record of secular change. Int. Geol. Rev. 49, 193–234.

Buiter, S.J.H., Govers, R., Wortel, M.J.R., 2002. Two-dimensional simulation of surface deformation caused by slab detachment. Tectonophysics 354, 192–210.

Burkett, E.R., Billen, M.I., 2009. Dynamics and implications of slab detachment due to ridge–trench collision. J. Geophys. Res. 114, B12402.

Burkett, E.R., Billen, M.I., 2010. Three-dimensionality of slab detachment due to ridge–trench collision: laterally simultaneous boudinage versus tear propagation. Geochem. Geophys. Geosyst. 11, Q11012.

Burov, E., Cloetingh, S., 2010. Plume-like upper mantle instabilities drive subduction initiation. Geophys. Res. Lett. 37, L03309.

Burov, E., Yamato, P., 2008. Continental plate collision, *P–T–t–z* conditions and unstable vs. stable plate dynamics: insights from thermo-mechanical modelling. Lithos 103, 178–204.

Burov, E., Jolivet, L., Le Pourhiet, L., Poliakov, A., 2001. A thermo-mechanical model of exhumation of high pressure (HP) and ultra-high pressure (UHP) metamorphic rocks in Alpine-type collision belts. Tectonophysics 342, 113–136.

Cagnioncle, A.M., Parmentier, E.M., Elkins-Tanton, L.T., 2007. Effect of solid flow above a subducting slab on water distribution and melting at convergent plate boundaries. J. Geophys. Res. 112, B09402.

Capitanio, F.A., Morra, G., Goes, S., 2007. Dynamic models of downgoing plate-buoyancy driven subduction: subduction motions and energy dissipation. Earth Planet. Sci. Lett. 262, 284–297.

Caricchi, L., Burlini, L., Ulmer, P., Gerya, T., Vassalli, M., Papale, P., 2007. Non-Newtonian rheology of crystal-bearing magmas and implications for magma ascent dynamics. Earth Planet. Sci. Lett. 264, 402–419.

Castro, A., Gerya, T.V., 2008. Magmatic implications of mantle wedge plumes: experimental study. Lithos 103, 138–148.

Castro, A., García-Casco, A., Fernández, C., Corretgé, L.G., Moreno-Ventas, I., Gerya, T., Löw, I., 2009. Ordovician ferrosilicic magmas: experimental evidence for ultrahigh temperatures affecting a metagreywacke source. Gondwana Res. 16, 622–632.

Castro, A., Gerya, T., Garcia-Casco, A., Fernandez, C., Diaz-Alvarado, J., Moreno-Ventas, I., Low, I., 2010. Melting relations of MORB-sediment melanges in underplated mantle wedge plumes; implications for the origin of Cordilleran-type batholiths. J. Petrol. 51, 1267–1295.

Chen, W.-P., Brudzinski, M.R., 2001. Evidence for a large-scale remnant of subducted lithosphere beneath Fiji. Science 292, 2475–2479.

Chopin, C., 2003. Ultrahigh-pressure metamorphism: tracing continental crust into mantle. Earth Planet. Sci. Lett. 212, 1–14.

Christensen, U.R., 1996. The influence of trench migration on slab penetration into the lower mantle. Earth Planet. Sci. Lett. 140, 27–39.

Christensen, U.R., Yuen, D.A., 1984. The interaction of a subducting lithospheric slab with a chemical or phase boundary. J. Geophys. Res. 89, 4389–4402.

Čížková, H., van Hunen, J., van den Berg, A.P., Vlaar, N.J., 2002. The influence of rheological weakening and yield stress on the interaction of slabs with the 670 km discontinuity. Earth Planet. Sci. Lett. 199, 447–457.

Čížková, H., van Hunen, J., van den Berg, A., 2007. Stress distribution within subducting slabs and their deformation in the transition zone. Phys. Earth Planet. Inter. 161, 202–214.

Clark, S.R., Stegman, D., Müller, R.D., 2008. Episodicity in back-arc tectonic regimes. Phys. Earth Planet. Inter. 171, 265–279.

Cloetingh, S.A.P.L., Wortel, M.J.R., Vlaar, N.J., 1982. Evolution of passive continental margins and initiation of subduction zones. Nature 297, 139–142.

Cloetingh, S., Burov, E., Matenco, L., Toussaint, G., Bertotti, G., Andriessen, P., Wortel, M., Spakman, W., 2004. Thermo-mechanical controls on the mode of continental collision in the SE Carpathians (Romania). Earth Planet. Sci. Lett. 218, 57–76.

Cloos, M., 1982. Flow melanges: numerical modelling and geologic constraints on their origin in the Fransiscan subduction complex, California. Geol. Soc. Am. Bull. 93, 330–345.

Cloos, M., Shreve, R.L., 1988a. Subduction-channel model of prism accretion, melange formation, sediment subduction, and subduction erosion at convergent plate margins. 1. Background and description. Pure Appl. Geophys. 128, 455–500.

Cloos, M., Shreve, R.L., 1988b. Subduction-channel model of prism accretion, melange formation, sediment subduction, and subduction erosion at convergent plate margins. 2. Implications and discussion. Pure Appl. Geophys. 128, 501–545.

Conder, J.A., Wiens, D.A., 2007. Rapid mantle flow beneath the Tonga volcanic arc. Earth Planet. Sci. Lett. 264, 299–307.

Condie, K.C., Pease, V., 2008. When did Plate Tectonics Begin on Planet Earth? In: The Geological Society of America, Special Paper, vol. 440. 294 pp.

Connolly, J.A.D., Podladchikov, Yu.Yu., 1998. Compaction-driven fuid fow in viscoelastic rock. Geodin. Acta (Paris) 11, 55–84.

Crameri, F., Kaus, B.J.P., 2010. Parameters that control lithospheric-scale thermal localization on terrestrial planets. Geophys. Res. Lett. 37, L09308.

Currie, C.A., Beaumont, C., Huismans, R.S., 2007. The fate of subducted sediments: a case for back-arc intrusion and underplating. Geology 35, 1111–1114.

Davies, G.F., 1992. On the emergence of plate-tectonics. Geology 20, 963–966.

Davies, G.F., 1999. Dynamic Earth. Cambridge University Press, New York.

Davies, G.F., 2006. Gravitational depletion of the early Earth's upper mantle and the viability of early plate tectonics. Earth Planet. Sci. Lett. 243, 376–382.

Davies, J.H., Stevenson, D.J., 1992. Physical model of source region of subduction zone volcanic. J. Geophys. Res. 97, 2037–2070.

Davies, H.J., von Blanckenburg, F., 1995. Slab break-off: a model of lithosphere detachment and its test in the magmatism and deformation of collisional orogens. Earth Planet. Sci. Lett. 129, 85–102.

de Wit, M.J., 1998. On Archean granites, greenstones, cratons and tectonics: does the evidence demand a verdict? Precambrian Res. 91, 181–226.

Dewey, J.F., 1969. Continental margins: a model for conversion of Atlantic type to Andean type. Earth Planet. Sci. Lett. 6, 189–197.

Dimalanta, C., Taira, A., Yumul, G.P., Tokuyama, H., Mochizuki, K., 2002. New rates of western Pacific island arc magmatism from seismic and gravity data. Earth Planet. Sci. Lett. 202, 105–115.

Doin, M.-P., Henry, P., 2001. Subduction initiation and continental crust recycling: the roles of rheology and eclogitization. Tectonophysics 342, 163–191.

Dvorkin, J., Nur, A., Mavko, G., Ben, A.Z., 1993. Narrow subducting slabs and the origin of back-arc basins. Tectonophysics 227, 63–79.

Duretz, T., Gerya, T.V., May, D.A., 2011. Numerical modelling of spontaneous slab break-off and subsequent topographic response. Tectonophysics 502, 244–256.

Ernst, W.G., 1977. Mineral parageneses and plate tectonic settings of relatively high-pressure metamorphic belts. Fortschr. Miner. 54, 192–222.

Faccenda, M., Burlini, L., Gerya, T.V., Mainprice, D., 2008a. Fault-induced seismic anisotropy by hydration in subducting oceanic plates. Nature 455, 1097–1101.

Faccenda, M., Gerya, T.V., Chakraborty, S., 2008b. Styles of post-subduction collisional orogeny: influence of convergence velocity, crustal rheology and radiogenic heat production. Lithos 103, 257–287.
Faccenda, M., Gerya, T.V., Burlini, L., 2009. Deep slab hydration induced by bending related variations in tectonic pressure. Nat. Geosci. 2, 790–793.
Faccenna, C., Davy, P., Brun, J.-P., Funiciello, R., Giardini, D., Mattei, M., Nalpas, T., 1996. The dynamics of back-arc extension: an experimental approach to the opening of the Tyrrhenian Sea. Geophys. J. Int. 126, 781–795.
Federico, L., Crispini, L., Scambelluri, M., Capponi, G., 2007. Ophiolite mélange zone records exhumation in a fossil subduction channel. Geology 35, 499–502.
Ferrari, L., 2004. Slab detachment control on mafic volcanic pulse and mantle heterogeneity in central Mexico. Geology 32, 77–80.
Gaherty, J.B., Hager, B.H., 1994. Compositional vs. thermal buoyancy and the evolution of subducted lithosphere. Geophys. Res. Lett. 21, 141–144.
Gerya, T.V., 2010. Introduction to Numerical Geodynamic Modelling. Cambridge University Press, 345 pp.
Gerya, T.V., Meilick, F.I., 2011. Geodynamic regimes of subduction under an active margin: effects of rheological weakening by fluids and melts. J. Metamorphic Geol. 29, 7–31.
Gerya, T.V., Stoeckhert, B., 2006. 2D numerical modeling of tectonic and metamorphic histories at active continental margins. Int. J. Earth Sci. 95, 250–274.
Gerya, T.V., Yuen, D.A., 2003. Rayleigh–Taylor instabilities from hydration and melting propel "cold plumes" at subduction zones. Earth Planet. Sci. Lett. 212, 47–62.
Gerya, T.V., Stoeckhert, B., Perchuk, A.L., 2002. Exhumation of high-pressure metamorphic rocks in a subduction channel—a numerical simulation. Tectonics 21, 1056.
Gerya, T.V., Yuen, D.A., Sevre, E.O.D., 2004a. Dynamical causes for incipient magma chambers above slabs. Geology 32, 89–92.
Gerya, T.V., Yuen, D.A., Maresch, W.V., 2004b. Thermomechanical modeling of slab detachment. Earth Planet. Sci. Lett. 226, 101–116.
Gerya, T.V., Connolly, J.A.D., Yuen, D.A., Gorczyk, W., Capel, A.M., 2006. Sesmic implications of mantle wedge plumes. Phys. Earth Planet. Inter. 156, 59–74.
Gerya, T.V., Connolly, J.A.D., Yuen, D.A., 2008a. Why is terrestrial subduction one-sided? Geology 36, 43–46.
Gerya, T.V., Perchuk, L.L., Burg, J.-P., 2008b. Transient hot channels: perpetrating and regurgitating ultrahigh-pressure, high temperature crust–mantle associations in collision belts. Lithos 103, 236–256.
Goes, S., Capitanio, F.A., Morra, G., 2008. Evidence of lower-mantle slab penetration phases in plate motions. Nature 451, 981–984.
Gorczyk, W., Gerya, T.V., Connolly, J.A.D., Yuen, D.A., Rudolph, M., 2006. Large-scale rigid-body rotation in the mantle wedge and its implications for seismic tomography. Geochem. Geophys. Geosyst. 7, Q05018.
Gorczyk, W., Willner, A.P., Gerya, T.V., Connolly, J.A.D., Burg, J.-P., 2007a. Physical controls of magmatic productivity at Pacific-type convergent margins: new insights from numerical modeling. Phys. Earth Planet. Inter. 163, 209–232.
Gorczyk, W., Gerya, T.V., Connolly, J.A.D., Yuen, D.A., 2007b. Growth and mixing dynamics of mantle wedge plumes. Geology 35, 587–590.
Gorczyk, W., Guillot, S., Gerya, T.V., Hattori, K., 2007c. Asthenospheric upwelling, oceanic slab retreat, and exhumation of UHP mantle rocks: insights from Greater Antilles. Geophys. Res. Lett. 34, L21309.
Goren, L., Aharonov, E., Mulugeta, G., Koyi, H.A., Mart, Y., 2008. Ductile deformation of passive margins: a new mechanism for subduction initiation. J. Geophys. Res. 113, B08411.
Grand, S., 1994. Mantle shear structure beneath the Americas and surrounding oceans. J. Geophys. Res. 99, 11591–11621.
Griffin, W.L., O'Reilly, S.Y., Abe, N., Aulbach, S., Davies, R.M., Pearson, N.J., Doyle, B.J., Kivi, K., 2003. The origin and evolution of Archean lithospheric mantle. Precambrian Res. 127, 19–41.
Grove, T.L., Till, C.B., Lev, E., Chatterjee, N., Medard, E., 2009. Kinematic variables and water transport control the formation and location of arc volcanoes. Nature 459, 694–697.
Gurnis, M., 1992. Rapid continental subsidence following the initiation and evolution of subduction. Science 255, 1556–1558.
Gurnis, M., Hall, C., Lavier, L., 2004. Evolving force balance during incipient subduction. Geochem. Geophys. Geosyst. 5, Q07001.
Hacker, B.R., Kelemen, P.B., Behn, M.D., 2011. Differentiation of the continental crust by relamination. Earth Planet. Sci. Lett., doi:10.1016/j.epsl.2011.05.024.
Hall, P.S., Kincaid, C., 2001. Diapiric flow at subduction zones: a recipe for rapid transport. Science 292, 2472–2475.
Hall, C.E., Gurnis, M., Sdrolias, M., Lavier, L.L., Muller, R.D., 2003. Catastrophic initiation of subduction following forced convergence across fractures zones. Earth Planet. Sci. Lett. 212, 15–30.
Hamilton, W.B., 1998. Archean magmatism and deformation were not products of plate tectonics. Precambrian Res. 91, 143–179.
Hansen, V.L., 2007. Subduction origin on early Earth: a hypothesis. Geology 35, 1059–1062.
Hebert, L.B., Antoshechkina, P., Asimow, P., Gurnis, M., 2009. Emergence of a low-viscosity channel in subduction zones through the coupling of mantle flow and thermodynamics. Earth Planet. Sci. Lett. 278, 243–256.
Hermann, J., Muntener, O., Scambelluri, M., 2000. The importance of serpentinite mylonites for subduction and exhumation of oceanic crust. Tectonophysics 327, 225–238.
Herzberg, C.T., Fyfe, W.S., Carr, M.J., 1983. Density constraints on the formation of the continental Moho and crust. Contrib. Mineral. Petrol. 84, 1–5.
Holbrook, W.S., Lizarralde, D., McGeary, S., Bangs, N., Diebold, J., 1999. Structure and composition of Aleutian island arc and implications for continental crustal growth. Geology 27, 31–34.
Honda, S., 2009. Numerical simulations of mantle flow around slab edges. Earth Planet. Sci. Lett. 277, 112–122.
Honda, S., Saito, M., 2003. Small-scale convection under the back-arc occurring in the low viscosity wedge. Earth Planet. Sci. Lett. 216, 703–715.
Honda, S., Yoshida, T., 2005. Application of the model of small-scale convection under the island arc to the NE Honshu subduction zone. Geochem. Geophys. Geosyst. 6, Q01002.
Honda, S., Saito, M., Nakakuki, T., 2002. Possible existence of small-scale convection under the back arc. Geophys. Res. Lett. 29, 20–43.
Honda, S., Yoshida, T., Aoike, K., 2007. Spatial and temporal evolution of arc volcanism in the northeast Honshu and Izu-Bonin arcs: evidence of small-scale convection under the island arc? Isl. Arc 16, 214–223.
Honda, S., Gerya, T., Zhu, G., 2010. A simple three-dimensional model of thermochemical convection in the mantle wedge. Earth Planet. Sci. Lett. 290, 311–318.
Hsu, K.J., 1971. Franciscan melange as a model for eugeosunclinal sedimentation and underthrusting tectonics. J. Geophys. Res. 76, 1162–1170.
Isacks, B., Molnar, P., 1969. Mantle earthquake mechanisms and the sinking of the lithosphere. Nature 223, 1121–1124.
Ito, E., Stern, R.J., 1986. Oxygen-isotopic and strontium-isotopic investigations of subduction zone volcanism—the case of the Volcano arc and the Marianas island-arc. Earth Planet. Sci. Lett. 76, 312–320.
Iwamori, H., 1998. Transportation of H_2O and melting in subduction zones. Earth Planet. Sci. Lett. 160, 65–80.
Iwamori, H., 2000. Deep subduction of H_2O and deflection of volcanic chain towards back-arc near triple junction due to lower temperature. Earth Planet. Sci. Lett. 181, 41–46.
Iwamori, H., 2004. Phase relations of peridotites under H_2O-saturated conditions and ability of subducting plates for transportation of H_2O. Earth Planet. Sci. Lett. 227, 57–71.
Iwamori, H., 2007. Transportation of H_2O beneath the Japan arcs and its implications for global water circulation. Chem. Geol. 239, 182–198.
Jadamec, M.A., Billen, M.I., 2010. Reconciling surface plate motions with rapid three-dimensional mantle flow around a slab edge. Nature 465, 338–341.
Jolivet, L., Tamaki, K., Fournier, M., 1994. Japan Sea, opening history and mechanism: a synthesis. J. Geophys. Res. 99, 22237–22259.
Kelemen, P.B., Rilling, J.L., Parmentier, E.M., Mehl, L., Hacker, B.R., 2004. Thermal structure due to solid-state flow in the mantle wedge beneath arcs. In: Eiler, J.M. (Ed.), Inside the Subduction Factory, Geophys. Monogr. Ser., vol. 138. AGU, Washington, DC, pp. 293–311.
Kelley, K.A., Plank, T., Grove, T.L., Stolper, E.M., Newman, S., Hauri, E., 2006. Mantle melting as a function of water content beneath back-arc basins. J. Geophys. Res. 111, B09208.
Kemp, D.V., Stevenson, D.J., 1996. A tensile, flexural model for the initiation of subduction. Geophys. J. Int. 125, 73–94.
Keskin, M., 2003. Magma generation by slab steepening and break-off beneath subduction–accretion complex: an alternative model for collision-related volcanism in Eastern Anatolia, Turkey. Geophys. Res. Lett. 30, 1–4.
Kimura, J., Yoshida, T., 2006. Contributions of slab fluid, mantle wedge and crust to the origin of quaternary lavas in the NE Japan arc. J. Petrol. 47, 2185–2232.
Kimura, J.-I., Hacker, B.R., van Keken, P.E., Kawabata, H., Yoshida, T., Stern, R.J., 2009. Arc basalt simulator version 2, a simulation for slab dehydration and fluid-fluxed mantle melting for arc basalts: modeling scheme and application. Geochem. Geophys. Geosyst. 10, Q09004.
Kodaira, S., Sato, T., Takahashi, N., Ito, A., Tamura, Y., Tatsumi, Y., Kaneda, Y., 2006. Seismological evidence for variable growth of crust along the Izu intraoceanic arc. J. Geophys. Res. 112, B05104.
Kodaira, S., Sato, T., Takahashi, N., Miura, S., Tamura, Y., Tatsumi, Y., Kaneda, Y., 2007. New seismological constraints on growth of continental crust in the Izu-Bonin intra-oceanic arc. Geology 35, 1031–1034.
Krebs, M., Maresch, W.V., Schertl, H.-P., Münker, C., Baumann, A., Draper, G., Idleman, B., Trapp, E., 2008. The dynamics of intra-oceanic subduction zones: a direct comparison between fossil petrological evidence (Rio San Juan Complex, Dominican Republic) and numerical simulation. Lithos 103, 106–137.
Lallemand, S., Heuret, A., Faccenna, C., Funiciello, F., 2008. Subduction dynamics as revealed by trench migration. Tectonics 27, TC3014.
Leat, P.T., Larter, R.D., 2003. Intra-oceanic subduction systems: introduction. In: Larter, R.D., Leat, P.T. (Eds.), Intra-oceanic Subduction Systems: Tectonic and Magmatic Processes. Geol. Soc. London, vol. 219. , pp. 1–17 (Special Publication).
Li, Z., Gerya, T.V., 2009. Polyphase formation and exhumation of HP-UHP rocks in continental subduction zone: Numerical modeling and application to the Sulu UHP terrane in eastern China. J. Geophys. Res. 114, B09406.
Li, Z., Gerya, T.V., Burg, J.P., 2010. Influence of tectonic overpressure on *P–T* paths of HP-UHP rocks in continental collision zones: thermo-mechanical modelling. J. Metamorphic Geol. 28, 227–247.
Li, C., van der Hilst, R.D., Engdahl, E.R., Burdick, S., 2008. A new global model for *P* wave speed variations in Earth's mantle. Geochem. Geophys. Geosyst. 9, Q05018.
Liou, J.G., Tsujimori, T., Zhang, R.Y., Katayama, I., Maruyama, S., 2004. Global UHP metamorphism and continental subduction/collision: The Himalayan model. Int. Geol. Rev. 46, 1–27.
Lister, G.S., Forster, M.A., Rawling, T.J., 2001. Episodicity during orogenesis. In: Miller, J.A., Holdsworth, R.E., Buick, I.S., Hand, M. (Eds.), Continental Reactivation and Reworking. Geol. Soc. London, vol. 184. , pp. 89–113 (Special Publication).

Loiselet, C., Braun, J., Husson, L., Le Carlier de Veslud, C., Thieulot, C., Yamato, P., Grujic, D., 2010. Subducting slabs: jellyfishes in the Earth's mantle. Geochem. Geophys. Geosyst. 11, Q08016.
Long, M.D., Silver, P., 2008. The subduction zone flow field from seismic anisotropy: a global view. Science 319, 315–318.
Macera, P., Gasperini, D., Ranalli, G., Mahatsente, R., 2008. Slab detachment and mantle plume upwelling in subduction zones: an example from the Italian South–Eastern Alps. J. Geodyn. 45, 32–48.
Manea, V.C., Manea, M., Kostoglodov, V., Sewell, G., 2005. Thermo-mechanical model of the mantle wedge in Central Mexican subduction zone and a blob tracing approach for the magma transport. Phys. Earth Planet. Inter. 149, 165–186.
Marques, F.O., Gerya, T., Nikolaeva, K., 2008. Subduction initiation at a passive margin: a prototype candidate. In: 33rd International Geological Congress, Abstract Volume , Oslo, Norway.
Mart, Y., Aharonov, E., Mulugeta, G., Ryan, W., Tentler, T., Goren, L., 2005. Analogue modelling of the initiation of subduction. Geophys. J. Int. 160, 1081–1091.
Maruyama, S., Liou, J.G., Terabayashi, M., 1996. Blueschists and eclogites in the world and their exhumation. Int. Geol. Rev. 38, 485–594.
Matsumoto, T., Tomoda, Y., 1983. Numerical-simulation of the initiation of subduction at the fracture-zone. J. Phys. Earth 31, 183–194.
McKenzie, D.P., 1977. The initiation of trenches: a finite amplitude instability. In: Talwani, M., Pitman III, W.C. (Eds.), Island Arcs, Deep Sea Trenches and Back-Arc Basins, Maurice Ewing Series, vol. 1. AGU, Washington, DC, pp. 57–61.
Michaud, F., Royer, J.Y., Bourgois, J., Dyment, J., Calmus, T., Bandy, W., Sosson, M., Mortera-Gutiérrez, C., Sichler, B., Rebolledo-Viera, M., Pontoise, B., 2006. Oceanic-ridge subduction vs. slab break off: plate tectonic evolution along the Baja California Sur continental margin since 15 Ma. Geology 34, 13–16.
Miller, S.A., Collettini, C., Chiaraluce, L., Cocco, M., Barchi, M., Kaus, B.J.P., 2004. Aftershocks driven by a high-pressure CO_2 source at depth. Nature 427, 724–727.
Minear, J.W., Toksöz, M.N., 1970. Thermal regime of a downgoing slab and new global tectonics. J. Geophys. Res. 75, 1397–1419.
Mishin, Y.A., Gerya, T.V., Burg, J.-P., Connolly, J.A.D., 2008. Dynamics of double subduction: numerical modeling. Phys. Earth Planet. Inter. 171, 280–295.
Mitchell, A.H.G., 1984. Initiation of subduction of post-collision foreland thrusting and back-thrusting. J. Geodyn. 1, 103–120.
Morra, G., Regenauer-Lieb, K., Giardini, D., 2006. Curvature of oceanic arcs. Geology 34, 877–880.
Morra, G., Yuen, D.A., Boschi, L., Chatelaine, P., Koumoutsakose, P., Tackley, P.J., 2010. The fate of the slabs interacting with a density/viscosity hill in the mid-mantle. Phys. Earth Planet. Inter. 180, 271–282.
Müeller, S., Phillips, R.J., 1991. On the initiation of subduction. J. Geophys. Res. 96, 651–665.
Nakajima, J., Hasegawa, A., 2003a. Estimation of thermal structure in the mantle wedge of northeastern Japan from seismic attenuation data. Geophys. Res. Lett. 30, 1760.
Nakajima, J., Hasegawa, A., 2003b. Tomographic imaging of seismic velocity structure in and around the Onikobe volcanic area, northeastern Japan: implications for fluid distribution. J. Volcanol. Geotherm. Res. 127, 1–18.
Nikolaeva, K., Gerya, T.V., Connolly, J.A.D., 2008. Numerical modelling of crustal growth in intraoceanic volcanic arcs. Phys. Earth Planet. Inter. 171, 336–356.
Nikolaeva, K., Gerya, T.V., Marques, F.O., 2010. Subduction initiation at passive margins: numerical modeling. J. Geophys. Res. 115, B03406.
Nikolaeva, K., Gerya, T.V., Marques, F.O., 2011. Numerical analysis of subduction initiation risk along the Atlantic American passive margins. Geology 39, 463–466.
Niu, Y., O'Hara, M.J., Pearce, J.A., 2003. Initiation of subduction zones as a consequence of lateral compositional buoyancy contrast within the lithosphere: a petrological perspective. J. Petrol. 44, 851–866.
Obata, M., Takazawa, E., 2004. Compositional continuity and discontinuity in the Horoman peridotite, Japan, and its implication for melt extraction processes in partially molten upper mantle. J. Petrol. 45, 223–234.
Ohtani, E., Litasov, K., Hosoya, T., Kubo, T., Kondo, T., 2004. Water transport into the deep mantle and formation of a hydrous transition zone. Phys. Earth Planet. Inter. 143–144, 255–269.
O'Neill, C., Lenardic, A., Moresi, L., Torsvik, T.H., Lee, C.-T.A., 2007a. Episodic precambrian subduction. Earth Planet. Sci. Lett. 262, 552–562.
O'Neill, C., Jellinek, A.M., Lenardic, A., 2007b. Conditions for the onset of plate tectonics on terrestrial planets and moons. Earth Planet. Sci. Lett. 261, 20–32.
Oxburg, E.R., Parmentier, E.M., 1977. Compositional and density stratification in oceanic lithosphere—causes and consequences. J. Geol. Soc. London 133, 343–355.
OzBench, M., Regenauer-Lieb, K., Stegman, D.R., Morra, G., Farrington, R., Hale, A., May, D.A., Freeman, J., Bourgouin, L., Muhlhaus, H., Moresi, L., 2008. A model comparison study of large-scale mantle-lithosphere dynamics driven by subduction. Phys. Earth Planet. Inter. 171, 224–234.
Pascal, G., Dubois, J., Barazangi, M., Isacks, B.L., Oliver, J., 1973. Seismic velocity anomalies beneath the New Hebrides island arc: evidence for a detached slab in the upper mantle. J. Geophys. Res. 78, 6998–7004.
Peacock, S.M., 1987a. Creation and preservation of subduction related inverted metamorphic gradients. J. Geophys. Res. 92, 12763–12781.
Peacock, S.M., 1987b. Serpentinization and infiltration metasomatism in the Trinity peridotite, Klamath province, northern California: implications for subduction zones. Contrib. Mineral. Petrol. 95, 55–70.
Peacock, S., 1990a. Numerical simulation of metamorphic pressure–temperature–time paths and fluid production in subduction slabs. Tectonics 9, 1197–1211.
Peacock, S., 1990b. Fluid processes in subduction zones. Science 248, 329–337.
Peacock, S.M., 1993. The importance of blueschist → eclogite dehydration reactions in the subduction oceanic crust. Geol. Soc. Am. Bull. 105, 684–694.
Peacock, S.M., 1996. Thermal and petrologic structure of subduction zones. In: Bebout, G.E., et, al. (Eds.), Subduction: Top to Bottom. Geophys. Monogr. Ser., vol. 96. AGU, Washington, DC, pp. 119–133.
Pérez-Gussinyé, M., Metois, M., Fernández, M., Vergés, J., Fullea, J., Lowry, A.R., 2009. Effective elastic thickness of Africa and its relationship to other proxies for lithospheric structure and surface tectonics. Earth Planet. Sci. Lett. 287, 152–167.
Platt, J.P., 1993. Exhumation of high-pressure rocks: a review of concepts and processes. Terra Nova 5, 119–133.
Poli, S., Schmidt, M.W., 1995. H_2O transport and release in subduction zones: experimental constraints on basaltic and andesitic systems. J. Geophys. Res. 100, 22299–22314.
Poli, S., Schmidt, M.W., 2002. Petrology of subducted slabs. Annu. Rev. Earth Planet. Sci. 30, 207–235.
Pope, D., Willett, C., 1998. Thermal–mechanical model for crustal thickening in the central Andes driven by ablative subduction. Geology 26, 511–514.
Qin, J., Lao, S., Li, Y., 2008. Slab break-off model for the Triassic post-collisional adakitic granitoids in the Qinling Orogen, Central China: zircon U–Pb ages, geochemistry, and Sr–Nd–Pb isotopic constraints. Int. Geol. Rev. 50, 1080–1104.
Quinteros, J., Sobolev, S.V., Popov, A.A., 2010. Viscosity in transition zone and lower mantle: implications for slab penetration. Geophys. Res. Lett. 37, L09307.
Ranero, C.R., Sallares, V., 2004. Geophysical evidence for hydration of the crust and mantle of the Nazca plate during bending at the North Chile trench. Geology 32, 549–554.
Regenauer-Lieb, K., Yuen, D.A., Branlund, J., 2001. The initiation of subduction: critically by addition of water? Science 294, 578–580.
Rey, P.F., Coltice, N., 2008. Neoarchean lithospheric strengthening and the coupling of Earth's geochemical reservoirs. Geology 36, 635–638.
Reymer, A., Schubert, G., 1984. Phanerozoic addition rates to the continental crust and crustal growth. Tectonics 3, 63–77.
Ribe, N.M., Stutzmann, E., Ren, Y., van der Hilst, R., 2007. Buckling instabilities of subducted lithosphere beneath the transition zone. Earth Planet. Sci. Lett. 254, 173–179.
Richard, G.C., Bercovici, D., 2009. Water-induced convection in the Earth's mantle transition zone. J. Geophys. Res. 114, B01205.
Richard, G., Bercovici, D., Karato, S.-I., 2006. Slab dehydration in the Earth's mantle transition zone. Earth Planet. Sci. Lett. 251, 156–167.
Ring, U., Brandon, M.T., Willett, S.D., Lister, G.S., 1999. In: Ring, U., Brandon, M.T., Lister, G.S., Willett, S.D. (Eds.), Exhumation Processes: Normal Faulting, Ductile Flow, and Erosion, Geol. Soc., vol. 154. , pp. 1–27 (Special Publication).
Ringwood, A.E., Green, D.H., 1966. An experimental investigation of the gabbro-eclogite transformation and some geophysical implications. Tectonophysics 3, 383–427.
Rogers, R.D., Karason, H., van der Hilst, R.D., 2002. Epeirogenic uplift above a detached slab in northern Central America. Geology 30, 1031–1034.
Rozhko, A.Y., Podladchikov, Y.Y., Renard, F., 2007. Failure patterns caused by localized rise in pore-fluid overpressure and effective strength of rocks. Geophys. Res. Lett. 34, L22304.
Rubatto, D., Hermann, J., 2001. Exhumation as fast as subduction. Geology 29, 3–6.
Rudnick, R.L., 1995. Making continental crust. Nature 378, 571–578.
Rudnick, R.L., Gao, S., 2003. Composition of the continental crust. In the Crust (Rudnick, R.L. (Ed.)), 3 Treatise on Geochemistry (Holland, H.D., Turekian, K.K. (Eds.)), Elsevier-Pergamon, Oxford. pp. 1–64.
Rüpke, L.H., Phipps Morgan, J., Hort, M., Connolly, J., 2004. Serpentine and the subduction zone water cycle. Earth Planet. Sci. Lett. 223, 17–34.
Sajona, F.G., Maury, R.C., Bellon, H., Cotten, J., Defant, M., 1996. High field strength element enrichment of Pliocene–Pleistocene island arc basalts, Zamboanga Peninsula, western Mindanao (Philpiipnes). J. Petrol. 37, 693–726.
Sajona, F.G., Maury, R.C., Prouteau, G., Cotten, J., Schiano, P., Bellon, H., Fontaine, L., 2000. Slab melt as metasomatic agent in island arc magma mantle sources, Negros and Batan (Philippines). Isl. Arc 9, 472–486.
Schellart, W.P., Freeman, J., Stegman, D.R., Moresi, L., May, D., 2007. Evolution and diversity of subduction zones controlled by slab width. Nature 446, 308–311.
Schmeling, H., 2000. Partial melting and melt segregation in a convecting mantle. In: Bagdassarov, N., Laporte, D., Thompson, A.B. (Eds.), Physics and Chemistry of Partially Molten Rocks. Kluwer Academic Publisher, Dordrecht, pp. 141–178.
Schmeling, H., Babeyko, A.Y., Enns, A., Faccenna, C., Funiciello, F., Gerya, T., Golabek, G.J., Grigull, S., Kaus, B.J.P., Morra, G., Schmalholz, S.M., van Hunen, J., 2008. A benchmark comparison of spontaneous subduction models—towards a free surface. Phys. Earth Planet. Inter. 171, 198–223.
Schmidt, M.W., Poli, S., 1998. Experimentally based water budgets for dehydrating slabs and consequences for arc magma generation. Earth Planet. Sci. Lett. 163, 361–379.
Sdrolias, M., Müller, R.D., 2006. Controls on back-arc basin formation. Geochem. Geophys. Geosyst. 7, Q04016.
Shreve, R.L., Cloos, M., 1986. Dynamics of sediment subduction, melange formation, and prism accretion. J. Geophys. Res. 91, 10229–10245.
Sizova, E., Gerya, T., Brown, M., Perchuk, L.L., 2010. Subduction styles in the Precambrian: insight from numerical experiments. Lithos 116, 209–229.
Sleep, N.H., 2007. Plate tectonics through time. In: Stevenson, D. (Ed.), Treatise on Geophysics: Evolution of the Earth, vol. 9, pp. 145–169.
Sobolev, S.V., Babeyko, A.Y., 2005. What drives orogeny in the Andes? Geology 33, 617–620.
Solomatov, V.S., 2004. Initiation of subduction by small-scale convection. J. Geophys. Res. 109, B05408.

Sperner, B., Lorenz, F., Bonjer, K., Hettel, S., Müller, B., Wenzel, F., 2001. Slab break-off—abrupt cut or gradual detachment? New insights from the Vrancea Region (SE Carpathians, Romania). Terra Nova 13, 139–172.
Spiegelman, M., Kelemen, P.B., Aharonov, E., 2001. Causes and consequences of flow organization during melt transport: the reaction infiltration instability in compactible media. J. Geophys. Res. 106, 2061–2077.
Stadler, G., Gurnis, M., Burstedde, C., Wilcox, L.C., Alisic, L., Ghattas, O., 2010. The dynamics of plate tectonics and mantle flow: from local to global scales. Science 329, 1033–1038.
Stegman, D.R., Freeman, J., Schellart, W.P., Moresi, L., May, D., 2006. Influence of trench width on subduction hinge retreat rates in 3D models of slab rollback. Geochem. Geophys. Geosyst. 7, Q03012.
Stegman, D.R., Farrington, R., Capitanio, F.A., Schellart, W.P., 2010. A regime diagram for subduction styles from 3D numerical models of free subduction. Tectonophysics 483, 29–45.
Stern, R.J., 2002. Subduction zones. Rev. Geophys. 40, 3-1-3-38.
Stern, R.J., 2004. Subduction initiation: spontaneous and induced. Earth Planet. Sci. Lett. 226, 275–292.
Stern, R.J., 2005. Evidence from ophiolites, blueschists, and ultrahigh-pressure metamorphic terranes that the modern episode of subduction tectonics began in Neoproterozoic time. Geology 33, 557–560.
Stern, R.J., 2007. When and how did plate tectonics begin? Theoretical and empirical considerations. Chin. Sci. Bull. 52, 578–591.
Stern, R.J., Bloomer, S.H., 1992. Subduction zone infancy: examples from the Eocene Izu-Bonin-Mariana and Jurassic California arcs. Geol. Soc. Am. Bull. 104, 1621–1636.
Stoeckhert, B., Gerya, T.V., 2005. Pre-collisional high pressure metamorphism and nappe tectonics at active continental margins: a numerical simulation. Terra Nova 17, 102–110.
Syracuse, E.M., van Keken, P.E., Abers, G.A., 2010. The global range of subduction zone thermal models. Phys. Earth Planet. Inter. 183, 73–90.
Tackley, P.J., 1998. Self-consistent generation of tectonic plates in threedimensional mantle convection. Earth Planet. Sci. Lett. 157, 9–22.
Tackley, P.J., 2000. Self-consistent generation of tectonic plates in time-dependent, three-dimensional mantle convection simulations. Part 1: Pseudo-plastic yielding. Geochem. Geophys. Geosyst. 1, 2000GC000036.
Tackley, P.J., 2011. Living dead slabs in 3D: the dynamics of compositionally-stratified slabs entering a "slab graveyard" above the core-mantle boundary. Phys. Earth Planet. Inter., doi:10.1016/j.pepi.2011.04.013.
Tackley, P., Nakagawa, T., Crameri, F., Connolly, J., Deschamps, F., Kaus, B., Gerya, T., 2010. The importance of mineral physics and a free surface in large-scale numerical models of mantle convection and plate tectonics. Geophys. Res. Abstr. 12, EGU2010-11007.
Taira, A., Saito, S., Aoike, K., Morita, S., Tokuyama, H., Suyehiro, K., Takahashi, N., Shinohara, M., Kiyokawa, S., Naka, J., Klaus, A., 1998. Nature and growth rate of the Northern Izu-Bonin (Ogasawara) arc crust and their implications for continental crust formation. Isl. Arc 7, 395–407.
Tamura, Y., 1994. Genesis of island arc magmas by mantle derived bimodal magmatism: evidence from the Shirahama Group, Japan. J. Petrol. 35, 619–645.
Tamura, Y., Tatsumi, Y., Zhao, D.P., Kido, Y., Shukuno, H., 2002. Hot fingers in the mantle wedge: new insights into magma genesis in subduction zones. Earth Planet. Sci. Lett. 197, 105–116.
Tao, W., O'Connell, R., 1992. Ablative subduction: a two-sided alternative to the conventional subduction model. J. Geophys. Res. 97, 8877–8904.
Taylor, S.R., 1967. The origin and growth of continents. Tectonophysics 4, 17–34.
Taylor, S.R., McLennan, S.M., 1985. In: Hallam, A. (Ed.), The Continental Crust: Its Composition and Evolution. Blackwell, Melbourne, p. 328.
Toth, J., Gurnis, M., 1998. Dynamics of subduction initiation at pre-existing fault zones. J. Geophys. Res. 103, 18053–18067.
Toussaint, G., Burov, E., Jolivet, L., 2004. Continental plate collision: unstable vs. stable slab dynamics. Geology 32, 33–36.
Trompert, R., Hansen, U., 1998. Mantle convection simulations with rheologies that generate plate-like behavior. Nature 395, 686–689.
Uyeda, S., Ben-Avraham, Z., 1972. Origin and development of the Philippine Sea. Nature 240, 176–178.
Ueda, K., Gerya, T., Sobolev, S.V., 2008. Subduction initiation by thermal–chemical plumes. Phys. Earth Planet. Inter. 171, 296–312.
van der Hilst, R.D., Engdahl, E.R., Spakman, W., Nolet, G., 1991. Tomographic imaging of subducted lithosphere below northwest Pacific island arcs. Nature 353, 37–43.
van der Hilst, R.D., 1995. Complex morphology of subducted lithosphere in the mantle beneath the Tonga trench. Nature 374, 154–157.
van der Hilst, R.D., Widiyantoro, S., Engdahl, E.R., 1997. Evidence for deep mantle circulation from global tomography. Nature 386, 578–584.
Van der Lee, S., Regenauer-Lieb, K., Yuen, D.A., 2008. The role of water in connecting past and future episodes of subduction. Earth Planet. Sci. Lett. 273, 15–27.
van de Zedde, D.M.A., Wortel, M.J.R., 2001. Shallow slab detachment as a transient source of heat at midlithospheric depths. Tectonics 20, 868–882.
van Hunen, J., Allen, M.B., 2011. Continental collision and slab break-off: a comparison of 3D numerical models with observations. Earth Planet. Sci. Lett. 302, 27–37.
van Hunen, J., van den Berg, A., 2008. Plate tectonics on the early Earth: limitations imposed by strength and buoyancy of subducted lithosphere. Lithos 103, 217–235.
Van Hunen, J., van den Berg, A.P., Vlaar, N.J., 2000. A thermo-mechanical model of horizontal subduction below an overriding plate. Earth Planet Sci. Lett. 182, 157–169.
Van Hunen, J., van den Berg, A.P., Vlaar, N.J., 2004. Various mechanisms to induce shallow flat subduction: a numerical parameter study. Phys. Earth Planet. Inter. 146, 179–194.
Van Keken, P.E., King, S.D., 2005. Thermal structure and dynamics of subduction zones: insights from observations and modeling. Phys. Earth Planet. Inter. 149, 1–6.
van Keken, P.E., Kiefer, B., Peacock, S.M., 2002. High resolution models of subduction zones: implications for mineral dehydration reactions and the transport of water into the deep mantle. Geochem. Geophys. Geosyst. 3, 1056.
van Keken, P.E., Currie, C., King, S.D., Behn, M.D., Cagnioncle, A., He, J., Katz, R.F., Lin, S.-C., Parmentier, E.M., Spiegelman, M., Wang, K., 2008. A community benchmark for subduction zone modeling. Phys. Earth Planet. Inter. 171, 187–197.
van Stiphout, T., Kissling, E., Wiemer, S., Ruppert, N., 2009. Magmatic processes in the Alaska subduction zone by combined 3D b value imaging and targeted seismic tomography. J. Geophys. Res. 114, B11302.
van Thienen, P., van den Berg, A.P., Vlaar, N.J., 2004. Production and recycling of oceanic crust in the early Earth. Tectonophysics 386, 41–65.
Vlaar, N.J., Wortel, M.J.R., 1976. Lithospheric aging, instability and subduction. Tectonophysics 32, 331–351.
Warren, C.J., Beaumont, C., Jamieson, R.A., 2008. Modelling tectonic styles and ultra-high pressure (UHP) rock exhumation during the transition from oceanic subduction to continental collision. Earth Planet. Sci. Lett. 267, 129–145.
Widiyantoro, S., Kennett, B.L.N., van der Hilst, R.D., 1999. Seismic tomography with P and S data reveals lateral variations in the rigidity of deep slabs. Earth Planet. Sci. Lett. 173, 91–100.
Wilmsen, M., Fürsich, F., Seyed-Emmani, K., Majidifard, M.R., Taheri, J., 2009. The Cimmerian Orogeny in northern Iran/tectono-stratigraphic evidence in the foreland. Terra Nova 21, 211–218.
Wong, A., Ton, S.Y.M., Wortel, M.J.R., 1997. Slab detachment in continental collision zones: an analysis of controlling parameters. Geophys. Res. Lett. 24, 2095–2098.
Wortel, M.J.R., Spakman, W., 2000. Subduction and slab detachment in the Mediterranean–Carpathian region. Science 290, 1910–1917.
Wyss, M., Hasegawa, A., Nakajima, J., 2001. Source and path of magma for volcanoes in the subduction zone of northeastern Japan. Geophys. Res. Lett. 28, 1819–1822.
Yamato, P., Agard, P., Burov, E., Le Pourhiet, L., Jolivet, L., Tiberi, C., 2007. Burial and exhumation in a subduction wedge: mutual constraints from thermomechanical modeling and natural *P–T–t* data (Sch. Lustrés, western Alps). J. Geophys. Res. 112, B07410.
Yamato, P., Burov, E., Agard, P., Le Pourhiet, L., Jolivet, L., 2008. HP-UHP exhumation during slow continental subduction: self-consistent thermodynamically and thermo-mechanically coupled model with application to the Western Alps. Earth Planet. Sci. Lett. 271, 63–74.
Yoshioka, S., Wortel, M.J.R., 1995. Three-dimensional numerical modeling of detachment of subducted lithosphere. J. Geophys. Res. 100, 20233–20244.
Yoshioka, S., Yuen, D.A., Larsen, T.B., 1994. Slab weakening: thermal and mechanical consequences for slab detachment. Isl. Arc 40, 89–103.
Zhao, D.P., 2001. Seismological structure of subduction zones and its implications for arc magmatism and dynamics. Phys. Earth Planet. Inter. 127, 197–214.
Zhao, D.P., Hasegawa, A., Horiuchi, S., 1992. Tomographic imaging of P and S wave velocity structure beneath north-eastern Japan. J. Geophys. Res. 97, 19909–19928.
Zhao, D.P., Mishra, O.P., Sanda, R., 2002. Influence of fluids and magma on earthquakes: seismological evidence. Phys. Earth Planet. Inter. 132, 249–267.
Zhu, G., Gerya, T.V., Yuen, D.A., Honda, S., Yoshida, T., Connolly, J.A.D., 2009. 3D dynamics of hydrous thermalchemical plumes in oceanic subduction zones. Geochem. Geophys. Geosyst. 10, Q11006.
Zhu, G., Gerya, T.V., Honda, S., Tackley, P.J., Yuen, D.A., 2011. Influences of the buoyancy of partially molten rock on 3D plume patterns and melt productivity above retreating slabs. Phys. Earth Planet. Inter. 185, 112–121.